

**STRUCTURAL ANALYSIS AND DESIGN
OF A FOUR METER CLASS
ALTAZIMUTH TELESCOPE WITH A MENISCUS MIRROR**

by

Rambabu Bavirisetty

A Dissertation Submitted to the Faculty of the
DEPARTMENT OF CIVIL ENGINEERING AND ENGINEERING MECHANICS

In Partial Fulfillment of the Requirements
For the Degree of

DOCTOR OF PHILOSOPHY

In the Graduate College

THE UNIVERSITY OF ARIZONA

1 9 9 2

INFORMATION TO USERS

This manuscript has been reproduced from the microfilm master. UMI films the text directly from the original or copy submitted. Thus, some thesis and dissertation copies are in typewriter face, while others may be from any type of computer printer.

The quality of this reproduction is dependent upon the quality of the copy submitted. Broken or indistinct print, colored or poor quality illustrations and photographs, print bleedthrough, substandard margins, and improper alignment can adversely affect reproduction.

In the unlikely event that the author did not send UMI a complete manuscript and there are missing pages, these will be noted. Also, if unauthorized copyright material had to be removed, a note will indicate the deletion.

Oversize materials (e.g., maps, drawings, charts) are reproduced by sectioning the original, beginning at the upper left-hand corner and continuing from left to right in equal sections with small overlaps. Each original is also photographed in one exposure and is included in reduced form at the back of the book.

Photographs included in the original manuscript have been reproduced xerographically in this copy. Higher quality 6" x 9" black and white photographic prints are available for any photographs or illustrations appearing in this copy for an additional charge. Contact UMI directly to order.

U·M·I

University Microfilms International
A Bell & Howell Information Company
300 North Zeeb Road, Ann Arbor, MI 48106-1346 USA
313/761-4700 800.521-0600

Order Number 9225174

**Structural analysis and design of a four meter class altazimuth
telescope with a meniscus mirror**

Bavirisetty, Rambabu, Ph.D.

The University of Arizona, 1992

U·M·I

**300 N. Zeeb Rd.
Ann Arbor, MI 48106**

**STRUCTURAL ANALYSIS AND DESIGN
OF A FOUR METER CLASS
ALTAZIMUTH TELESCOPE WITH A MENISCUS MIRROR**

by

Rambabu Bavirisetty

A Dissertation Submitted to the Faculty of the
DEPARTMENT OF CIVIL ENGINEERING AND ENGINEERING MECHANICS

In Partial Fulfillment of the Requirements
For the Degree of

DOCTOR OF PHILOSOPHY

In the Graduate College

THE UNIVERSITY OF ARIZONA

1 9 9 2

THE UNIVERSITY OF ARIZONA
GRADUATE COLLEGE

2

As members of the Final Examination Committee, we certify that we have read
the dissertation prepared by Rambabu Bavirisetty
entitled Structural Analysis and Design of A Four Meter Class Altazimuth
Telescope with a Meniscus Mirror

and recommend that it be accepted as fulfilling the dissertation requirement
for the Degree of Doctor of Philosophy.

Ralph M. Richard

25 Sep 91
Date

B. R. Simon

25 Sep 91
Date

D. G. DeDepp

Sep 25 1991
Date

Date

Date

Final approval and acceptance of this dissertation is contingent upon the
candidate's submission of the final copy of the dissertation to the Graduate
College.

I hereby certify that I have read this dissertation prepared under my
direction and recommend that it be accepted as fulfilling the dissertation
requirement.

Ralph M. Richard
Dissertation Director

12 Nov 91
Date

STATEMENT BY AUTHOR

This dissertation has been submitted in partial fulfillment of requirements for an advanced degree at The University of Arizona and is deposited in the University Library to be made available to borrowers under the rules of the Library.

Brief quotations from this dissertation are allowable without special permission, provided that accurate acknowledgement of source is made. Requests for permission for extended quotation from or reproduction of this manuscript in whole or in part may be granted by the head of the major department or the Dean of the Graduate College when in his or her judgement the proposed use of the material is in the interests of scholarship. In all other instances, however, permission must be obtained from the author.

SIGNED: N. Lambah

ACKNOWLEDGEMENTS

The author would like to extend his deep gratitude and appreciation to his academic advisor and dissertation director, Dr. Ralph M. Richard, Professor of Civil Engineering and Engineering Mechanics, for his constant encouragement and constructive critique.

The suggestions of Professors Dr. D. A. DaDeppo, Dr. B. R. Simon, and Dr. T. Kundu are acknowledged and appreciated. Sincere thanks are extended to D. Blanco, Research engineer at Steward Observatory, for many rewarding discussions pertaining to this study.

Special acknowledgements are due to Dr. B. R. Simon for providing financial assistance during the course of his graduate studies. The author wishes to express his appreciation to the Steward Observatory personnel for the help extended to him during the association.

The encouragement and support of his parents and sisters is deeply appreciated. As a token of his appreciation for their unending love, patience, and understanding, he proudly dedicates this dissertation to his parents, Suguna and Krishna Moorthy Bavirisetty and sisters, Padmaja, Rajani, and Radhika.

TABLE OF CONTENTS

	Page
LIST OF ILLUSTRATIONS	8
LIST OF TABLES.....	11
ABSTRACT.....	13
CHAPTER 1. INTRODUCTION	14
1.1 Background.....	14
1.2 Primary Mirror Technology.....	16
1.3 Telescope Mounting.....	17
1.4 Design Criteria and Error Budget	18
1.5 Primary Mirror Support.....	19
1.6 Objectives	22
1.7 Organization.....	22
CHAPTER 2. PRIMARY MIRROR.....	32
2.1 Background.....	32
2.2 Theoretical and Closed Form Solutions	33
2.2.1 Classical Theory of Thin Flat Circular Plate Loaded Transversely.....	33
2.2.2 Deflections of a Circular Mirror on a Ring of Point Supports	34
2.2.3 Thin Flat Circular Mirror with Linearly Varying Thickness radially on Multiple Point Supports.....	36
2.2.4 Closed Form Solution for Thin Flat Mirror With Uniform Thickness.....	37

TABLE OF CONTENTS *continued*

	Page
2.2.5 Tapered Mirror with a Central Hole	38
2.2.6 Circular Light Weight Mirror	39
2.2.7 Circular Mirror with Cassegrain Hole on One or Two Axial Ring Supports	40
2.3 Analysis and Design of a Support System of a Primary Mirror using the Finite Element Method and Wavefront analysis	41
2.3.1 Specifications and Design Target	41
2.3.2 Handling Stresses in Primary Mirrors	42
2.3.3 Determination of Number of Support Points	44
2.3.4 Optimization Procedure	45
2.3.5 Preprocessor	45
2.3.6 Postprocessor	46
2.3.7 Effect of Finite Element Grid Pattern on the Fringe Analysis	46
2.3.8 Effect of Mesh Refinement on the Peak to Valley Displacement	47
2.3.9 Axial Support System	47
2.3.10 Radial Support System	49
2.3.11 Bellofram Supports	50
2.4 Frequency Analysis of the Primary Mirror	51
2.5 Summary	52
CHAPTER 3. OPTICAL SUPPORT STRUCTURE	104
3.1 Background	104
3.2 Trunnion Beam	105
3.3 Forward Truss Structure for the Four Meter Telescope	105
3.4 Summary	106

TABLE OF CONTENTS *continued*

	Page
CHAPTER 4. DESIGN OF THE PRIMARY MIRROR CELL, FORK, AND SECONDARY MIRROR	112
4.1 Background	112
4.2 Design of the Primary Mirror Cell.....	112
4.3 Design of the Fork	113
4.4 Analysis of Support System of a Secondary Mirror.....	114
4.5 Summary	116
CHAPTER 5. ANALYSIS OF THE TELESCOPE ASSEMBLY.....	130
CHAPTER 6. OPTIMIZATION PROCEDURES.....	134
6.1 Background	134
6.2 Proposed Optimization Procedures.....	136
6.3 Optimization of Mirror Support System Using Modal Frequencies.....	139
6.4 Summary	141
CHAPTER 7. CONCLUSIONS	151
GLOSSARY	153
LIST OF REFERENCES	155

LIST OF ILLUSTRATIONS

Figure	Page
1.1 Primary mirror technology	26
1.2 Most commonly used telescope mounts	27
1.3 Typical error budget distribution of the telescope image quality	28
1.4 Telescope orientation	29
1.5 Mirror support system - Lever with counter weight	30
1.6 Main components of an altazimuth telescope	31
2.1 (A) Circular plate on a ring of point supports	63
2.1 (B) Thickness variation model	63
2.2 (A) Mirror with linearly varying thickness	64
2.2 (B) Mirror with a central hole	64
2.3 (A) Meniscus mirror	65
2.3 (B) Finite element model of the meniscus mirror	66
2.4 Ray tracing and spot diagram	67
2.5 Diameter that encloses 80% energy	68
2.6 Finite element model for the handling stress analysis	69
2.7 Different handling methods	70
2.8 Contour plot and spot diagram for a three point support system	71
2.9 Contour plot and spot diagram for a six point (-Z) support system	72
2.10 Contour plot and spot diagram for a nine point (-Z) support system	73
2.11 Contour plot and spot diagram for a nine point (+Z) support system ...	74
2.12 Contour plot and spot diagram for a nine point (-Y) support system	75
2.13 Contour plot and spot diagram for a six point (+Z) support system	76

LIST OF ILLUSTRATIONS *continued*

Figure	Page
2.14 (A) Flow chart describing the optical performance evaluation procedure .	77
2.14 (B) Organization of program FRINGE	78
2.15 Different grid patterns generated by the preprocessor	79
2.16 Different grid patterns used in finite element analysis of mirrors.....	80
2.17 Three, six, and eighteen point support locations	81
2.18 Contour plot and spot diagram for a three point support system (zenith).....	82
2.19 Contour plot and spot diagram for a three point support system (horizon).....	83
2.20 Contour plot and spot diagram for a six point support system (zenith).....	84
2.21 Contour plot and spot diagram for a six point support system (horizon).....	85
2.22 Contour plot and spot diagram for an eighteen point support system (zenith)	86
2.23 Contour plot and spot diagram for an eighteen point support system (horizon).....	87
2.24 Contour plot and spot diagram for a sixty six point support system (zenith)	88
2.25 Contour plot and spot diagram for a sixty six point support system (horizon).....	89
2.26 Optimum support locations for the four meter mirror	90
2.27 Simple model for the vibration modes procedure.....	91
2.28 Zero leakage rolling diaphragm installed in a cylinder	92
2.29 Axial and radial support systems for the four meter meniscus mirror	93

LIST OF ILLUSTRATIONS *continued*

Figure	Page
2.30 Alternative scheme of supporting the mirror	94
2.31 Contour plot and spot diagram for mode 1	95
2.32 Contour plot and spot diagram for mode 2	96
2.33 Contour plot and spot diagram for mode 3	97
2.34 Contour plot and spot diagram for mode 4	98
2.35 Contour plot and spot diagram for mode 5	99
2.36 Contour plot and spot diagram for mode 6	100
2.37 Contour plot and spot diagram for mode 7	101
2.38 Contour plot and spot diagram for mode 8	102
2.39 Contour plot and spot diagram for mode 9	103
3.1 Different telescope truss geometries	111
4.1 Primary mirror cell and trunnion beam	124
4.2 Finite element model of the cell and OSS	125
4.3 Altazimuth fork	126
4.4 Finite element model of the fork	127
4.5 Secondary mirror for the four meter telescope	128
4.6 (A) Honeycomb mirror	129
4.6 (B) Meniscus mirror with equivalent thickness	129
5.1 Finite element model of the telescope assembly	133
6.1 Simple Truss for Optimization Procedure	147
6.2 Optimization of a Cantilever Beam	148
6.3 Optimization of a Simply Supported Beam	149
6.4 Model used for the modal frequencies procedure	150

LIST OF TABLES

Table	Page
1.1 Some large telescopes.....	24
1.2 Typical materials for mirror blanks.....	25
2.1 Primary mirror specifications.....	53
2.2 Handling stresses in the primary mirror.....	54
2.3 Effect of mesh refinement on the peak to valley displacement.....	55
2.4 Three ring support optimization (Zenith).....	56
2.5 Three ring support optimization (Horizon).....	57
2.6 Four ring support optimization (Zenith).....	58
2.7 Four ring support optimization (Horizon).....	59
2.8 Axial support system.....	60
2.9 Radial support system.....	61
2.10 Modal frequencies for plate and shell models.....	62
3.1 Primary and secondary mirror specifications.....	107
3.2 Frequencies and deflections of different telescope trusses.....	108
3.3 Mode shapes of the original structure.....	109
3.4 Mode shapes of the optimized structure.....	110
4.1 Mode shapes of the optimized cell structure.....	117
4.2 Total weight on the elevation axis.....	118
4.3 Mass moments of inertia on the elevation axis.....	119
4.4 Mode shapes of the optimized fork.....	120
4.5 Honeycomb mirror specifications.....	121

LIST OF TABLES *continued*

Table	Page
4.6 Material properties of the secondary mirror.....	122
4.7 (A) Gravity deflections of the secondary mirror with a three point support system (Zenith)	123
4.7 (B) Gravity deflections of the secondary mirror with a three point support system (Horizon)	123
4.8 (A) Gravity deflections of the secondary mirror with a six point support system (Zenith)	124
4.8 (B) Gravity deflections of the secondary mirror with a six point support system (Horizon)	124
5.1 Mode shapes of the optimized telescope.....	131
5.2 Gravity deflections (Horizon - Zenith)	132
6.1 Optimality criteria	142
6.2 Structural optimization of a truss using modal analysis	143
6.3 Structural optimization of a cantilever beam using modal analysis.....	144
6.4 Structural optimization of a simply supported beam using modal analysis.....	145
6.5 Optimization using modal frequencies	146

ABSTRACT

Structural analysis and design of a four meter class altazimuth telescope was performed using the finite element program MSC/NASTRAN. Optical performance of the mirror was evaluated using the program FRINGE. Structural and optical performance was optimized based on reduction of the root mean square (rms) wavefront deflections of the mirror surface and minimization of the self weight of the telescope using natural mode shapes of the finite element model.

A procedure to optimize the support locations for the primary mirror using the piston frequency from the free vibration analysis was proposed. Finite element models for the mirror were automatically generated by a special purpose pre-processor developed for this study. Optimized support locations and the support systems are presented for a four meter meniscus mirror. Preparation of an input data file for the optical performance evaluation program FRINGE from the NASTRAN structural deformation data was achieved using a post-processor which was developed for this specific case study. Procedures to achieve the optimum criteria are presented.

Analysis and design of mirror cell, secondary mirror, optical support structure, and fork are presented. Both static and free vibration analyses were performed on all the components of the telescope. Comparisons were made wherever approximate solutions were available. Also, primary mirror handling analysis, mesh refinement study, effect of grid pattern of the finite element model on the FRINGE analysis are presented.

CHAPTER 1

INTRODUCTION

1.1 Background

Most of the methods by which the physical constitution of the star systems studied require telescopes of large dimensions. As astronomers are concentrating their efforts to make more accurate observations in angular resolution, spectral resolution, and time resolution for varieties of brightness of celestial objects, the need for the large telescopes is increasing tremendously. To research the farthest reaches of the universe in time and in space even fainter objects need to be studied in detail. This requires the light collecting power which can be provided only by large telescopes. The efforts that have led to the construction of the large telescopes in use today have been rewarded by outstanding discoveries. Sometimes it is thought that the space telescopes are the future of astronomy as the disturbing effects of earth's atmosphere can be avoided. But, the cost of these space telescopes (US Space telescope – 1.5 Billion dollars) and the accessibility criteria encourages the development of ground based telescopes. Table 1.1 lists some ground based large telescopes. Also, a super giant telescope is very costly to operate. As the telescope becomes wider in its aperture, the quantity of light it collects increases in proportion to the square of the aperture. The primary mirror with a large diameter results in increased image resolution and increased optical power to the received signal, thus increasing the signal-to-noise ratio. The higher signal-to-noise ratio, in turn, results in the telescope pointing accuracy. However, when the ratio

of the thickness to aperture of the primary mirror material is the same as the conventional value, the weight of the primary mirror increases in proportion to the third power of the aperture. Because of this fact along with the pessimistic estimates of the image quality, a large array of small telescopes (3.5m - 5m) is preferable to the construction of a very large telescope ($\geq 10\text{m}$). The field committee report (Astronomy and Astrophysics for 1980's) of the United States National Academy of Sciences has expanded this line of argument still further, saying

“... telescopes in the 2m-5m class have furnished essential follow on observations and identifications of a multitude of objects discovered in other wavelength regions by spacecraft or complementary ground facilities. Such telescopes are essential for timely observation for transient phenomena, long term survey and surveillance program, general support of space astronomy”,

As most of the research departments in astronomy depend highly on the oversubscribed national telescopes such as U. S. 4- meter telescope, there is a tremendous need for a versatile, highly instrumented, high technology, simple and low weight 3.5m - 5m telescope. There are many technical problems remain unsolved and there is no general agreement concerning a design of a large telescope of this size. Thus design criteria for these telescopes has been a challenge for many engineers and scientists. The speed of data collection has been increasing enormously by technical breakthrough in the performance of detectors and in the automation of telescopes. For example, the Hale 5 meter telescope is now in equal in photon collecting power to a 30 meter telescope with 1950 style detection. Therefore, the technical advancement in the performance of telescopes certainly proved fruitful. But, the increase in the weight of the instruments directly effects the structural performance of the telescope and the image quality. So, there is a need for the research to improve the structural performance of the telescope to counteract the reasons mentioned above.

1.2 Primary Mirror Technology

The structural design approach for a large telescope depends largely on the primary mirror technology. For example it may be a single monolithic mirror or a segmented mirror or a set of monolithic mirrors each one being a primary mirror of a smaller telescope mounted on one single mount or on independent mounts as shown in the Figure 1.1. A monolithic mirror is bound to be the most reliable because of the relative simplicity of the support system compared with that of a segmented mirror. The meniscus mirror is preferred to the light weight honeycomb mirror for this size as it is cost effective. Also, the support system is much simpler for the meniscus mirror. Of the two available support systems active and passive, the actively supported mirror performs better than a passively supported mirror in imaging. The former offers an additional possibility of correction of forces in situ, that the passively supported mirror does not have. Wilson, Franza, and Noethe (1984) presented the basic principles and layout of the primary support of European Southern Observatory's 3.5 meter New Technology Telescope (NTT). They have designed the axial supports as passive supports with active modulation possibilities. A monolithic actively corrected primary mirror is the best choice in terms of reliability of operation and performance. Zerodur glass is chosen for its superior stiffness to weight ratio and thermal characteristics over the other materials used for the mirror blanks. Table 1.2 lists some of the typical thermal and mechanical properties of the materials used for the mirror blanks.

Thickness of the mirror also plays a great role in the selection of the support system for solid substrates. Mirrors with diameter to thickness ratios between 10 and 20 are common. But, if the ratio is more than 20, the support system becomes more complicated in order to hold the mirror in the required optical shape regardless of the deformation of the supporting cell structure. Ballio, Contro, Poggi, and

Citterio (1984) used finite elements to design the active support system for the ESO's one meter meniscus mirror with the diameter to thickness ratio greater than 20.

1.3 Telescope Mounting

Telescope mounting is another critical issue which is selected according to the mirror technology. For segmented mirrors the altitude-altitude (alt-alt) mounting shown in Figure 1.2 is suitable. However, altitude-azimuth (alt-az) mounting can be used also. Alt-az mounting, which is standard for modern telescope designs, combines compactness, low mass and vertical symmetry is suitable for the monolithic mirrors. The initial main drawback of this mounting, which is the need for driving two axes, is no longer a problem. The forbidden zone around the zenith, where tracking becomes impossible, has in practice never been a real difficulty. Both alt-az and alt-alt mountings are shown in the Figure 1.2. Alt-Az mounting was chosen to provide the benefits of reduced weight, cost, and lower and repeatable deflections which lead to higher pointing accuracy. For example, the overall weight of the William Herschel telescope is 190 tons (compared with about 360 tons for equatorially mounted telescope). The structural benefits of an altazimuth mounting with its freedom from large bending moments were very evident during the course of this study.

Most of the large telescopes (e.g., 4.2 meter Herschel telescope, 7.5 meter Texas telescope, 10.0 meter UC Berkely telescope, US 15.0 meter telescope, Crimean 25.0 meter telescope) intend to use alt-az mounts because of the substantial cost saving associated with their construction as compared to other mounts.

Telescope technology has burgeoned with new innovations over the past few years. But, every innovation to be exploited must have a clear scientific purpose

or at the minimum, lead to simplification of design, construction, or maintainance. Otherwise the risks can not be justified. Stated in the Report of the Astronomy Survey Committee (1982), the University of Michigan's proposal for 2.4 meter telescope, "... for a 2.4 meter telescope, the alt-az mount offers no significant advantages but some disadvantages such as field rotation and zenith dead zone...". There are certain choices in the design of 4 meter class telescopes that can add enormously to its future scientific productivity without major price penalty. The alt-az mount is a case in point. The important criterion for the suitability of the mounting technique is the performance level required. Balick, Mannery, and Seigmund (1983) have proposed some design concepts of a precision, versatile, and inexpensive 4 meter class telescope. They outlined a general philosophy and preliminary concepts for the design.

1.4 Design Criteria and Error Budget

Large mirrors are susceptible to deformations due to internal stresses, temperature gradients, and thermal property inhomogeneties. Changes in orientation of the optic during use are also of significance, especially in regard to gravitational and thermal effects.

Design problems for large telescopes due to self weight and additional weight from the instruments have been a challenge to engineers and scientists. The structural deflections of the mirror in different orientations of the telescope are the criteria for the optical system. Imposed error budget on optical performance is the driving parameter behind the methodology applied during the design process. Structural performance of each component of the telescope is studied and optimized before evaluating the optical performance of the assembled structure. Based on the imposed error budget and the design requirements, such as the root mean square

wavefront variation over the optical surface, peak-to-valley deflection, and the 80% of the encircled energy criterion, the improvements are made. Typical error budget distribution of the telescope image quality is shown in Figure 1.3. The next generation of large optical telescopes will have thin, short focus primary mirrors to reduce the weight and cost of the telescope.

1.5 Primary Mirror Support

Primary mirror support system is the most critical part of the structural design of the telescope. Two principal causes for mirror deformation are the gravity and temperature non-uniformities. Couder (1931) studied the gravitational and thermal deflections of large astronomical mirrors. More recently, the entire field of support and testing of astronomical mirrors was reviewed in a symposium reported by Crawford, Meinel, and Stockton (1968). Several specific mirror supports are described by Pearson (1980).

Telescope orientation during operation significantly effects the gravity deflections. Two extreme cases commonly dealt with in optical design are the ZENITH position and the HORIZON position with the optical axis as shown in Figure 1.4. Selke (1970,1971) proposed closed form solutions for gravity deflections of flat mirrors with diameter to thickness ratio less than 10 on one or two ring continuous supports at optimized radial locations using thick plate theory. Niedenfuhr, Leissa, and Gaitens (1965) have proposed a method of analyzing shallow shells of revolution supported elastically on concentric ring supports. The results were compared with the classical elasticity solutions. Grundmann (1983) investigated different types of passive support systems suitable for a thin meniscus type mirror in a 3 meter optical telescope. The diameter to thickness ratio in this case is 25. Nelson, Lubliner, and Mast (1982) have described the general concepts, scaling laws, and given some

specific examples (infinite plates and circular flat plates) for supporting thin plates on a number of discrete points. But for any real mirror support system, an analysis that includes the detailed shape (central hole, variable thickness) and curvature is essential. Richard and Williams (1985) have used finite element methods to analyze large mirrors and their support structures. Ray and Chang (1986) have analyzed an 8 meter class cellular primary mirror using a commercially available finite element program. An analytic approach for a circular plate on multipoint support was developed by Williams and Brinson (1974). Schwesinger (1954) developed a theoretical approach for evaluating the optical effect of flexure in vertically mounted (HORIZON case) precision mirrors. A parametric design study of light weight mirror shapes with various support conditions was performed by Cho (1989). Procedures and modeling techniques to achieve the optimum (the lightest and stiffest mirror shape) were addressed in his report. Concave flat back, double concave, single arch, double arch, solid SXA, and foam core mirrors were some of the mirrors he considered in his study, for the improvement in the optical performance. Malvick (1968,1972) utilized dynamic relaxation technique to analyze a large mirror with a central hole, flat back, and spherically dished front surface under the gravity load. Using this technique, the deformation of the optical surface can be found for any proposed support system and any desired orientation of the mirror. This technique is an iterative scheme and requires significant CPU time.

Vukobratovich, Iraninejad, Richard, Hansen, and Melugin (1982) analyzed light weight mirrors in two different orientations , HORIZON and ZENITH, and evaluated the optical performance of the mirrors. Kowalskie (1978), Yoder (1986), and Vukobratovich (1988) have discussed various mounting techniques for small and large horizontal axis and vertical axis thick mirrors. Bliss (1966), Grundmann (1983), Wilson, Franza, and Noethe (1984), Hill (1990), and Kodaira (1990) have

described the active and passive support mechanisms for large mirrors. For thin mirrors, the stiffness is so small that severe force accuracy is required. Therefore, a conventional mirror support system such as lever with counterweight is not applicable as shown in Figure 1.5. Itoh (1987) presented a detailed design of support mechanism for the 7.5 meter Japanese National Large Telescope's thin mirror. Meier (1988) proposed a self balancing hydraulic support system superposed by an active correction system for a 2.7 meter thin meniscus mirror. The optimum support locations are usually determined using iterative methods. Structural deflections of the optical surface are computed first using a classical solution or computational methods such as finite element method. Then, the optical performance is evaluated from the structural data. A Number of studies have been made to quantify the structural data and evaluate the optical performance in terms of optical aberrations such as piston, tilt, spherical aberration, and coma. Anderson (1982) developed the program FRINGE for use in wide variety of optical tests and fabrication problems. Program FRINGE is described in appendix B. Cho (1989) used program FRINGE to perform parametric studies on light weight mirrors. Bella (1987) developed a method to least-mean square fit Zernike polynomials to optical component deformation from finite element structural analysis. This procedure uses a pre-processor to a commercially available finite element package MSC/NASTRAN and allows the polynomial fit to be calculated during dynamic response as well as static loading. Both the authors used Zernike polynomials to describe optical fringe analysis and the wavefront errors. Even though there are several optimization programs available to solve optimal control problems, they can not be used to solve the optimization problems in mirror support design because of the many design parameters involved in the optical system. For this reason, finite element methods and fringe analysis are extensively used in the mirror design, mirror support design, and telescope design areas.

1.6 Objectives

The main objective of this research is to design a stiff, low weight telescope structure for a meniscus mirror with altazimuth mounting. The preliminary optimization of the mirror support system is an iterative process with NASTRAN and FRINGE analyses and can be lengthy. A simplified procedure is proposed and investigated. Also, a new procedure which optimizes the stiffness and weight of a structure is proposed and will be applied to several telescope structures to demonstrate the effectiveness of the algorithm.

1.7 Organization

In this research, analysis and design of a 4 meter class altazimuth mount telescope was performed. The primary mirror is a thin $f/1.5$ mirror with a diameter to thickness ratio of 35. Improvements in the optical performance were based on optimizing the support locations of the mirror, minimizing the overall weight of the telescope using modal analysis, and imposed optical constraints considering both the ZENITH and HORIZON cases. The optical performance of a four meter thin meniscus mirror (4.5 inches thick) is optimized for its best RMS and 80% energy criteria using the finite element package MSC/NASTRAN and optical surface evaluation program FRINGE. Contour plots, energy plots, and spot diagrams are included for the optimized support configuration. Also, handling stress analysis was performed for the primary mirror. Natural frequency analyses were conducted for the mirror and other structural components of the telescope. Chapter 2 presents the primary mirror support optimization. Shown in Figure 1.6 are the important components of a four meter class altazimuth telescope. Optimization of the Optical Support Structure (OSS) was based on the minimization of the weight using a

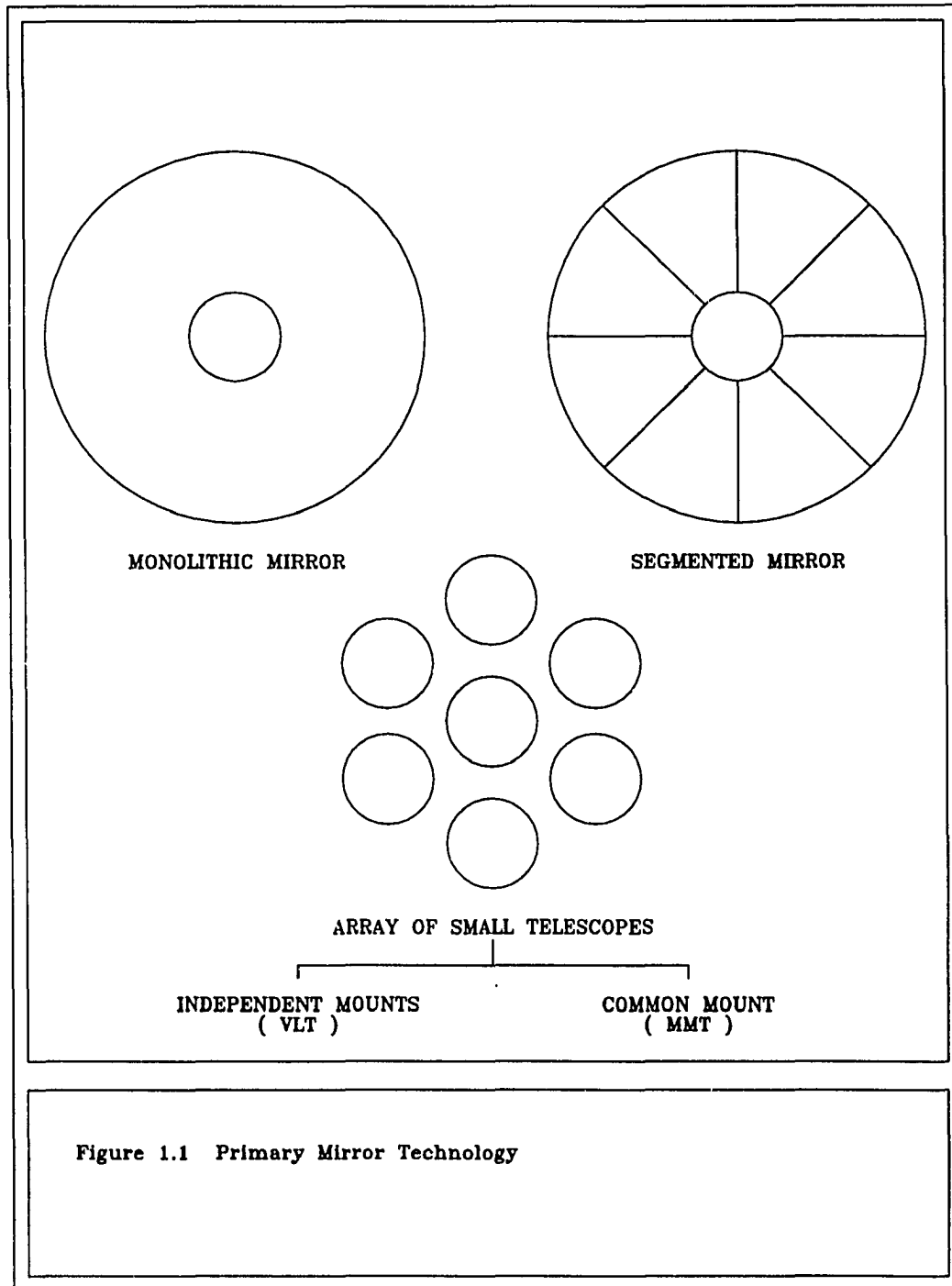
modal analysis algorithm. This procedure is described in Chapter 6. In Chapter 4, vibrational analyses of the primary cell, analysis and design of the fork, and analysis of support system of a secondary mirror are presented. In Chapter 5, finite element analysis of the complete telescope is presented. Chapter 7 summarizes the results and presents the conclusions.

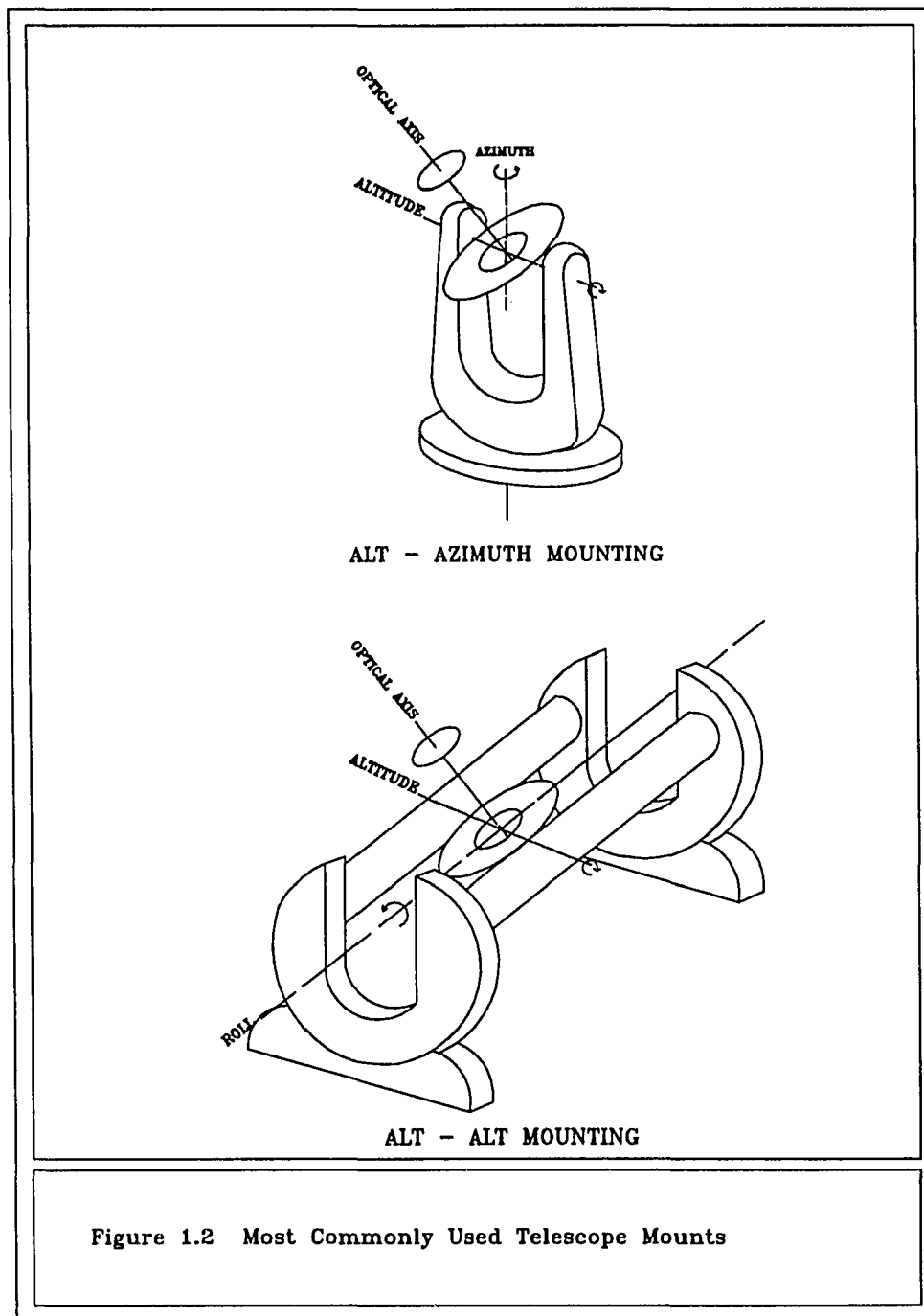
TABLE 1.1 SOME LARGE TELESCOPES

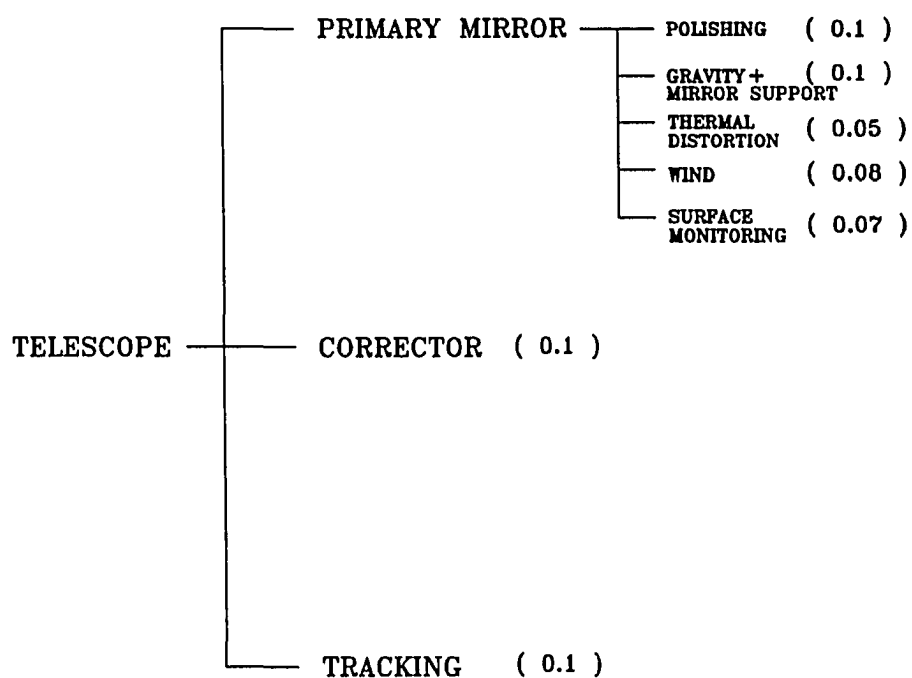
TELESCOPE	SIZE	DESCRIPTION
HALE	5.0m	Located on Mt. Palomar In Operation
SHANE	3.0m	At Lick Observatory In Operation
NTT	3.5m	New Technology Telescope At European Southern Observatory In Operation
VLT	15.0m	Very Large Telescope At European Southern Observatory Proposed
SUNDAI	0.75m	Altazimuth Mount In Operation
MMT	6 × 1.8 m	Multiple Mirror Telescope on Mt. Hopkins In Operation
LEST	2.4m	Large European Solar Telescope
COLUMBUS	11.0m	In The Design Phase To be built on Mt. Graham
TMT	10.0m	Keck Ten Meter Telescope (Segmented Mirror) University Of California Under Construction
JNLT	7.5m	Japanese National Large Telescope Proposed
UTT	7.6m	University of Texas Telescope Proposed

TABLE 1.2 TYPICAL MATERIALS FOR MIRROR BLANKS

Material	Young's Modulus (E , 10^6 lb/in^2)	Poisson's Ratio (ν)	Coefficient Of Thermal Expansion (α , $10^{-6}/^\circ F$)	Weight Density (ρ , lb/in^3)
Zerodur	13.2	0.21	0.03	0.092
Fused Silica (Corning 7940)	10.7	0.17	0.32	0.092
Aluminum (6061-T6)	10.0	0.33	13.0	0.098
Borosilicate	9.86	0.20	1.77	0.080
Silica (ULE)	9.57	0.17	0.03	0.079
Invar	21.0	0.30	0.55	0.293
Stainless Steel (321)	28.0	0.30	9.30	0.290
SXA	16.0	0.30	7.30	0.100
Titanium (Ti-6Al-4V)	16.5	0.31	5.30	0.160



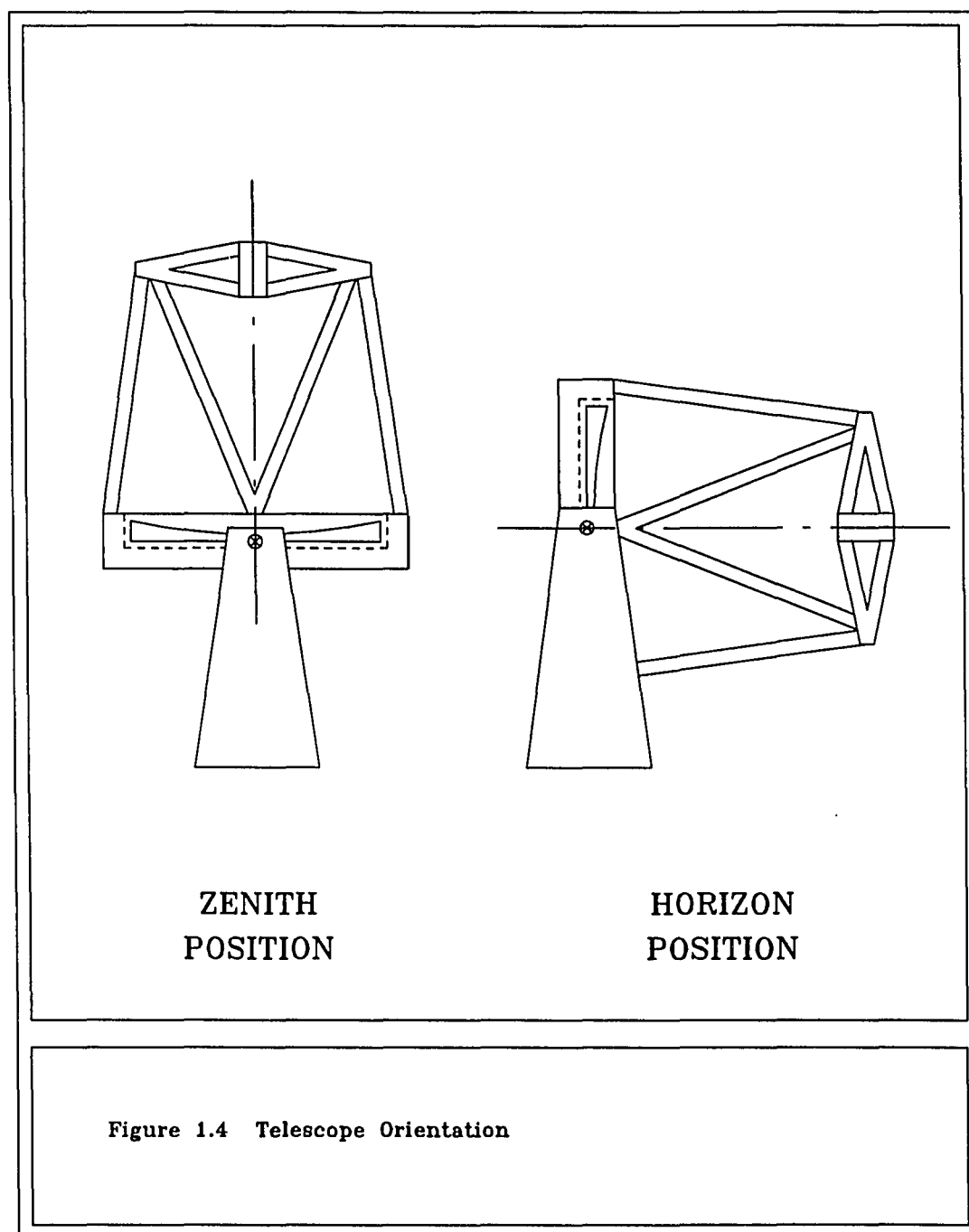




Note : Values shown in the brackets are rms deflections in waves.

$$1 \text{ Wave} = 0.6330 \times 10^{-6} \text{ m}$$

Figure 1.3 Typical Error Budget Distribution of the Telescope Image Quality



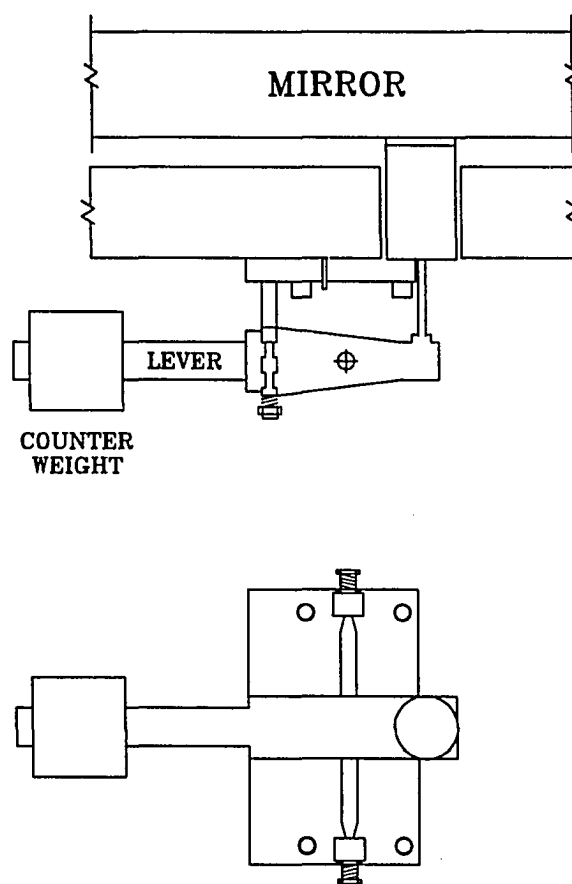
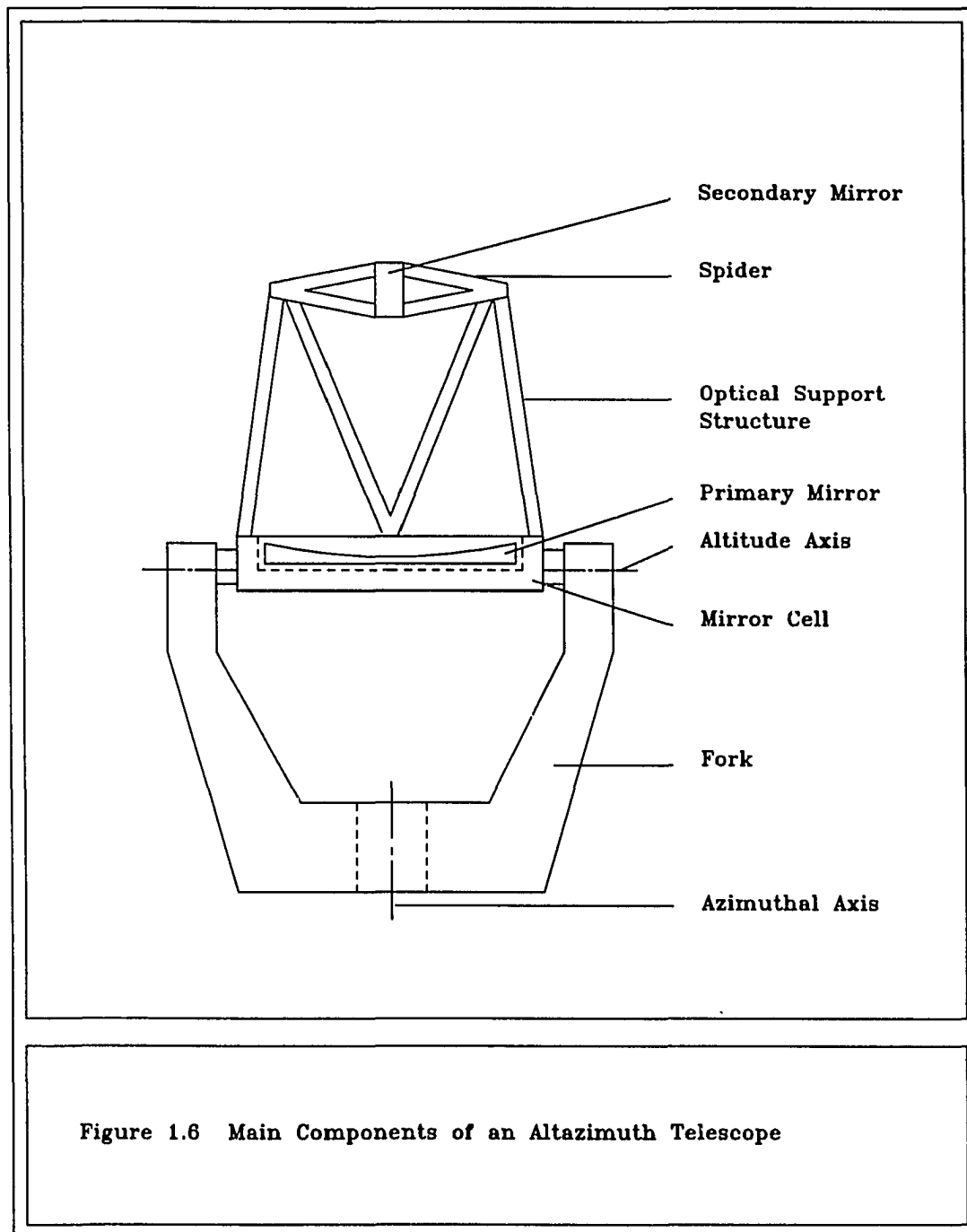


Figure 1.5 Mirror Support System - Lever With Counter Weight



CHAPTER 2

PRIMARY MIRROR

2.1 Background

The surface deflection of a large thin mirrors due to gravity is an important design consideration for a large telescope. High quality telescopes typically require that the mirror deformations be limited to a small fraction of the wavelength of the light ($\text{rms} = 0.05 \text{ to } 0.20 \lambda$, where λ is the design wavelength of the light) for the telescope.

The solutions expressed in an analytical form for general support patterns for various mirror shapes (with curvature, with and without Cassegrain hole, with and without variation in the thickness, etc.,) are very valuable and allow rapid evaluation of different support geometries without numerical analysis. Theoretical models based on classical thin plate theory were developed by several researchers in the past. But, most of the theoretical models were developed for the mirrors pointing zenith, i.e., gravity in the direction normal to the aperture. A mirror support system must be able to carry the load both axially and radially as the telescope points to different zenith angles. So, the existing theoretical and closed form solutions do not cover entire problem domain and thus the finite element analysis is still a very useful tool in the design of a support system for a large mirror. In the following section, brief descriptions of several theoretical models and closed form solutions are presented.

2.2 Theoretical and Closed form Solutions

Seven solutions which are relevant to this study are presented in this section.

They are:

- 2.2.1) Classical theory of thin circular plate
- 2.2.2) Deflections of a circular plate on a ring of point supports
- 2.2.3) Deflections of a circular mirror with radially varying thickness on multiple support points
- 2.2.4) Thin flat mirror with uniform thickness
- 2.2.5) Tapered mirror with a central hole
- 2.2.6) Lightweight circular mirror
- 2.2.7) Circular mirror with central hole on axial supports of one ring and two rings

2.2.1 Classical Theory of thin flat circular plate loaded transversely:

Classical theory of thin flat transversely loaded plates from Timoshenko and Krieger (1970) is summarized in this section.

$$\nabla^4 w = \frac{q}{D} \quad (2.1)$$

Where, ∇^4 is the operator given by

$$\begin{aligned} \nabla^4 &= \left(\frac{\partial^2}{\partial x^2} + \frac{\partial^2}{\partial y^2} \right) \left(\frac{\partial^2}{\partial x^2} + \frac{\partial^2}{\partial y^2} \right) \\ &= \left(\frac{\partial^2}{\partial r^2} + \frac{1}{r} \frac{\partial}{\partial r} + \frac{1}{r^2} \frac{\partial^2}{\partial \theta^2} \right) \end{aligned}$$

w = Transverse deflection of the plate

q = Transverse load per unit area

D = Flexural rigidity of the plate

For a given boundary condition, i.e., mounting arrangements, the maximum deflection is proportional to $\frac{q}{D}$. For transversely loaded plates, the load per unit area q is proportional to the weight per unit area. The flexural rigidity D is the stiffness per unit perimeter of a representative subsection of the plate. For solid plate,

$$D = \frac{Eh^3}{12(1 - \nu^2)}$$

Where,

E = Young's Modulus

ν = Poisson's Ratio

h = Thickness of the plate

Equation 2.1 for uniformly varying thin flat mirror can be written as,

$$\nabla^2 (D \nabla^2 w) = q \quad (2.2)$$

2.2.2 Deflections of a circular mirror on a ring of point supports:

The deflections of thin, constant thickness plate are of great interest in optical support systems. Nelson, Lubliner, and Mast (1982) derived a solution for the deflections of a circular plate on a ring of point supports for a uniformly loaded plate of a radius a and flexural rigidity D , with total load of P , is supported by k point supports loaded at $r = b$, $b = \beta a$, and $0 < \beta < 1$. This model is illustrated in Figure 2.1 (A).

$$\theta = \frac{2j\pi}{k} \quad j = 1, 2, \dots, k$$

The deflection of the plate $w(r, \theta)$ is governed by the differential equation

$$D \nabla^4 w = \frac{-P}{\pi a^2} + \frac{P}{k} \sum_{j=1}^k \frac{\delta(r-b)}{b} \delta \left[\theta - \frac{2j\pi}{k} \right]$$

The Fourier series for $\sum_{j=1}^k \delta \left[\theta - \frac{2j\pi}{k} \right]$ is of form

$$\frac{a_0}{2} + \sum_{m=1}^{\infty} a_m \cos(km\theta)$$

with,

$$a_m = \frac{1}{\pi} \sum_{j=1}^k \int_0^{2\pi} \delta \left[\theta - \frac{2j\pi}{k} \right] \cos(km\theta) d\theta = \frac{k}{\pi}$$

hence the loading is

$$-\frac{P}{\pi a^2} + \frac{P}{2\pi b} \delta(r-b) + \frac{P}{\pi} \frac{\delta(r-b)}{b} \sum_{m=1}^{\infty} \cos(km\theta)$$

Assuming the deflection has the form

$$w(r, \theta) = \sum_{m=0}^{\infty} w_m(r) \cos(km\theta) \quad (2.3)$$

where w_0 is governed by

$$\frac{1}{r} \frac{d}{dr} \left\{ r \frac{d}{dr} \left[\frac{1}{r} \frac{d}{dr} \left(r \frac{dw}{dr} \right) \right] \right\} = -\frac{P}{\pi a^2} + \frac{P}{2\pi b} \delta(r-b)$$

i.e., w_0 is just the deflection of a plate supported on a ring of radius b . w_0 is obtained by superposing deflection of simply supported plates that are uniformly loaded and ring loaded, with loads equal and opposite. For $m \geq 1$, we have

$$\left[\frac{d^2}{dr^2} + \frac{1}{r} \frac{d}{dr} - \frac{k^2 m^2}{r^2} \right]^2 w_m = \frac{P}{\pi b D} \delta(r-b) \text{ for } r \neq b$$

The solution takes the form (with $n=km$)

$$w_m(r) = A_m r^n + B_m r^{n+2} + C_m r^{-n} + D_m r^{-n+2} \quad (2.4)$$

Where,

$$\begin{aligned}
 A_m a^n &= \frac{Pa^2}{8\pi D} \frac{\beta^n}{3+\nu} \left[(1-\nu) \left(\frac{1}{n-1} - \frac{\beta^2}{n} \right) + \frac{8(1+\nu)}{n^2(n-1)(1-\nu)} \right] \\
 B_m a^{n+2} &= -\frac{Pa^2}{8\pi D} \frac{\beta^n}{3+\nu} \left[(1-\nu) \left(\frac{1}{n} - \frac{\beta^2}{n+1} \right) \right] \\
 C_m a^{-n} &= -\frac{Pa^2}{8\pi D} \frac{\beta^{n+2}}{n(n+1)} \\
 D_m a^{-n+2} &= \frac{Pa^2}{8\pi D} \frac{\beta^n}{n(n-1)}
 \end{aligned}$$

Thus the solution to (2.3) can be obtained. It is given by equation (2.5) in (2.4), and (2.4) in (2.3).

2.2.3 Thin flat circular mirror with linearly varying thickness radially on multiple point supports:

Wan, Angel, and Parks (1989) modified the above procedure by Nelson to accomodate the thickness variation along the radius. Their procedure is described briefly in the following paragraph.

For a non flat mirror the flexural rigidity D is no longer a constant, so the equation to solve for the deflection becomes,

$$\nabla^2(D\nabla^2 w) = P$$

An approximation was made to divide the mirror in to several cylinders with constant thickness or height within each cylinder as shown in the Figure 2.1 (B), so that the flexural rigidity D is constant, so equation (2.3) can be used to solve for the displacements in each cylinder.

$$w_{0i} = -\frac{1}{f_i} \left[\frac{q_i}{8(1-\nu_0^2)} r^4 + \frac{1}{4} A_i r^2 (\ln r - 1) + \frac{1}{4} B_i r^2 + C_i \ln r + F_i \right]$$

$$w_{mi}(r) = \frac{1}{f_i}(A_m r^n + B_m r^{n+2} + C_m r^{-n} + D_m r^{-n+2})$$

The above equation ignores the scaling factor $\frac{Pa^2}{8\pi D}$, The factors q_i and f_i are defined as

$$q_i = \frac{h_i}{h} \text{ and } f_i = \frac{h_i^3}{h^3}$$

h_i and h are the mirror thickness at the i th cylinder and at the center. r_0 is the radius of the central hole in terms of the fraction of mirror radius. The terms q_i and f_i take into account the different self-weight and flexural rigidity of different cylinders.

2.2.4 Closed form solution for thin flat mirrors with uniform thickness

Nelson (1982) has developed expressions for a optimum multipoint supports. For the root mean square deflection (δ_{rms}) for an N point support is given as

$$\delta_{rms} = \gamma_n \left(\frac{\rho h}{D} \right) \left(\frac{\pi r^2}{N} \right)^2 \left[1 + 2 \left(\frac{h}{u} \right)^2 \right]$$

Where,

γ_N = Constant depending on the support configuration

ρ = Density

D = Flexuaral rigidity = $\frac{Eh^3}{12(1-\nu^2)}$

r = Radius of the mirror

h = Mirror thickness

ν = Poisson's ratio

E = Young's Modulus

u = Support effective length = $\frac{\gamma}{\sqrt{N}}$

Then the peak-to-valley deflection (δ_{pv}) is given by

$$\delta_{pv} = K \delta_{rms}$$

where K is the support constant. Note that, this solution is for mirrors without a central hole. A central hole can cause errors of up to 140%. A table for the constant K for different configurations is given in the paper.

2.2.5 Tapered mirror with a central hole

Most Cassegrainian mirrors supported along the central hole are designed for deflection tolerances using the theory for solid, constant thickness plates. Where tolerances are critical, the mirror is usually made thicker, thereby reducing the deflection, but also increasing the weight of the mirror. Weight can be reduced by using a honeycomb design. However, manufacturing problems result because of the inherent complexity. To circumvent the disadvantages of excessive weight of solid, constant thickness design and the complexity of the honeycomb design, a lightweight, yet simple design would be a solid mirror of linearly varying thickness, decreasing in thickness from center to the outer edge. Because of linearly varying thickness may provide the best solution under combined deflection and weight restraints, a design basis is required. Prevenslik (1968) used the small deflection theory and developed a closed form solution for mirror with linearly varying thickness for fixed and simply supported boundary conditions along the central hole. This variable thickness model is shown in the Figure 2.2 (A).

The maximum deflection w_{max} of the variable thickness mirror given by

$$w_{max} = K \frac{8(1-x_1)^2}{27x_2^4} \frac{\rho r_2^4}{E h_1^2}$$

where K is a deflection coefficient. The deflection coefficients for simply supported and conditions were presented in the paper.

x_1 = Inner dimensionless radius = $\frac{r_1}{a}$

x_2 = Outer dimensionless radius = $\frac{r_2}{a}$

r_1 = Inner radius

r_2 = Outer radius

ρ = Density

E = Young's modulus

h_1 = Thickness at inner radius

2.2.6 Circular light weight mirror

Several researchers have worked extensively on the lightweight mirrors. Barnes (1969,1972), Pepi (1987), and Sheng (1988) have developed closed form equations to compute self weight deflections of light weight mirrors. Barnes developed an approximate expression for the combined bending and shear deflections for a cored mirror configuration. Pepi introduced a closed form solution which estimates the self weight deflections of a light weight mirror. It is given as

$$w_{max} = \frac{Cqr_0^4}{Et_m^3}$$

Where,

q = Uniform load per unit area

C = Pepi's Coefficient

t_m = Modified thickness for the honeycomb structure

$t_m = t$ for a solid mirror

r_0 = Radius of the mirror

E = Young's modulus

2.2.7 Circular mirror with Cassegrain hole on one or two axial ring supports

To obtain an idea of the effect of a Cassegrain (central) hole, Pearson (1968) used a flat circular plate on one or more rings for support and obtained the midplane deflection of the mirror. Shown in Figure 2.2 (B) is this model.

For a mirror with the hole and on two rings of supports, the maximum deflection is given as

$$w = K \left(\frac{a^4}{h^2} \right) \left[f_1 + M f_2|_{\xi_1} + (1 - M) f_2|_{\xi_2} \right]$$

where,

$$K = \frac{\delta g}{64 B}$$

δ = Density

g = Gravitational Constant

$$B = \frac{E}{12(1-\nu^2)}$$

E = Young's modulus

ν = Poisson's ratio

$$\xi = c/a$$

$$\alpha = b/a$$

$$\rho = r/a$$

$$\begin{aligned} f_1 &= (1 - \rho^2) \left[\rho^2 + 2 \left(\frac{3 + \nu}{1 + \nu} \right) \alpha^2 - \frac{8\alpha^4 \log_e \alpha}{1 - \alpha^2} - \left(\frac{5 + \nu}{1 + \nu} \right) \right] \\ &\quad + 8 \log_e \rho \left[\alpha^2 \rho^2 + \frac{1}{2} \left(\frac{3 + \nu}{1 - \nu} \right) \alpha^2 + \left(\frac{1 + \nu}{1 - \nu} \right) \frac{2\alpha^4 \log_e \alpha}{1 - \alpha^2} \right] \\ f_2 &= (1 - \xi^2) \left[4 \left(\frac{3 + \nu}{1 + \nu} \right) - 4 \left(\frac{1 - \nu}{1 + \nu} \right) \rho^2 - 8\alpha^2 - 8\alpha^2 \log_e \rho \right] \end{aligned}$$

$$\begin{aligned}
& + 8 \log_e \xi \left[\xi^2(1 - \alpha^2) + \rho^2 - \alpha^2 + 2 \left(\frac{1 + \nu}{1 - \nu} \right) \alpha^2 \log_e \rho \right] \\
& \quad \text{for } \alpha \leq \rho \leq \xi \\
f_2 = & (1 - \rho^2) \left[4 \left(\frac{3 + \nu}{1 + \nu} \right) - 4 \left(\frac{1 - \nu}{1 + \nu} \right) \xi^2 - 8\alpha^2 - 8\alpha^2 \log_e \xi \right] \\
& + 8 \log_e \xi \left[\rho^2(1 - \alpha^2) + \xi^2 - \alpha^2 + 2 \left(\frac{1 + \nu}{1 - \nu} \right) \alpha^2 \log_e \xi \right] \\
& \quad \text{for } \xi \leq \rho \leq 1
\end{aligned}$$

where M is the fraction of the total mirror weight supported on the inner ring at ξ_1 .

2.3 Analysis and Design of Support System of a Primary Mirror using the Finite Element Method and Wavefront Analysis

2.3.1 Specifications and Design Target

A four meter mirror with focal ratio of 1.5 ($f/d = 1.5$, where, f = focal length, d = diameter of the mirror) with a passive support system was considered for optimization. The primary mirror is treated as a thin shallow shell as shown in the Figure 2.3 (A). The geometry and material properties are shown in the Table 2.1. A high image quality of 0.1 arcsecs to 0.2 arcsecs (diameter that encloses the 80% energy) is the target for this four meter altazimuth telescope. The error budget for the primary mirror support is set at 0.05 arcsecs. The limit on rms deflections is set at 0.1 waves. Demonstrated in Figure 2.4 is how the spot diagram is obtained. Shown in Figure 2.5 is the diameter that encloses 80 % of the energy. Error analysis has been made mainly for the primary mirror. The gravitational deformations were computed by the finite element program MSC/NASTRAN and the optical performance was evaluated by the program FRINGE. Quadrilateral isoparametric plate bending elements were used to model the mirror.

2.3.2 Handling Stresses in Primary Mirrors

The primary mirror experiences several different handling stresses during fabrication, installation, and use. Lifting the mirror blank out of the mould, transportation to the shop, lifting and turning the mirror for the final figuring are only a few of the handling operations. Material properties and the structure of the mirror totally determine the amount of the risk involved in handling.

The type of risk is different for glass mirrors when compared to metal mirrors. For metal mirrors, the risk of permanent deformations that could occur if the micro yield strength (MYS) is exceeded. It is reported by European Southern Observatory (1988) personnel that a maximum stress of 50% of MYS is considered appropriate to avoid any permanent deformations. However, for glass, which in theory is perfectly elastic up to the point of fracture, the situation is more complex. The maximum stress value corresponding to the fracture can not be easily determined because it depends on several factors such as the surface quality and the dimensions of the surface under stress. A practical limit of 500 psi is recommended for handling stresses, although a higher stress for short period of time is unlikely to produce a fracture. The limit for the maximum stress is usually set at 750 psi for silica.

For a 4.5 inch thick Zerodur meniscus mirror blank a handling stress analysis has been evaluated for three different configurations, namely: lifting at three points, lifting in a carrying frame where the mirror is held at the outer and inner edge, and upside down turning in a frame with a 2×9 axial pads and a radial support belt at the outer edge. The finite element model shown in the Figure 2.6 was used for the stress analysis.

Shown in Figure 2.7 are the different handling methods. Shown in Figure 2.8 through Figure 2.13 are the contours and spot diagrams for the various handling

methods. A summary of the results of these analyses is presented in the Table 2.2, which lists different support configurations, the maximum peak-to-valley deformations that occur during the handling and the maximum equivalent stress (σ_e) which is given by the relation:

$$\sigma_e^2 = \frac{1}{\sqrt{2}} [(\sigma_1 - \sigma_2)^2 + (\sigma_2 - \sigma_3)^2 + (\sigma_3 - \sigma_1)^2]^{\frac{1}{2}}$$

Where, σ_1, σ_2 , and σ_3 are the principal stresses. The analysis is conservative because the load introduction into the mirror is considered to be made by point or knife edge supports. The use of pads will significantly reduce the stress levels in the mirror.

Therefore, the maximum stresses calculated with conservative point support approach are well below the 500 psi limit for Zerodur glass. However, necessary care has to be taken when specifying allowable additional loads, i.e., by impact, especially for the three point support case of the mirror. For transportation, the load can be uniformly spread over the mirror surface so that larger accelerations can be applied.

2.3.3 Determination of Number of Support Points

To determine the number of support points which are necessary to keep the rms error within an allowed budget, the following equation relating the parameters, the rms of the wavefront aberration, the number of supports (N), and the thickness (h) of the thin meniscus mirror is used.

$$rms \propto \frac{1}{(hN)^2}$$

Since h is not a variable in this model,

$$rms \propto \frac{1}{N^2}$$

$$\begin{aligned}
 N &\propto \frac{1}{\sqrt{rms}} \\
 N &= \frac{K}{\sqrt{rms}} \quad (2.3.3.1)
 \end{aligned}$$

Where, K = Constant, dependent on the material properties, thickness, etc.

Finite element analysis was made with three different support topologies. They were 3, 6, and 18 point support systems. The rms values were 39.336, 10.178, and 1.073 waves, respectively, for the zenith loading case. Using equation 2.3.3.1, K values for these three cases were calculated to be 18.81, 19.14, and 18.65, respectively. An approximate value of 19 was selected. The total number of support points to yield an rms value of 0.1 waves was then

$$N = \frac{K}{\sqrt{rms}} = \frac{19}{\sqrt{0.1}} = 60.08$$

Therefore at least 60 supports are estimated to yield an rms value of 0.1 waves with gravity in the direction normal to the aperture.

2.3.4 Optimization Procedure

A procedure to evaluate the optical performance of the meniscus mirror due to the effects of gravity has been done in a sequential manner as shown in the flowchart in Figure 2.14 (A) and (B). The finite element model of the mirror was created by a special purpose preprocessor for the finite element package NASTRAN. Finite element analysis was done on a Data General minicomputer model MV10000. A command file was then created for the program FRINGE. This file contains the information about the mirror geometry and the output required. Then FRINGE was run with the structural deformations as input data on CDC CYBER 175 and a micro computer IBM PS2. The rms value of the deformations of the optical surface from the output data was compared with the error budget. The above procedure

was repeated until the rms error was brought down to the 0.1 wave limit. The above procedure was repeated for the horizon pointing case also.

2.3.5 Preprocessor

A special purpose preprocessor was developed to generate the mesh automatically for three different grid patterns. These are:

- 1) Triangular grid pattern, Type 1
- 2) Triangular grid pattern, Type 2
- 3) Quadrilateral grid pattern

In case of quadrilateral grid pattern, the program gives the user a choice to generate the mesh automatically or input the radial distances of the nodal rings in a sequential manner. Examples for all three grid patterns are presented in the Figure 2.15. This special purpose preprocessor can generate circular mirror with and without holes, for the finite element program MSC/NASTRAN. Nodal points, element connectivity and other data such as material properties, solution type etc., is written in the user specified file. The input parameters for this preprocessor are:

- a) Inner and outer diameters of the mirror
- b) Radius of the curvature
- c) Number of nodes on the perimeter
- d) Material properties
- e) Solution type (gravity analysis or modal analysis)

2.3.6 Postprocessor

A simple postprocessor was developed to plot the undeformed, deformed plots of the finite element model. This program can also be used as preprocessor to check the geometry of the model before the analysis. For optical design purposes,

the wavefront aberrations such as tilt, defocus, coma, spherical aberrations etc., were computed using program FRINGE. A detailed description of the program FRINGE is given by Anderson (1982).

2.3.7 Effect of the Finite Element Grid Pattern on the FRINGE analysis

In the wavefront analysis using FRINGE, data from a mesh of equilateral triangles yields the lowest wavefront aberration for a given density of support points. In actual practice, the support points of the mirror are placed on concentric circles, following the axial symmetry of the mirror. Therefore the mesh of quadrilateral elements as shown in Figure 2.16 is practical for finite element analysis. Wavefront aberrations computed from model with quadrilateral elements usually yield data which are 5 to 15 % larger than the mesh of equilateral triangles. This is because of the fact that triangular elements are stiffer than quadrilateral elements. A three point support analysis was performed to demonstrate this fact. To make these two models comparable, the total number of nodal points which are to be used in FRINGE analyses were made approximately the same. Total number of nodes in triangular mesh were 162 and 163 in square mesh. These models represent the same primary mirror which is to be optimized, but with fewer number of nodal points. For quadrilateral grids, the rms deflection was 85.91 waves where as for the triangular grids the rms deflection was 80.36 waves. This means the aberrations computed from the quadrilateral mesh were 7 % higher than that of the triangular mesh. To simplify the generation of the structural model for the program NASTRAN, the quadrilateral mesh was chosen as it was on a conservative side.

2.3.8 Effect of Mesh Refinement on the peak to valley displacement

The iterative process described above consumes a significant amount of CPU time. To optimize the computer time, an analysis was done to minimize the

number of nodes in a finite element model without compromising accuracy in the results. Four models with 816, 1008, 1200, and 3360 nodes were analyzed with a two ring support system with a total number of 48 supports. The support radii were 32 and 73 inches. The rms value was computed for each case as listed in the Table 2.3. The peak to valley displacement which is the difference between the maximum and minimum values of the deflections of the finite element model was the criterion. A finite element model with 1200 nodes was selected on this basis. This model has 48 circumferential nodes for each of 25 rings. This mesh is shown in Figure 2.3 (B).

2.3.9 Axial Support System

As the telescope points at different zenith angles, the direction of gravity relative to the primary mirror changes. As a result of this, a mirror support system must be able to carry this force both in axial (normal to the mirror surface) and radial directions (parallel to the mirror surface). These two components generally have different support systems. The axial support system is a delicate and difficult design problem for the meniscus mirror. The axial support is provided by a force system applied along the backside of the mirror. The radial support is a system of forces applied at discrete points located along the midplane of the mirror. From the calculations described in section 2.3.3, the least number of point supports for the axial system is 60. It is at these points at which specified forces are applied.

In analyzing and optimizing a support system, it is emphasized that the supports provide specified forces, but do not by themselves define the position of the mirror. In case of N point supports, three of these support points can be specified to define the position of the mirror, but the other support points should in practice, be allowed to float in position and provide only the specified force. It follows from this, that deflections at the support points are not required to be zero for overall

optimized support. A three ring support system was optimized by varying the radii, forces, and rotation angles of each group to minimize the rms deflection. The support points of the mirror following the axial symmetry of the mirror, are placed in concentric rings. For this mirror, the procedure described in section 2.3.4 was followed. A three point, six point, and an eighteen point support systems were analyzed to study the effect of number of supports on rms deflection. These models are illustrated in Figure 2.17. The thin meniscus mirrors need a larger number of support nodes which are usually distributed over several support rings, each with circumferential equidistant nodes.

The contours and spot diagrams are presented in Figures 2.18 through 2.25. When analyzing the supports with multiple ring of supports a variety of point topologies become possible. Listed in Table 2.4 are some of the various support topologies analyzed before reaching the optimized three ring support system. The rms deflection value of 0.13 waves for the optimized three ring support is beyond the allowable error budget of 0.10 waves. Therefore a four ring support system was investigated and optimized to yield an rms value of 0.061 waves. The support locations are shown in Figure 2.26. Listed in Table 2.4 are various three ring geometries and the corresponding rms and peak to valley displacement values. Listed in Table 2.6 are the same for the four ring geometries. Listed in Table 2.8 are the force distribution for the optimized four ring support system for the zenith pointing case.

2.3.10 Radial Support System

When the telescope is pointing horizon, the optical axis is horizontal. The horizontal axis mirror is also deformed by the gravity, but not to the extent of one with its axis pointing to the zenith. This is one reason why mirrors are frequently

tested on edge. The deformations that occur in this case are not rotationally symmetrical about the mirror axis. There are two different solutions for the radial support system of a thin meniscus mirror.

- 1) Outer edge together with inner hole support.
- 2) Distributed point support at the back surface of the mirror or in the neutral plane.

In case of the outer edge support, a bending moment is introduced into the mirror, since the edge supports are not placed in the plane of the center of gravity of the mirror. Third and fifth order coma is introduced in the mirror because of this out-of-plane bending. The additional inner edge supports reduce these aberrations. In the second solution, the application of the radial supports at points of the neutral plane reduces the bending moments. Here in this section, the second solution is analyzed in detail in order to determine the magnitude of the forces necessary to keep the rms deflection within the error budget. For the analysis of the radial support system the same finite element model as in the case of the axial support system has been used. Similar to that of the axial support optimization, the analysis started with a three ring support system. The rms deflection value of 0.01 waves for the optimized three ring support with a total number of supports of 60 was well within the limits when compared to the allowable error budget of 0.10 waves. But to have the same support pattern as the axial support system, a four ring support system was investigated to yield an rms value of 0.006 waves. The total number of support points was 66 as shown in Figure 2.26. Listed in Table 2.5 are various three ring geometries and the corresponding rms and peak to valley displacement values. Listed in Table 2.7 are these results for the four ring geometries. Listed in Table 2.9 is the force distribution for the optimized four ring support system for the horizon pointing case.

2.3.11 Bellofram Supports

Recent large telescopes have usually employed a pneumatic system for the support of the primary mirror. A controller or regulator controls the pressure in either each ring of belloframs or individual belloframs. Multipoint mounts using pneumatic or hydraulic actuators are frequently used and have proved effective to support the force required. Bellofram rolling diaphragm is a tough, flexible seal with a unique configuration that permits relatively long piston strokes while completely eliminating sliding friction. Shown in Figure 2.28 is a zero leakage rolling diaphragm installed in a cylinder. The rolling action is smooth and effortless, completely without sliding contact and breakaway friction. With the outer flange clamped to the cylinder and center fastened to the piston head, the bellofram forms a perfect barrier, preventing blow-by leakage or pressure loss. It requires no lubrication of any kind. Bellofram rolling diaphragms are, in effect, pressure vessels having a variable volume and flexible moving side walls. These belloframs can function effectively with applied pressures of up to 1000 psi. Illustrated in Figures 2.29 and 2.30 are two possible support systems for the primary meniscus mirror using bellofram supports.

2.4 Frequency Analysis of the Primary Mirror

For a primary mirror with large diameter (diameter ≥ 3 meters), the resonant vibration of the mirror can become a significant factor in the design process and can no longer be neglected. The primary mirror of a telescope is often mounted in a configuration where the primary mirror is supported on three points at a radial distance of approximately $0.7 \times \text{diameter of the mirror}$ and are spaced at 120° and kinematically mounted. Such a support system can produce small tilt. Resonant mode shapes and frequencies depend on the manner they are supported. Also, the

free vibration analysis is very important for the design of the support system and the mirror cell in order to determine the dynamic response behavior due to the excitation by the wind gusts or telescope drives. The lowest eigen-frequency that can be excited by the dynamic loading is an important parameter for the dynamic response behavior. Natural frequencies of a flat circular plate can be computed using the following equation. This equation can be used for circular plates with central holes also. Blevins (1972) listed a dimensionless parameter (λ_{ij}) in a tabular form for different support conditions. The closed form solution is given as

$$f_{ij} = \frac{\lambda_{ij}}{2 \pi a^2} \left[\frac{E h^3}{12 \gamma (1 - \nu^2)} \right]^{\frac{1}{2}}$$

With,

$$i = 0, 1, 2, \dots$$

$$j = 0, 1, 2, \dots$$

Where,

f_{ij} = natural frequency

i = number of nodal diameters

j = number of nodal circles, not counting the boundary circles

E = Young's Modulus

h = thickness of the mirror

γ = mass per unit area

ν = Poisson's Ratio

λ_{ij} = dimensionless parameter

Cho (1989) and ESO (1987) have compared frequencies computed from both closed form solutions and finite element analyses for flat circular plates. Results indicate the frequencies computed from finite element analysis are within 5% of the closed form solution. A flat circular plate with a hole as well as the thin

shell model with the curvature have been analyzed using the finite element program MSC/NASTRAN to compute the vibration modes and frequencies. Table 2.10 summarizes the first ten frequencies for both plate and shell models. The corresponding contour plots and spot diagrams are shown in the figures 2.31 through 2.39. The comparison of plate and shell models show that only the radial modes are significantly higher in the shell model due to the stiffening effect of the curvature. Modes 3 and 5 are the defocussing modes. Eigen-frequencies of the shell model are 27% and 31% than corresponding eigen-frequencies of the plate model. Also, the order of modes 4 and 5 is reversed in the plate model, i.e., mode 4 of the shell model is same as mode 5 of the plate model and mode 5 of the shell model is same as mode 4 of the plate model.

2.5 Summary

Support point locations for both the axial and radial systems were achieved. The handling stresses were within the allowable limits. The high image quality of 0.010 arcsecs with an rms value of 0.06 waves was obtained with a four ring, 66 point support system.

TABLE 2.1 PRIMARY MIRROR SPECIFICATIONS

PARAMETER	VALUE
Outer Diameter	160 inches
Inner Diameter	30 inches
Thickness	4.5 inches
Radius of Curvature	480 inches
f/d	1.5
Weight	8066 lbs
Material	Zerodur
Young's Modulus	13.2×10^6 lbs/in ²
Poisson's Ratio	0.24
Weight Density	0.092 lbs/in ³

TABLE 2.2 HANDLING STRESSES IN THE PRIMARY MIRROR

Handling Device Configuration	Load Direction	Maximum Deflection (Waves)	Peak to Valley Displacement (Waves)	Maximum Equivalent Stress (psi)
3 Points	+1g	84.327	158.922	151.2
Carrying Frame (6 Points)	+1g	98.341	172.819	89.5
	-1g	98.341	172.819	86.1
Turning Frame (9 Points)				
Horizontal	+1g	18.469	32.078	79.2
Horizontal	-1g	18.289	31.860	76.6
Vertical	-1g	12.116	24.229	31.9

TABLE 2.3 EFFECT OF MESH REFINEMENT ON THE PEAK TO VALLEY DISPLACEMENT

No. Of Nodes	Peak to Valley Displacement (Waves)
816	4.821
1008	5.573
1200	6.622
3360	6.719

TABLE 2.4 THREE RING SUPPORT OPTIMIZATION (ZENITH)

MODEL #	RING LOCATIONS (inches)	TOTAL # OF SUPPORTS	rms (waves)	pv (waves)	SPOT DIAGRAM RADIUS (arc secs)
1	20,27,73	54	3.670	11.130	5.760
2	24,41,58	54	2.939	10.489	4.656
3	16,37,73	54	1.426	5.043	1.200
4	16,41,65	54	1.369	4.927	1.635
5	18,41,65	54	1.036	3.994	1.455
6	18,33,65	54	0.682	3.044	0.932
7	27,52,73	54	0.220	1.090	0.202
8	27,52,73	60	0.130	0.4540	0.060

TABLE 2.5 THREE RING SUPPORT OPTIMIZATION (HORIZON)

MODEL #	RING LOCATIONS (inches)	TOTAL # OF SUPPORTS	rms (waves)	pv (waves)	SPOT DIAGRAM RADIUS (arc secs)
1	24,41,58	60	0.447	3.252	0.692
2	20,27,73	60	0.237	1.640	0.381
3	18,41,65	60	0.129	1.167	0.278
4	16,46,65	60	0.126	1.118	0.297
5	18,33,65	60	0.118	1.073	0.252
6	16,37,73	60	0.108	0.711	0.240
7	27,46,73	60	0.028	0.170	0.099
8	27,52,73	60	0.010	0.057	0.013

TABLE 2.6 FOUR RING SUPPORT OPTIMIZATION (ZENITH)

MODEL #	RING LOCATIONS (inches)	TOTAL # OF SUPPORTS	rms (waves)	pv (waves)	SPOT DIAGRAM RADIUS (arc secs)
1	16,33,52,80	66	0.374	1.715	0.110
2	20,41,58,73	66	0.183	0.680	0.107
3	18,37,52,73	66	0.137	0.522	0.102
4	16,33,52,75	66	0.070	0.299	0.048
5	16,33,52,73	66	0.066	0.281	0.029
6	16,33,53,73	66	0.061	0.277	0.010

TABLE 2.7 FOUR RING SUPPORT OPTIMIZATION (HORIZON)

MODEL #	RING LOCATIONS (inches)	TOTAL # OF SUPPORTS	rms (waves)	pv (waves)	SPOT DIAGRAM RADIUS (arc secs)
1	16,33,52,80	66	0.084	0.182	0.083
2	20,41,58,73	66	0.066	0.110	0.059
3	18,37,52,73	66	0.022	0.101	0.046
4	16,33,52,75	66	0.012	0.055	0.033
5	16,33,52,73	66	0.010	0.045	0.020
6	16,33,53,73	66	0.006	0.037	0.010

TABLE 2.8 AXIAL SUPPORT SYSTEM

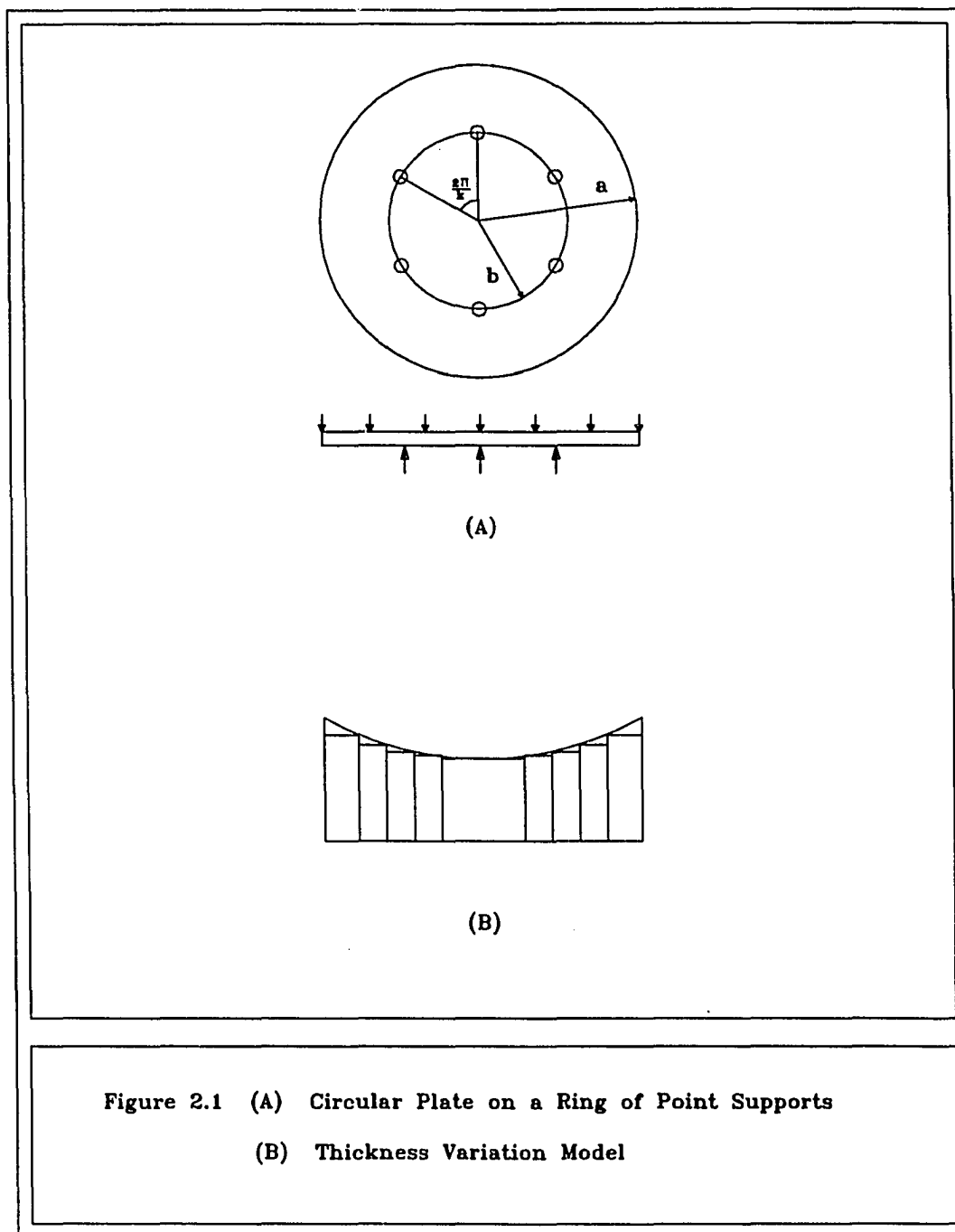
RING #	RADIUS (inches)	# OF SUPPORTS	ANGLE (°)	FORCE (lbs)
1	16	6	60	61.43
2	33	12	30	129.32
3	52	24	15	127.05
4	73	24	15	129.02

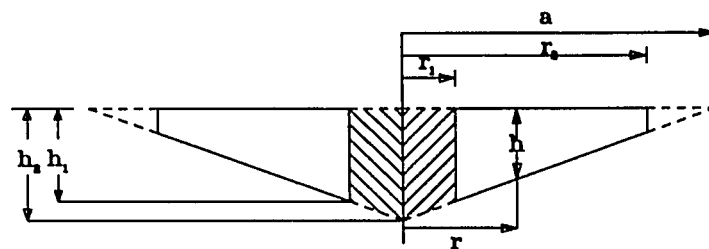
TABLE 2.9 RADIAL SUPPORT SYSTEM

RING #	RADIUS (inches)	# OF SUPPORTS	ANGLE (°)	FORCE (lbs)
1	16	6	60	122.20
2	33	12	30	122.20
3	52	24	15	122.20
4	73	24	15	122.20

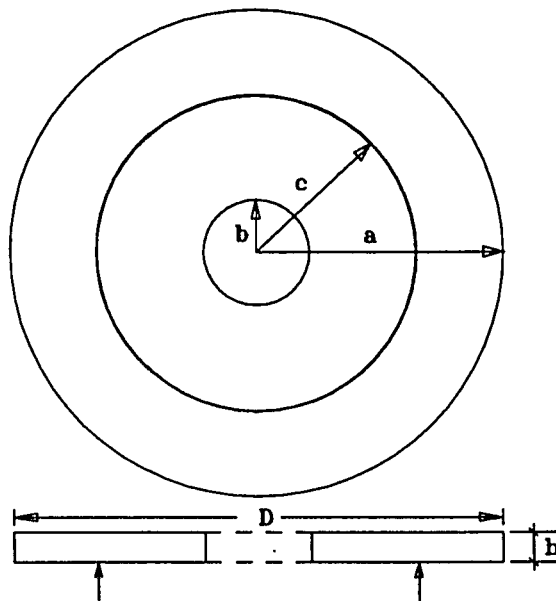
TABLE 2.10 MODAL FREQUENCIES FOR PLATE AND SHELL MODELS

Mode No.	Frequency (Hz)		Mode No.	Frequency (Hz)	
	Plate	Shell		Plate	Shell
1	30.48	34.46	6	98.09	104.10
2	30.48	34.46	7	98.09	104.10
3	55.16	70.30	8	150.70	158.28
4	85.35	90.40	9	150.70	158.28
5	73.82	97.10	10	169.14	178.80



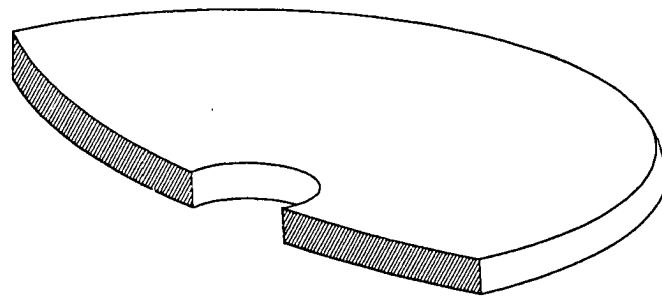


(A)



(B)

Figure 2.2 (A) Mirror with Linearly Varying Thickness
(B) Mirror with a Central Hole



MENISCUS MIRROR

Figure 2.3 (A) Meniscus Mirror

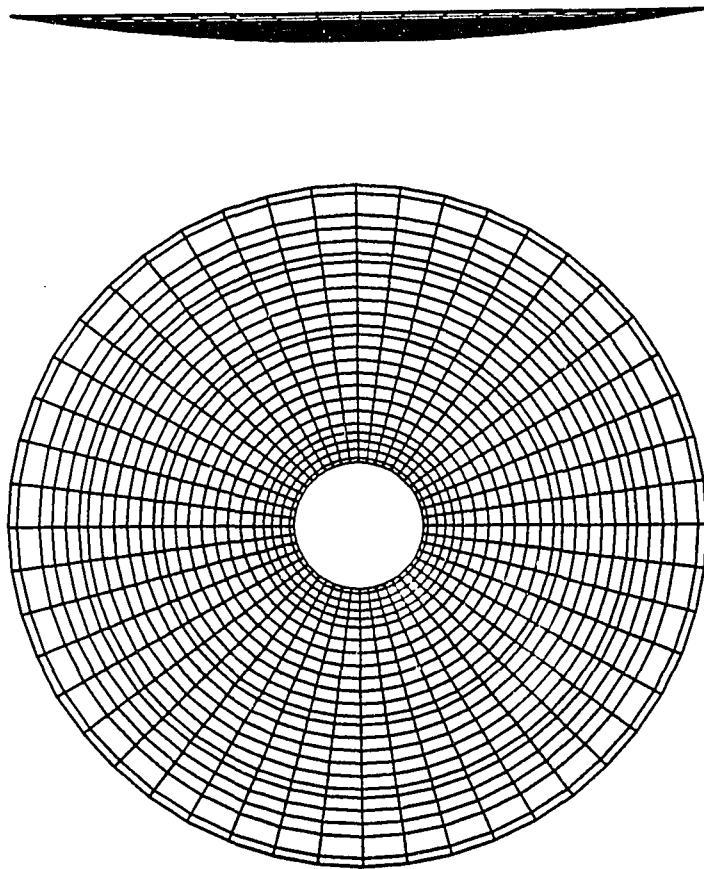
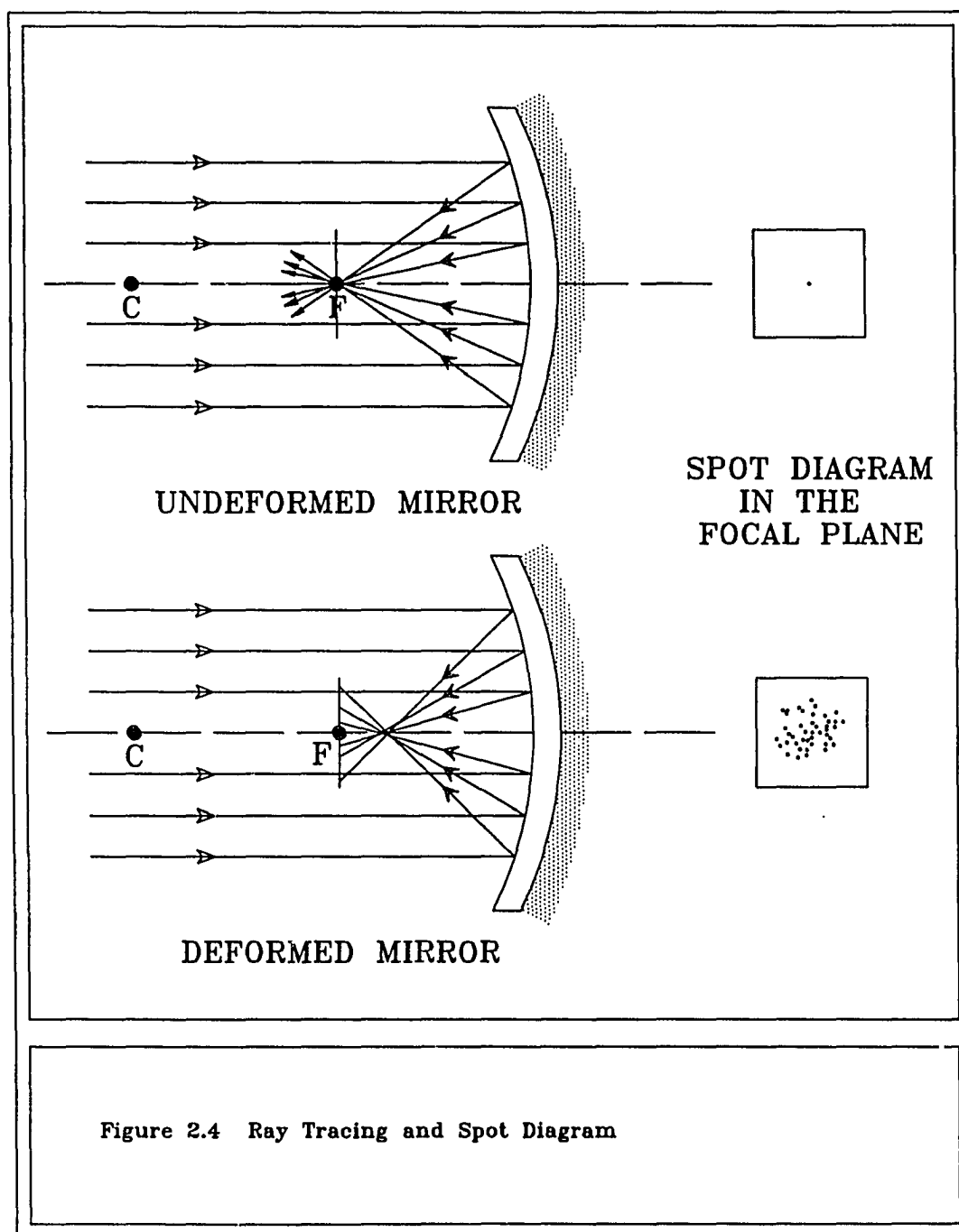
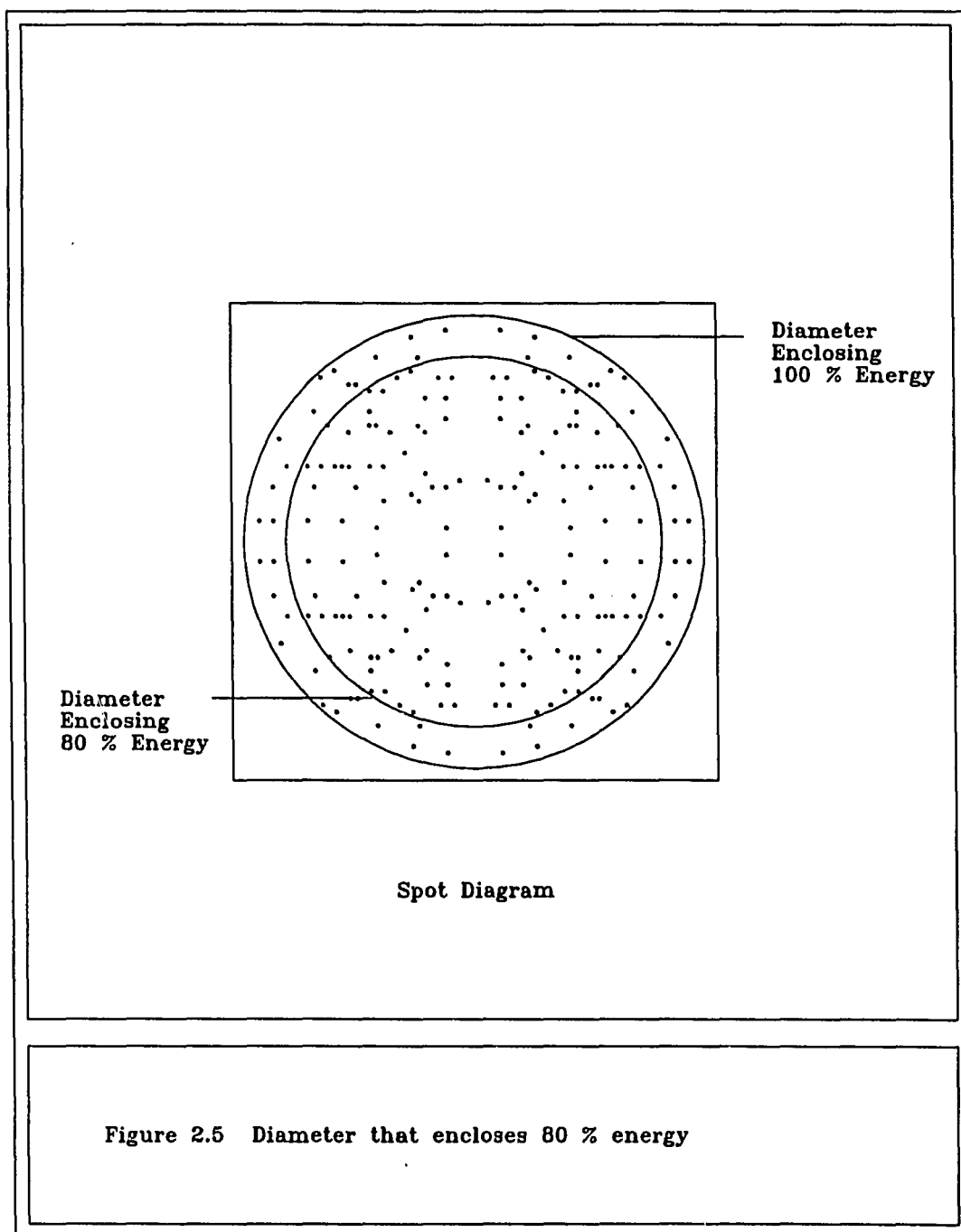
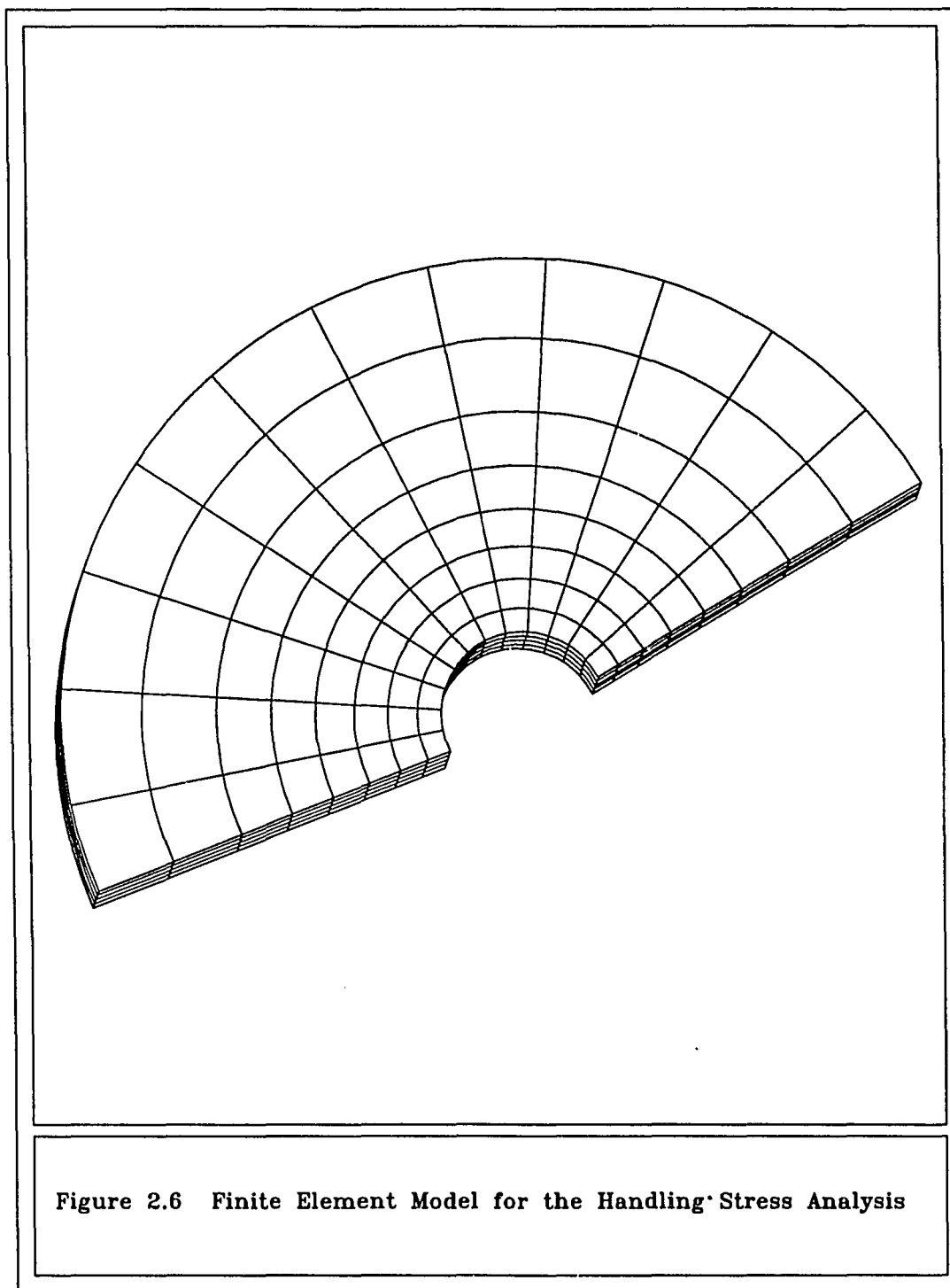
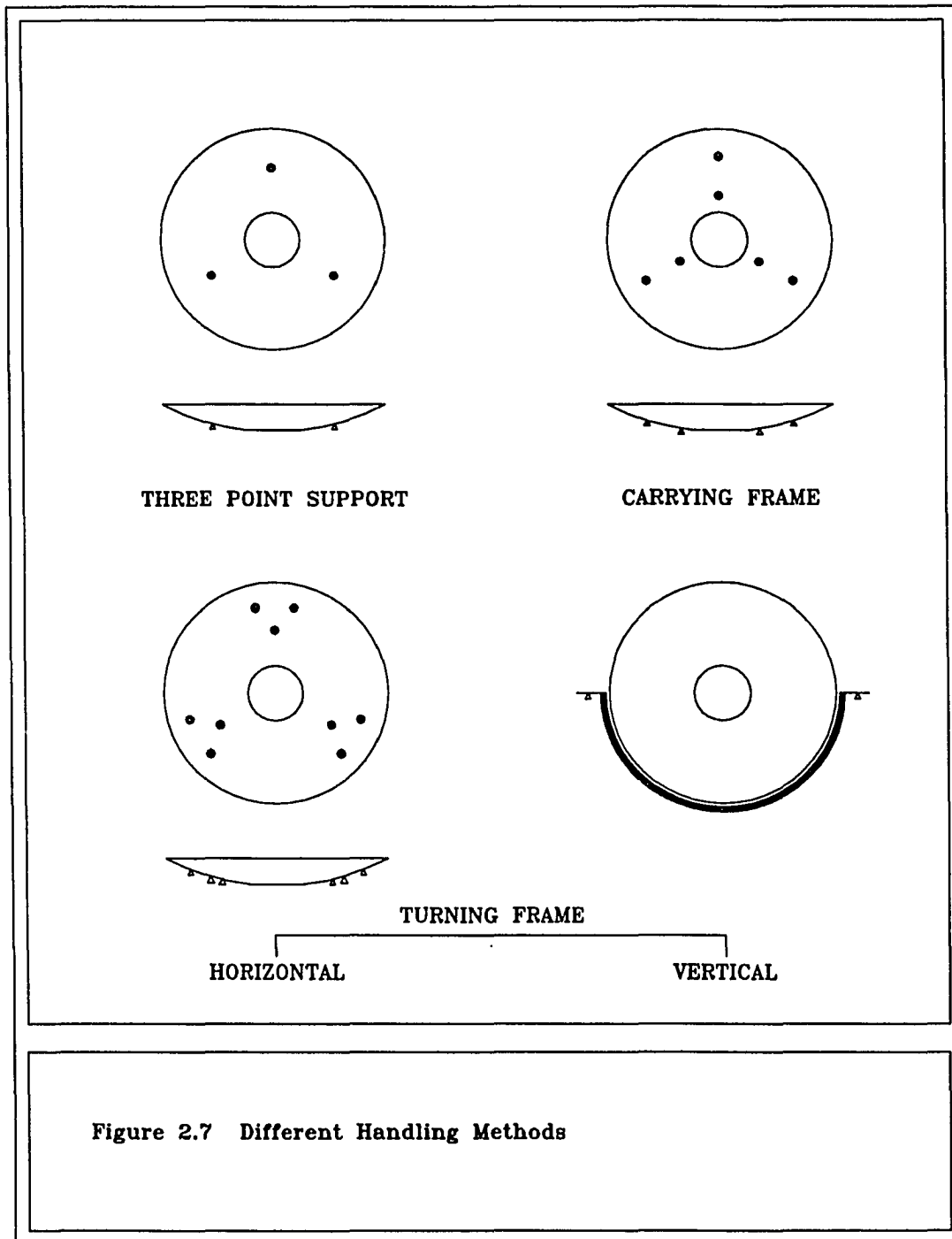


Figure 2.3 (B) Finite Element Model of the Primary Mirror









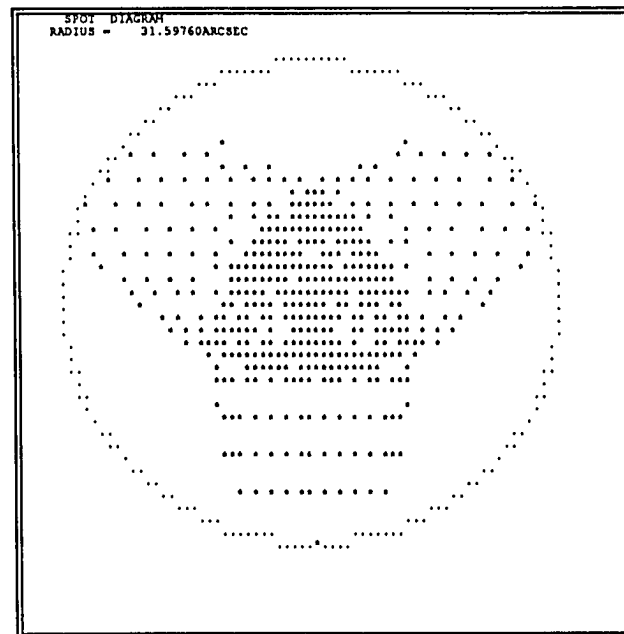
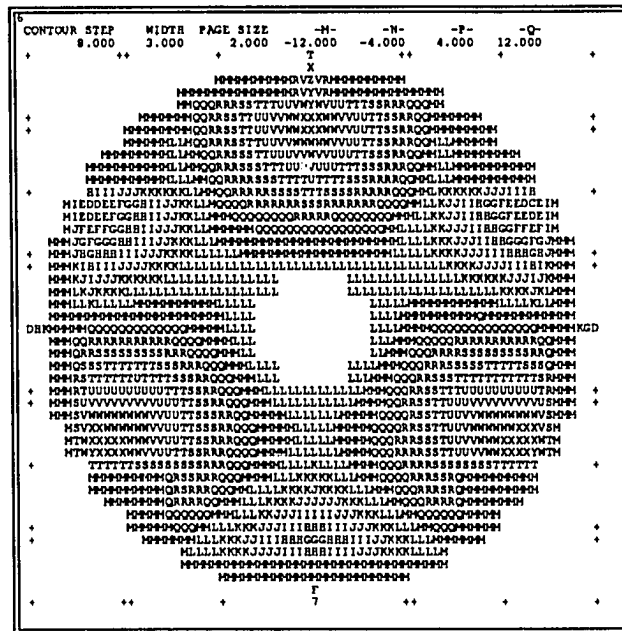


Figure 2.8 Contour Plot and Spot Diagram for a Three Point Support System

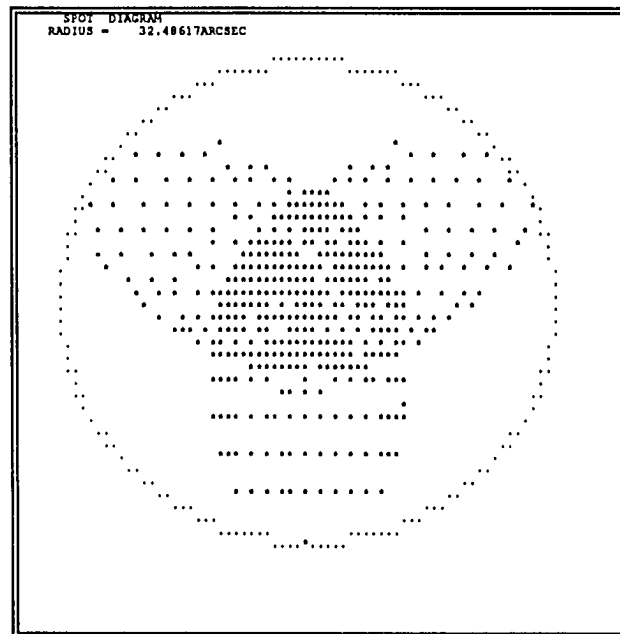
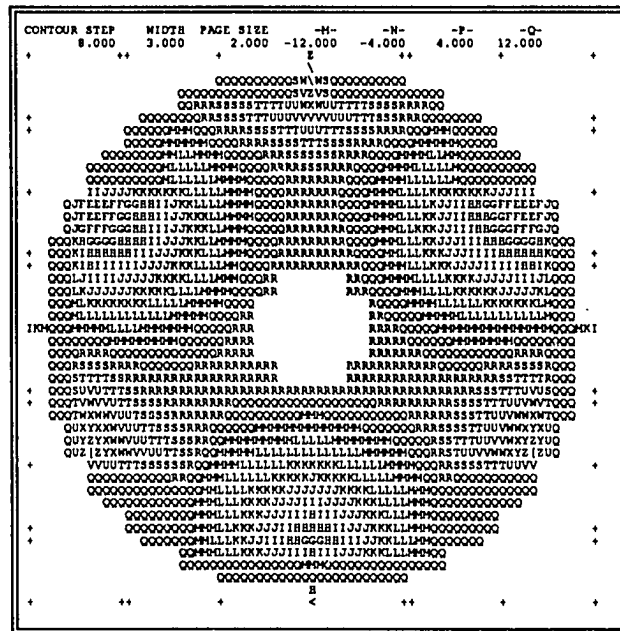


Figure 2.9 Contour Plot and Spot Diagram for a Six Point Support (-Z) System

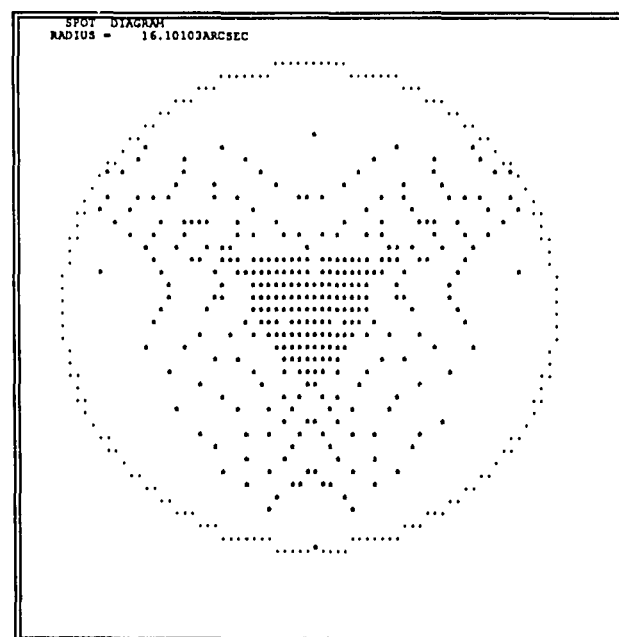
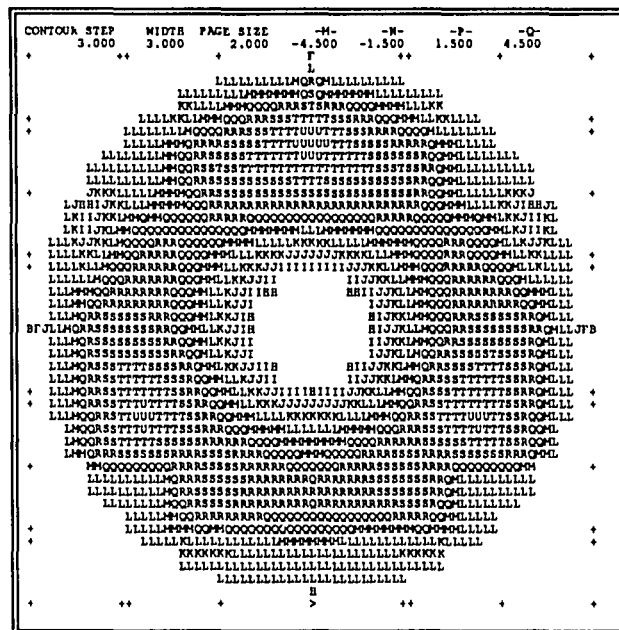


Figure 2.10 Contour Plot and Spot Diagram for a Nine Point Support (-Z) System

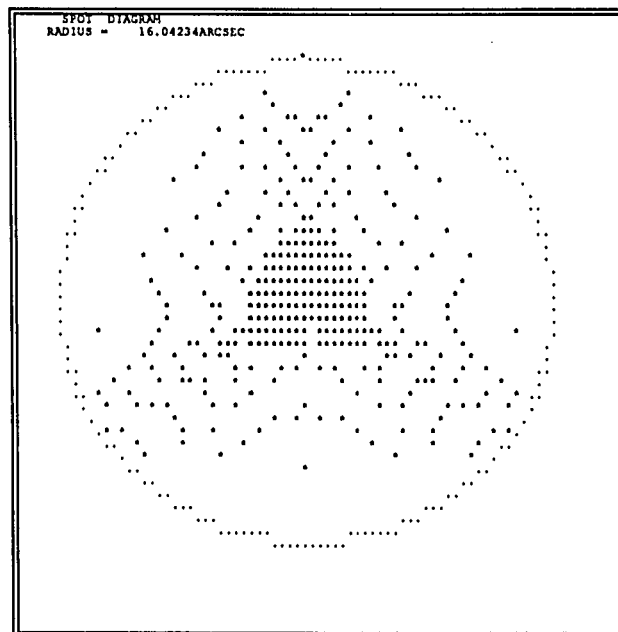


Figure 2.11 Contour Plot and Spot Diagram for a Nine Point Support (+Z) System

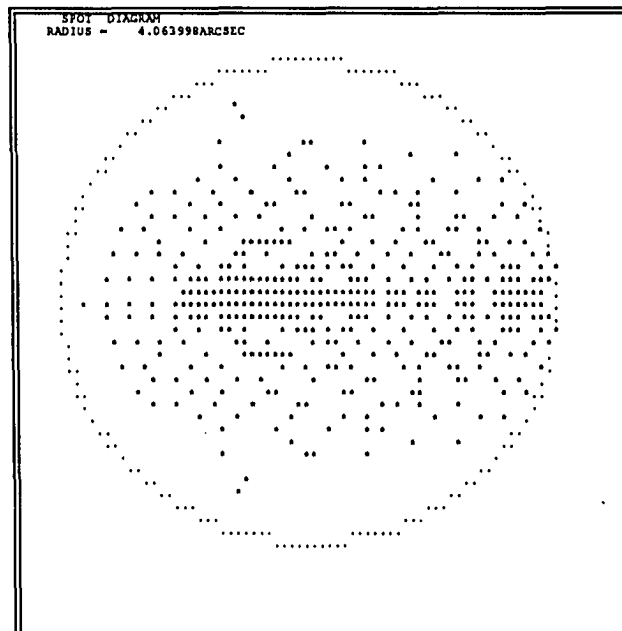
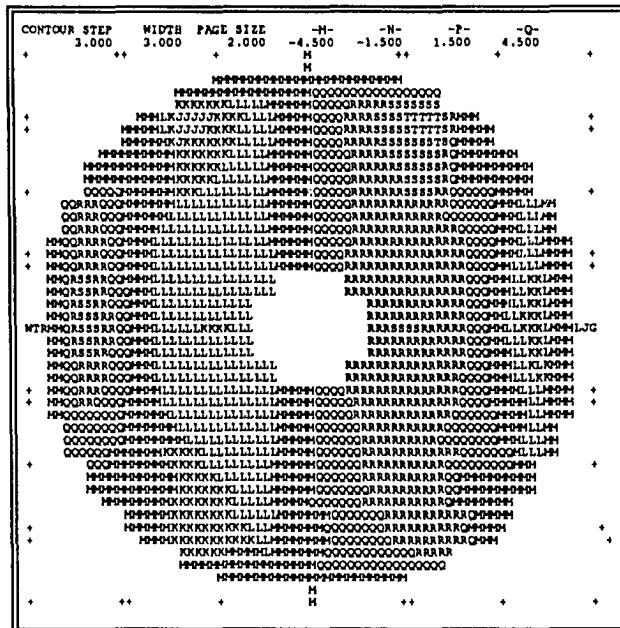


Figure 2.12 Contour Plot and Spot Diagram for a Six Point Support (-Y) System

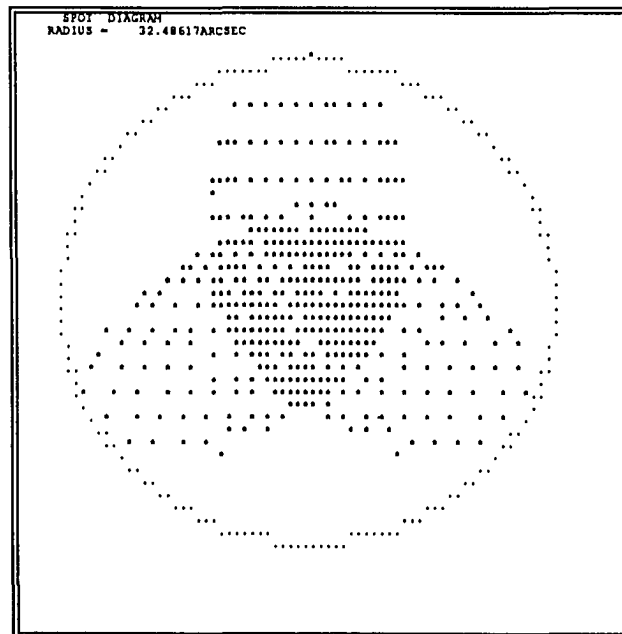
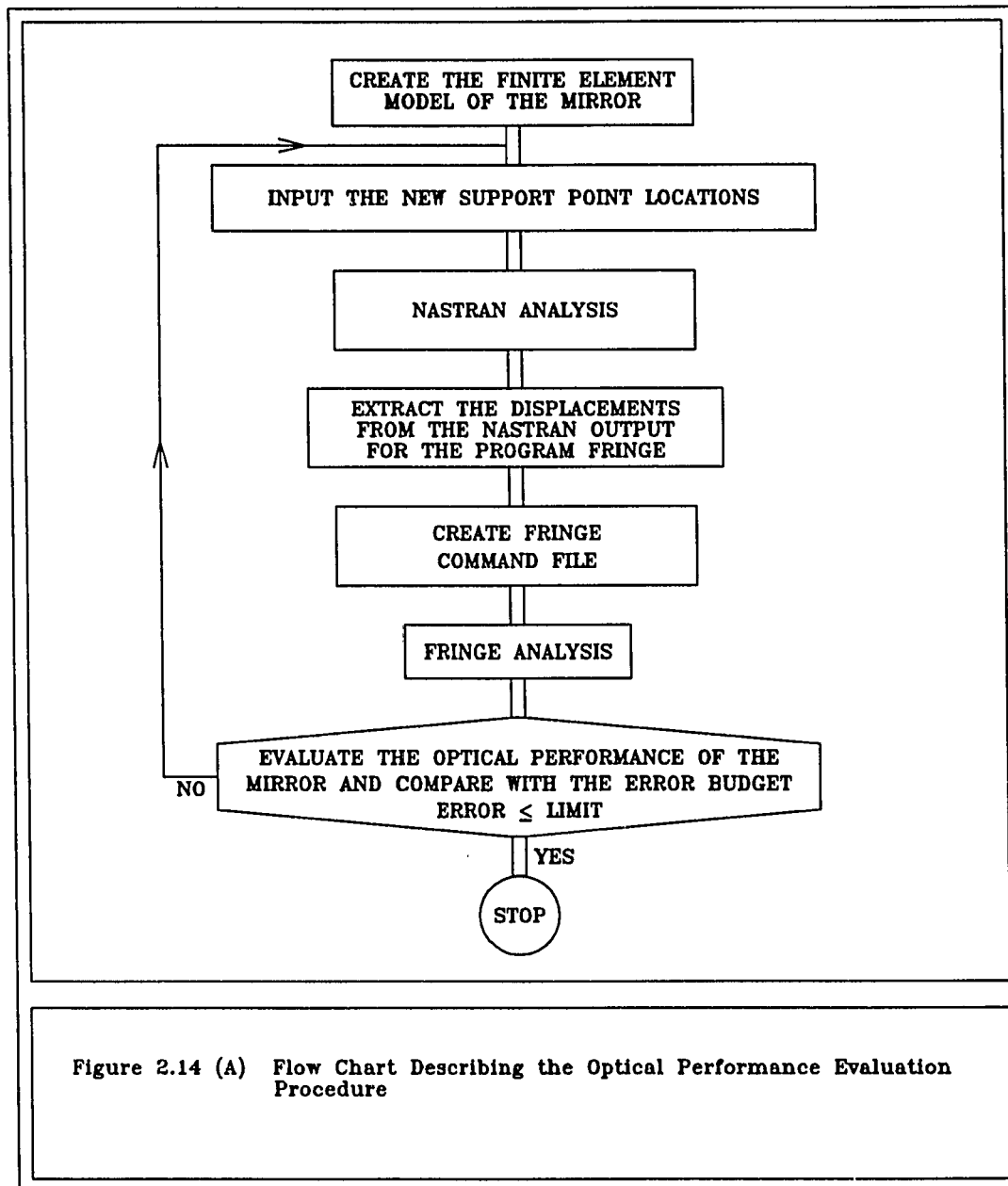
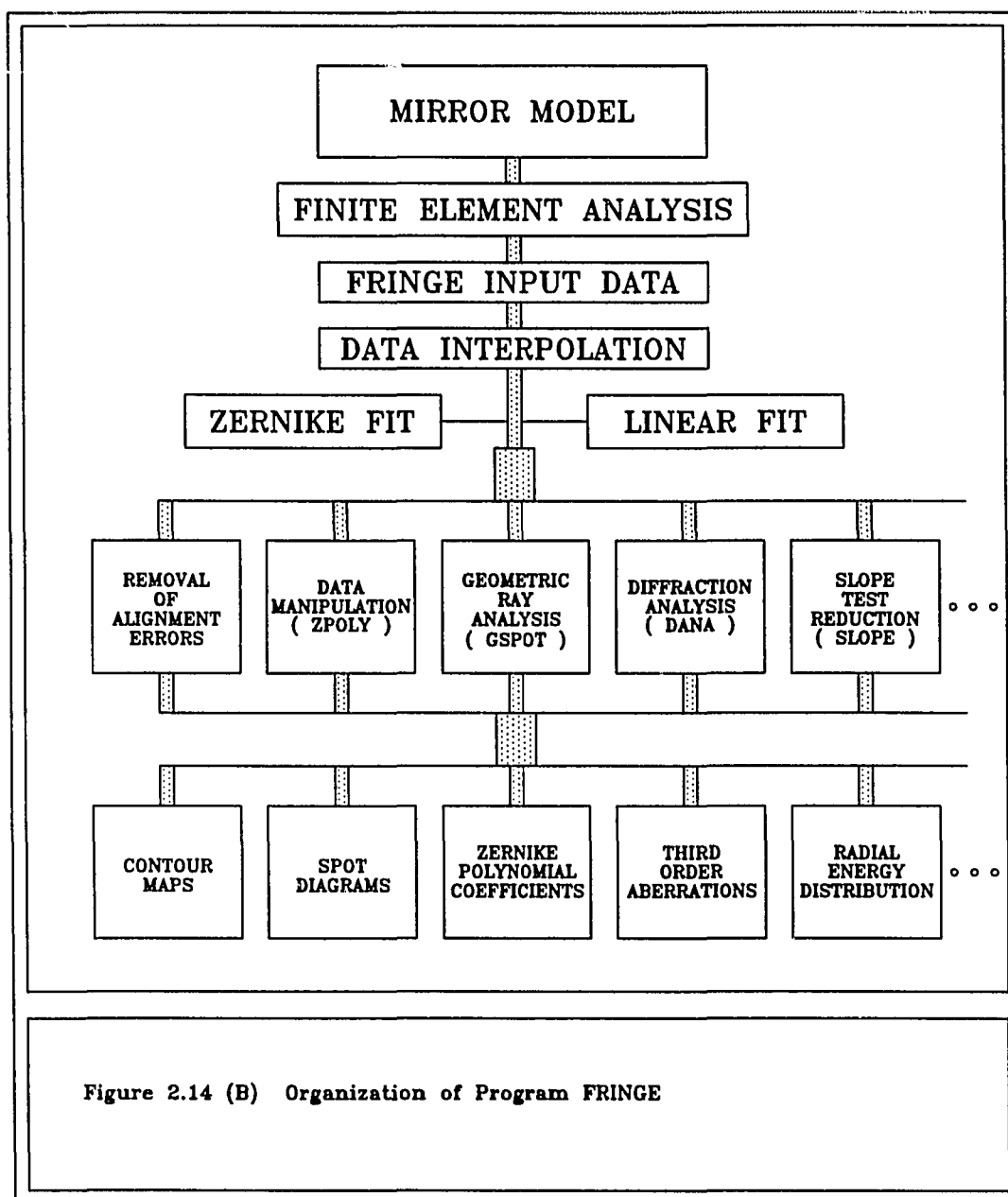
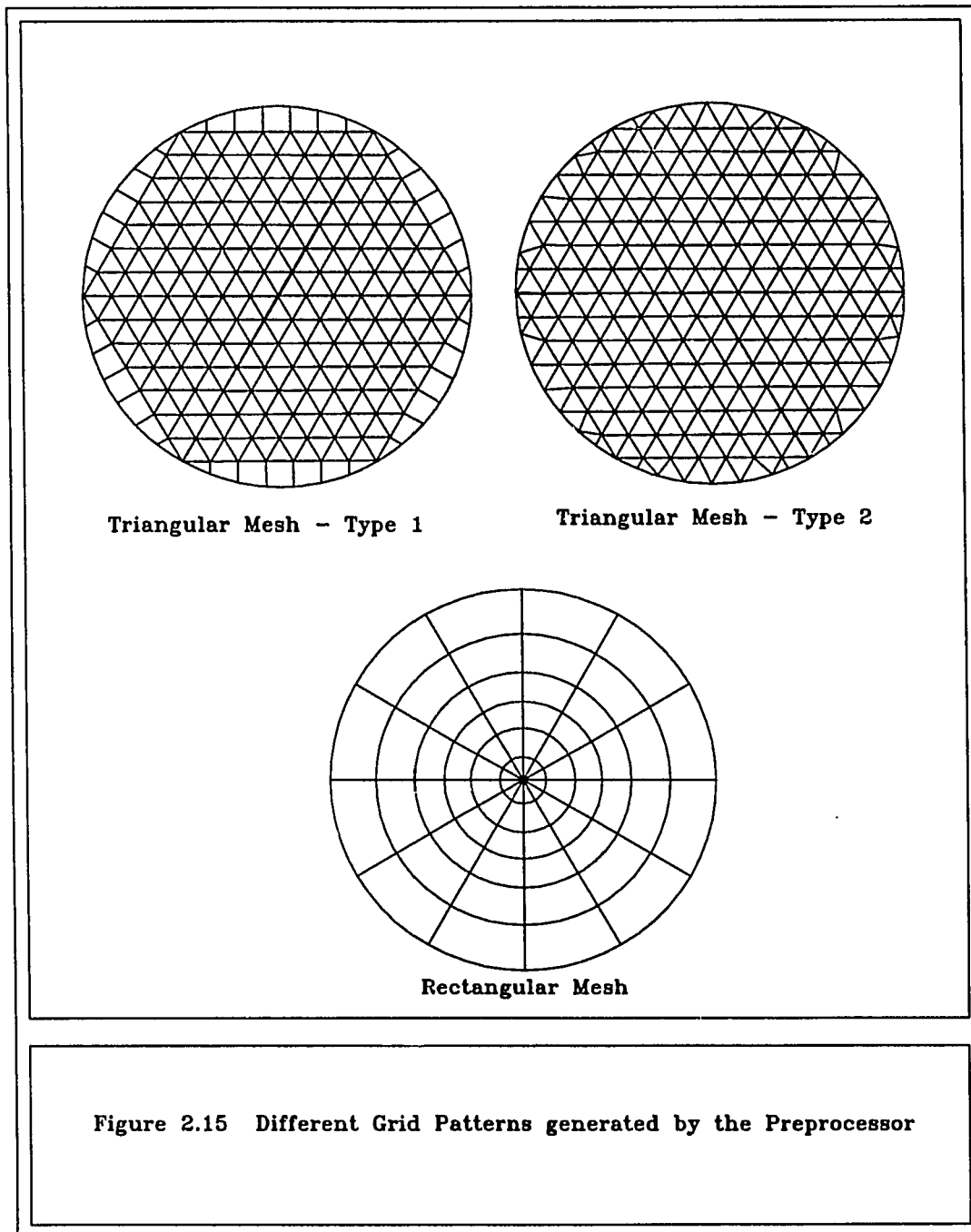
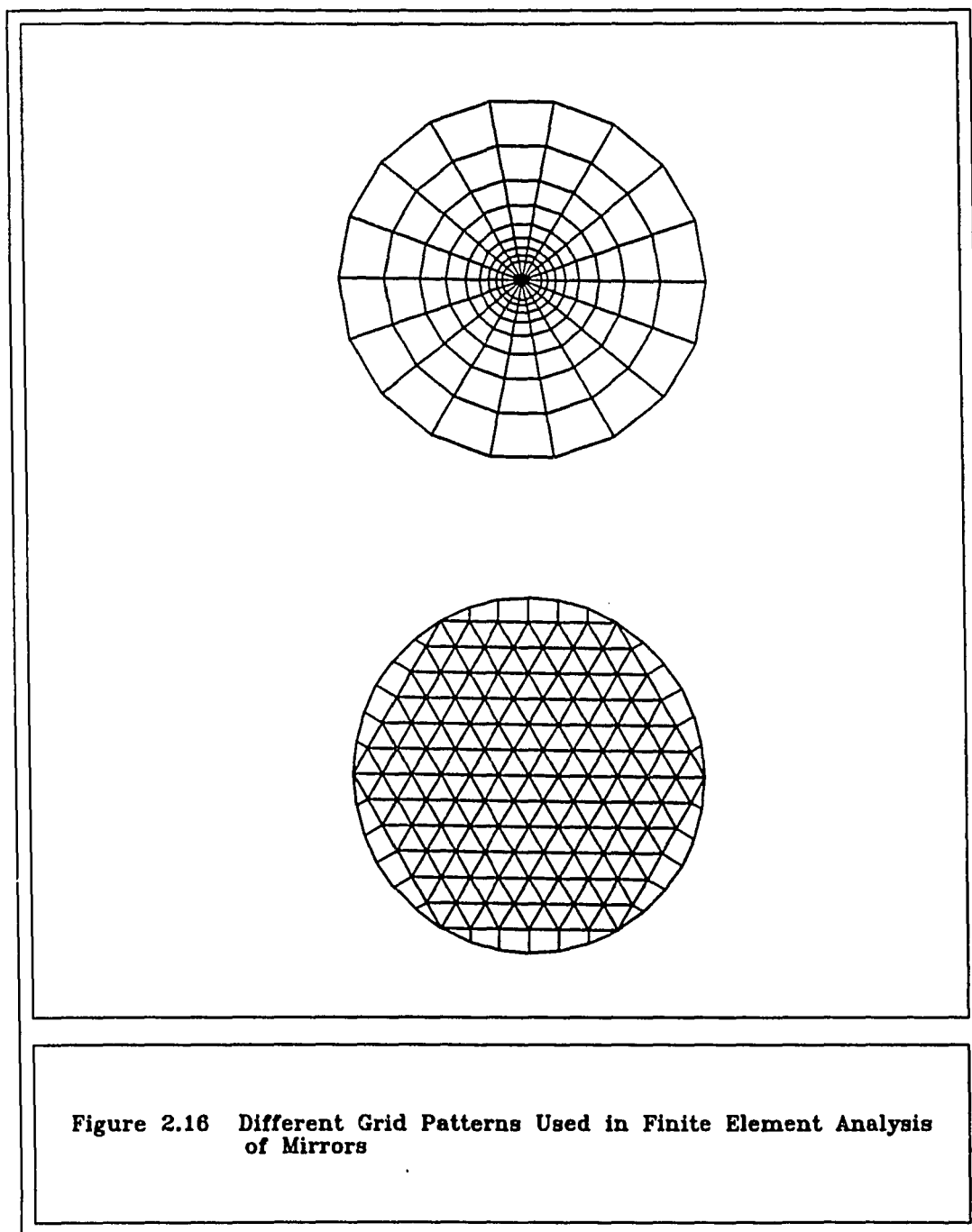


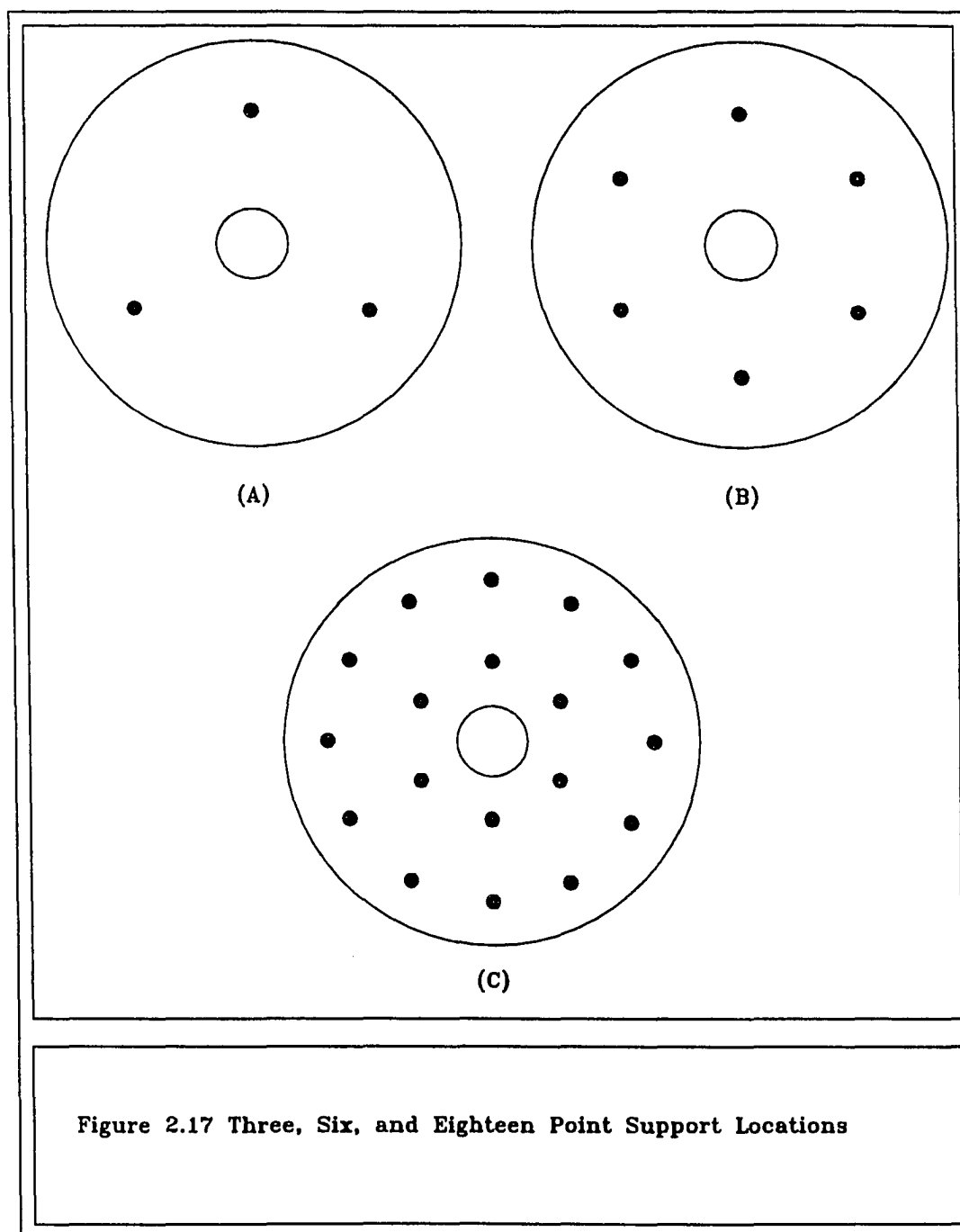
Figure 2.13 Contour Plot and Spot Diagram for a Six Point Support (+Z) System











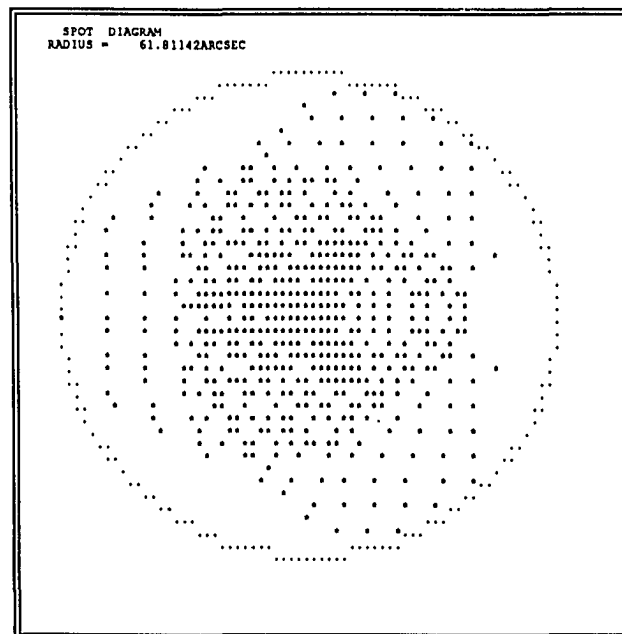


Figure 2.18 Contour Plot and Spot Diagram for a Three Point Support System (Zenith)

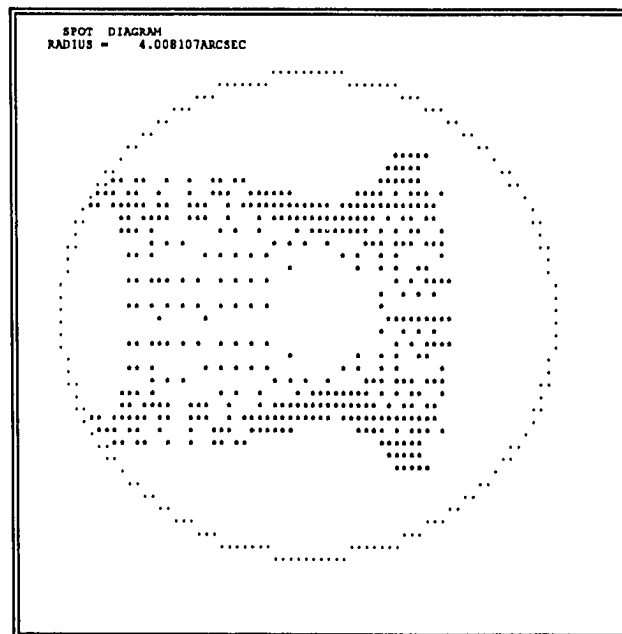


Figure 2.19 Contour Plot and Spot Diagram for a Three Point Support System (Horizon)

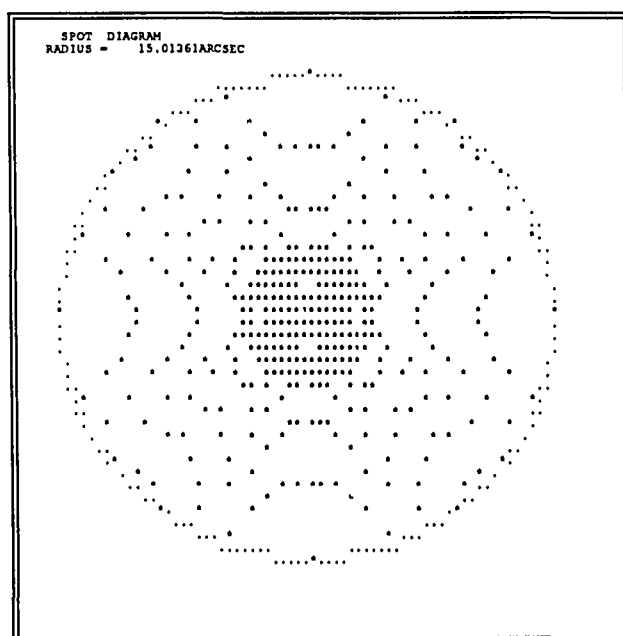


Figure 2.20 Contour Plot and Spot Diagram for a Six Point Support System (Zenith)

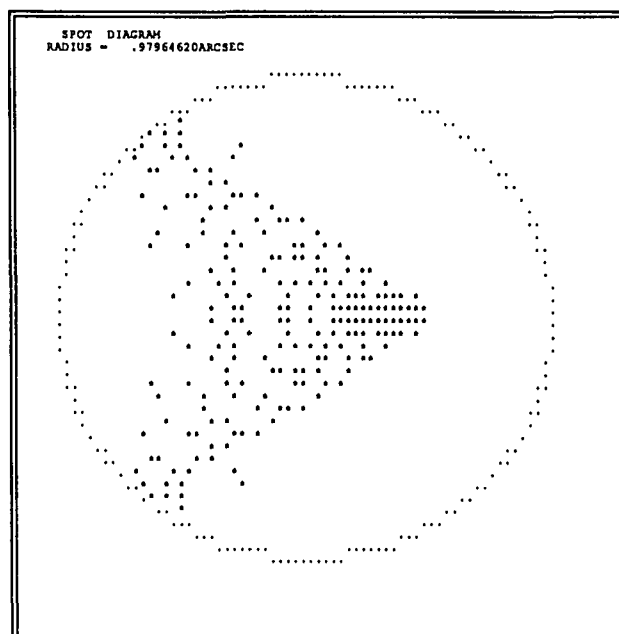


Figure 2.21 Contour Plot and Spot Diagram for a Six Point Support System (Horizon)

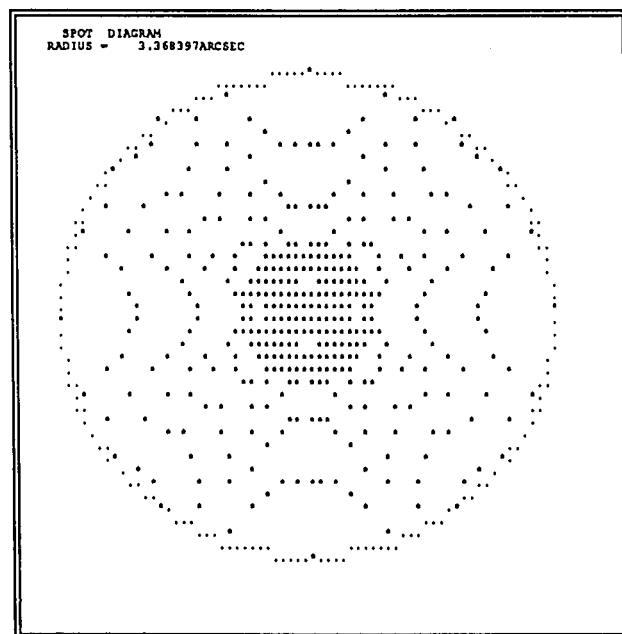
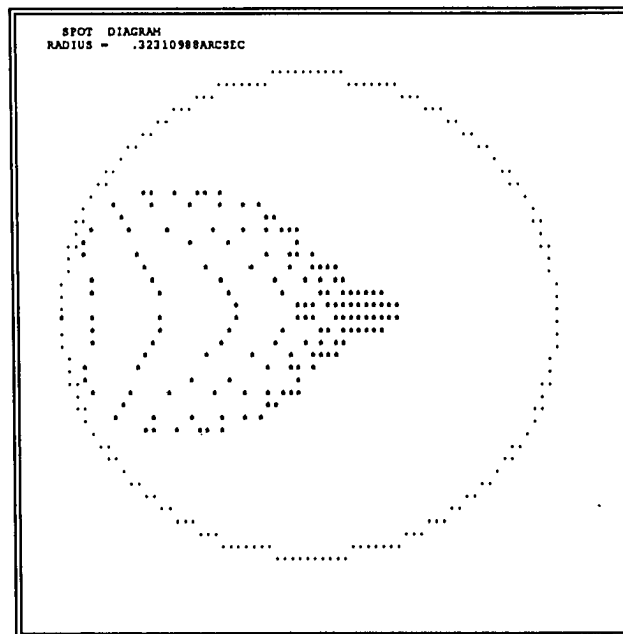


Figure 2.22 Contour Plot and Spot Diagram for 18 Point Support System (Zenith)



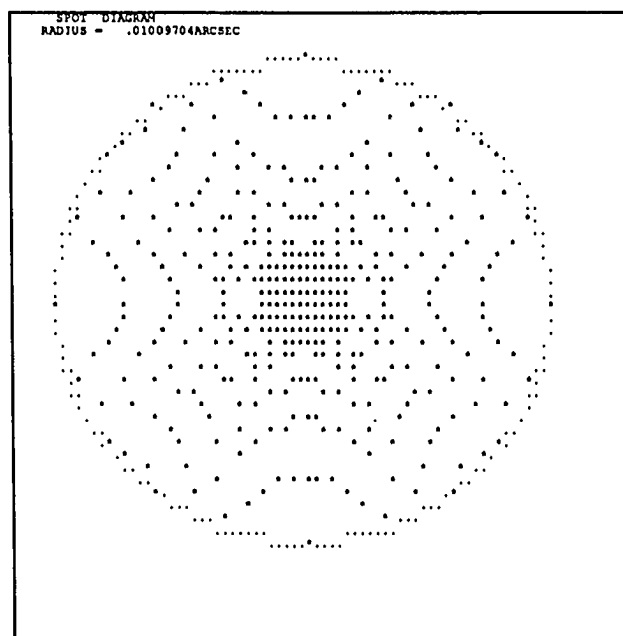


Figure 2.24 Contour Plot and Spot Diagram for Sixty Six Point support System (Zenith)

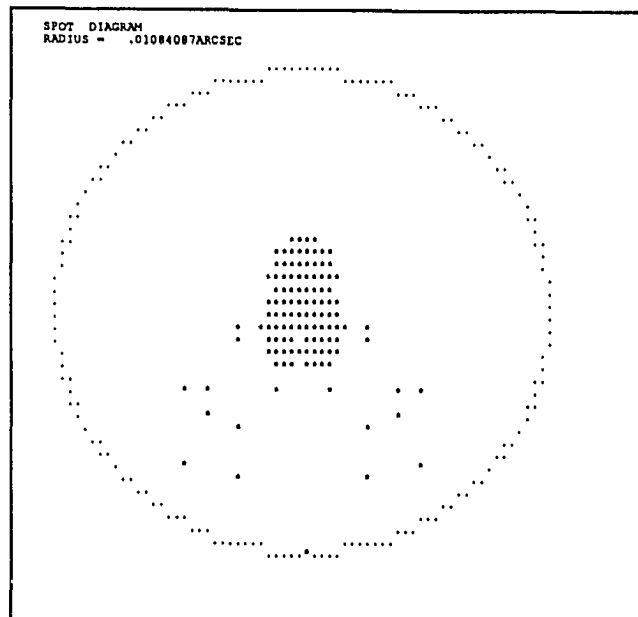
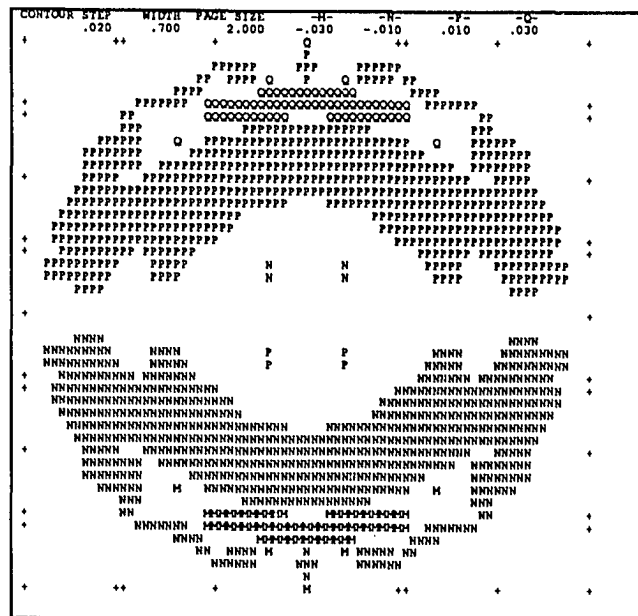
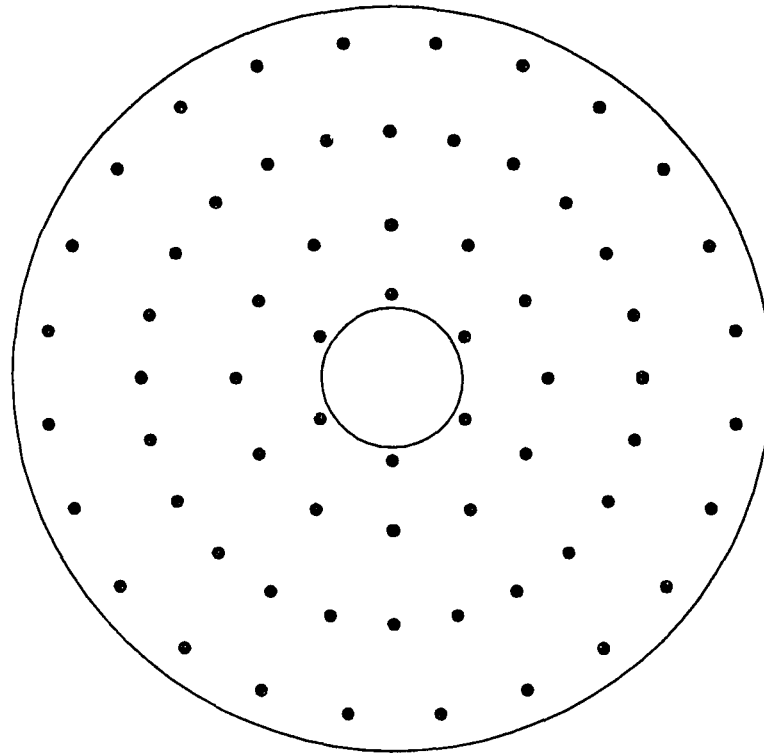


Figure 2.25 Contour Plot and Spot Diagram for Sixty Six Point support System (Horizon)



Outer Diameter = 160 in.

Inner Diameter = 30 in

Figure 2.26 Optimum Support Locations for the Four Meter Mirror

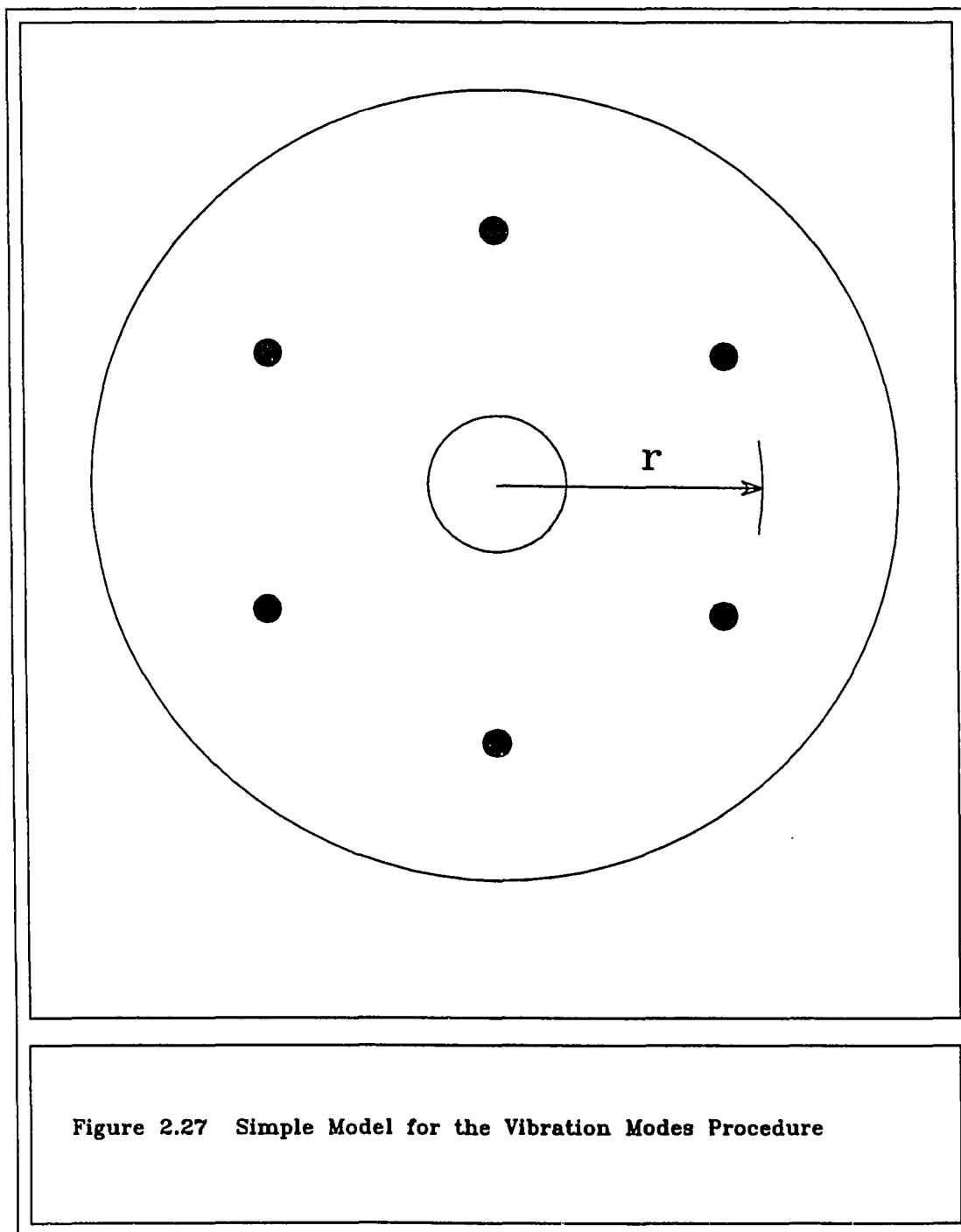


Figure 2.27 Simple Model for the Vibration Modes Procedure

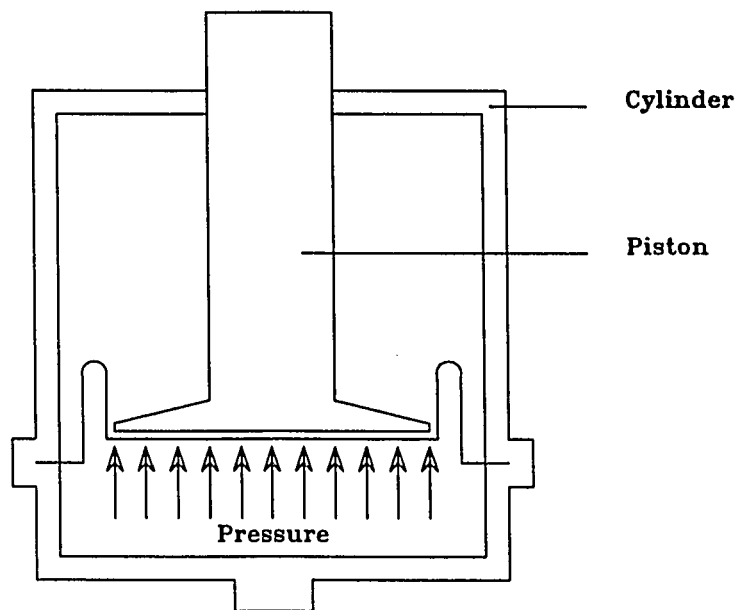
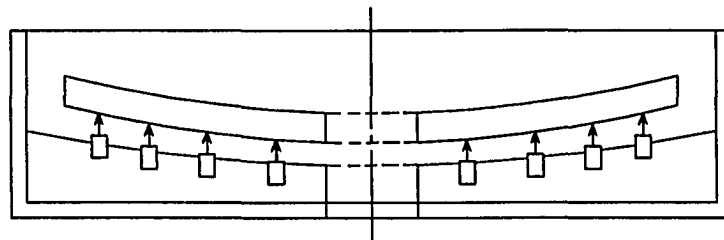
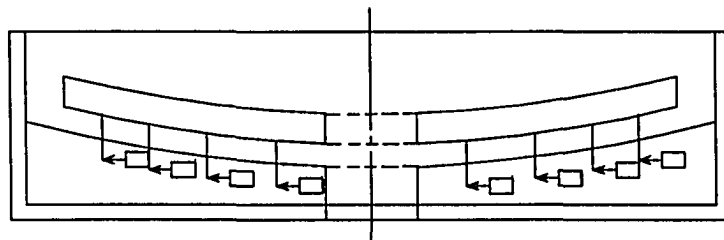


Figure 2.28 Zero Leakage Rolling Diaphragm Installed In Cylinder

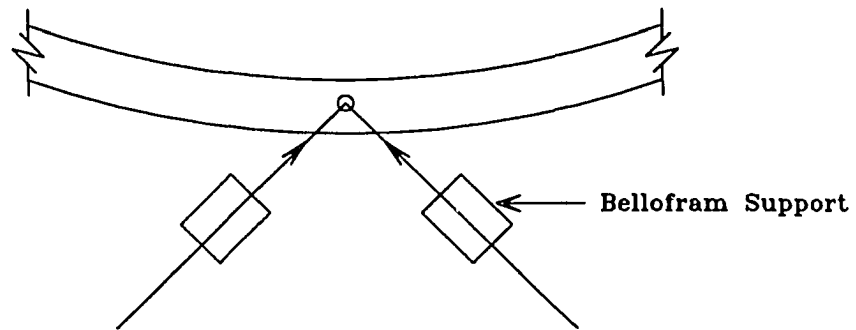


Axial Support System

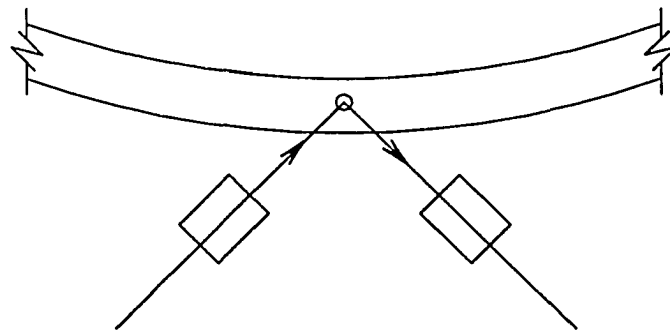


Radial Support System

Figure 2.29 Axial and Radial Support Systems for the Four Meter Mirror



Axial Support System



Radial Support System

Figure 2.30 Alternative Scheme of Supporting the Mirror

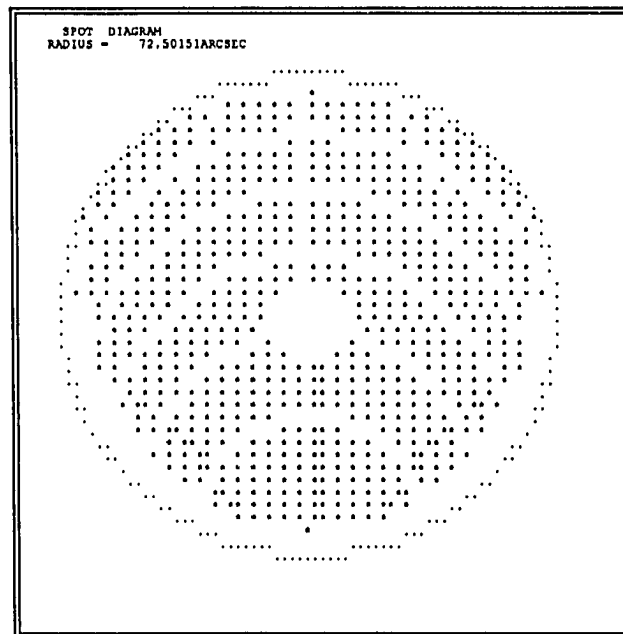
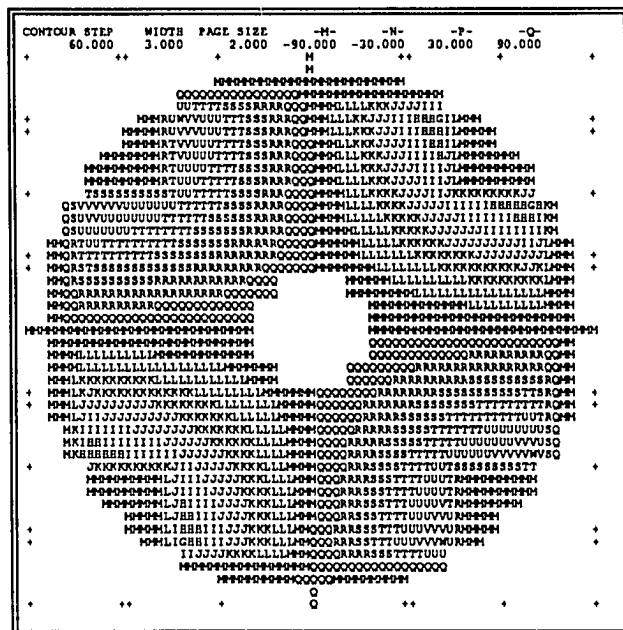


Figure 2.31 Contour Plot and Spot Diagram for Mode 1

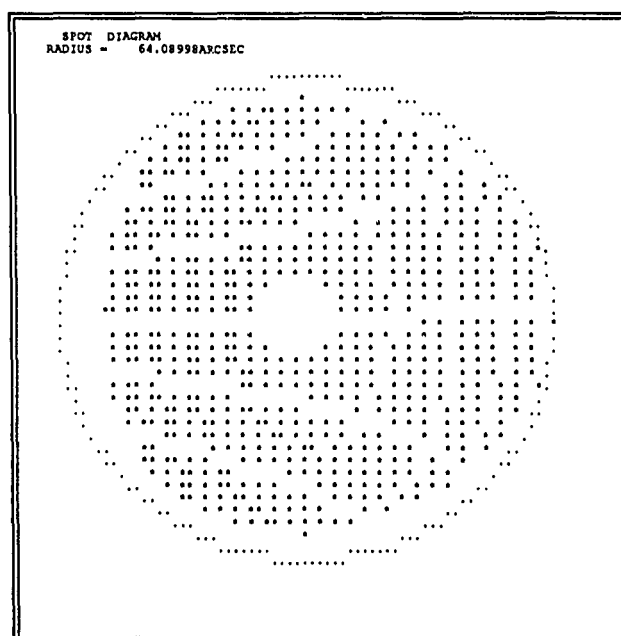


Figure 2.32 Contour Plot and Spot Diagram for Mode 2

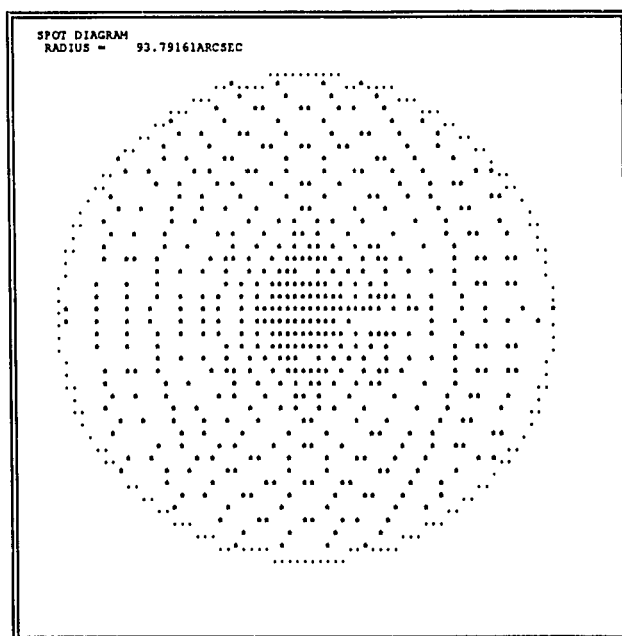


Figure 2.33 Contour Plot and Spot Diagram for Mode 3

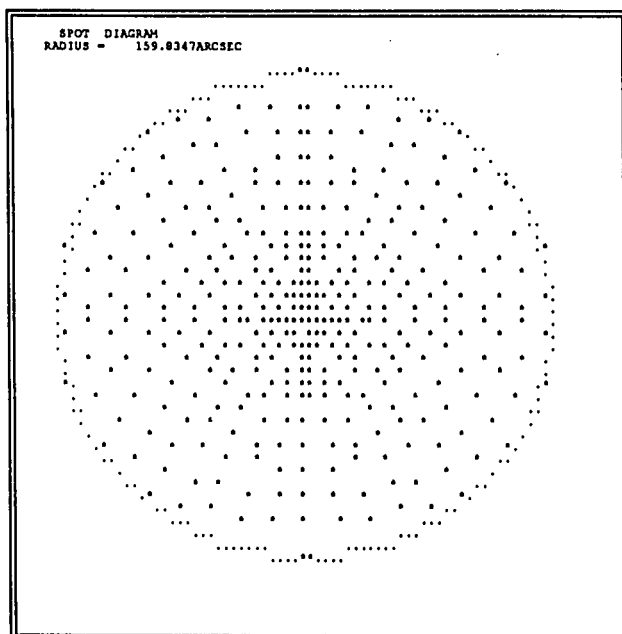
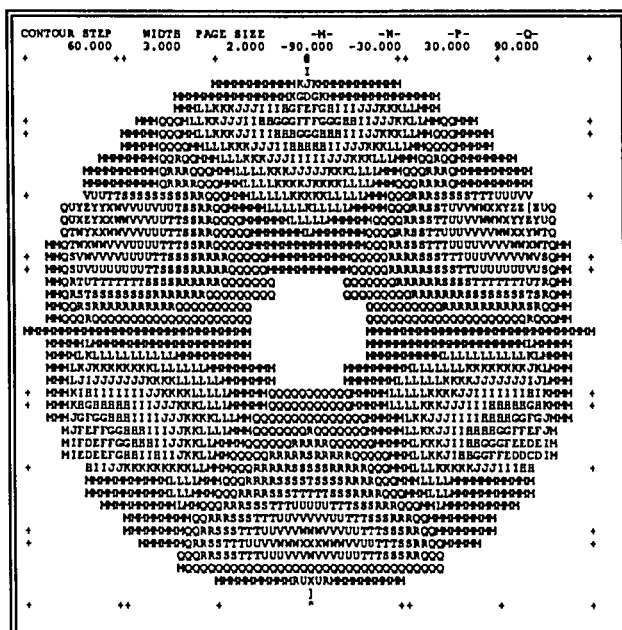


Figure 2.34 Contour Plot and Spot Diagram for Mode 4

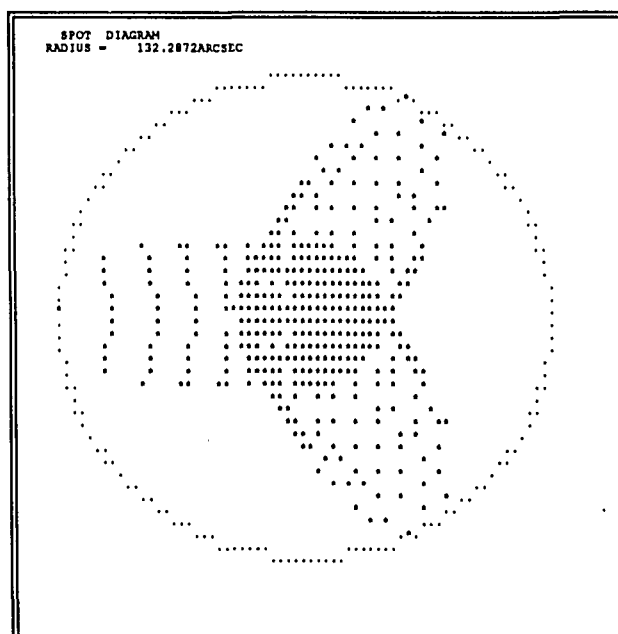


Figure 2.35 Contour Plot and Spot Diagram for Mode 5

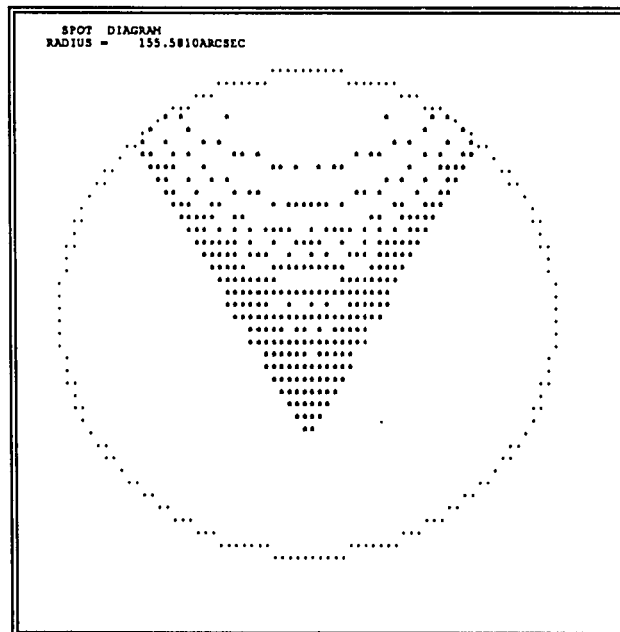


Figure 2.36 Contour Plot and Spot Diagram for Mode 6

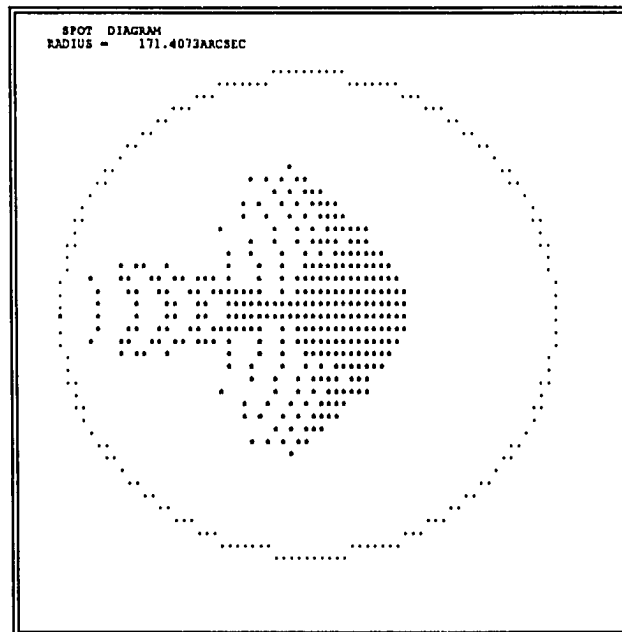


Figure 2.37 Contour Plot and Spot Diagram for Mode 7

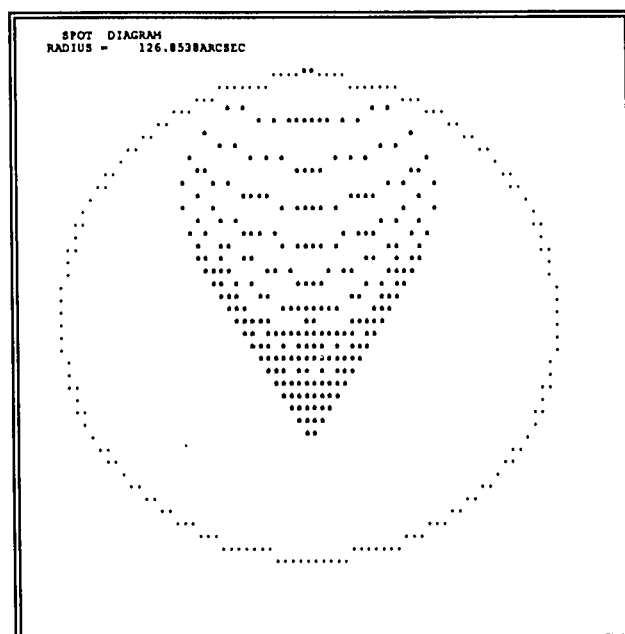


Figure 2.38 Contour Plot and Spot Diagram for Mode 8

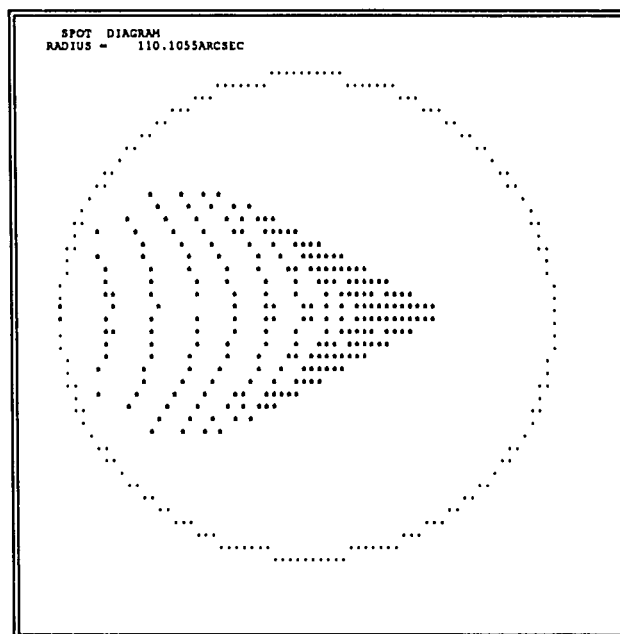
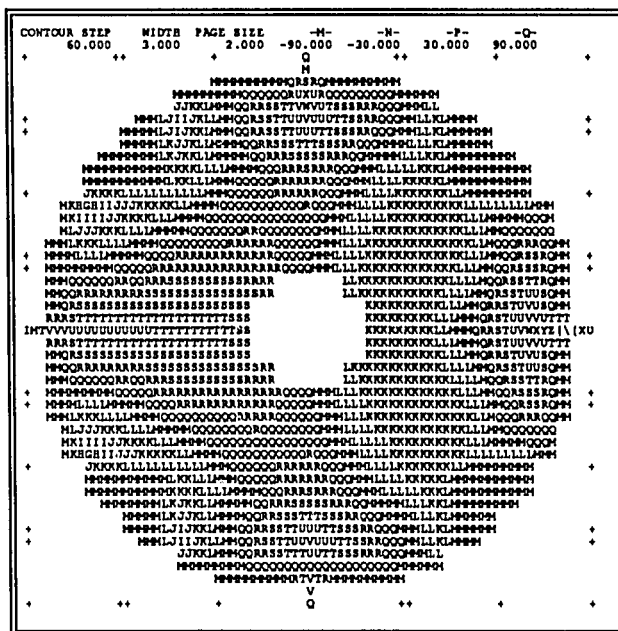


Figure 2.39 Contour Plot and Spot Diagram for Mode 9

CHAPTER 3

OPTICAL SUPPORT STRUCTURE

3.1 Background

The Optical Support Structure (OSS) is the upper part of the telescope truss structure with a task to maintain a zero pointing error condition when the telescope moves in the gravity field. It is a standard procedure to design the OSS so that the gravity deflection of the upper part (secondary mirror) and lower part (primary mirror) of the structure are balanced and thus maintain optical alignment. The OSS has the following main components:

- 1) Trunnion Beam
- 2) Forward Truss Structure
- 3) Primary Mirror Cell

The design of the truss also follows the principle of weight and stiffness optimization in order to minimize the gravity deflections. The structural eigen frequencies should be as high as possible in order to have a good dynamic performance of the truss, in order to maximize the frequency response of the telescope drives.

Therefore, the main design characteristics of the OSS design are light weight, small wind attack cross section, and high stiffness. Space tube structures are usually chosen to improve the performance with respect to the wind loading. In the finite element analysis of the OSS, the primary mirror, secondary mirror, and the instruments are considered as lumped masses. Given in Table 3.1 are the weights and geometry of the primary and secondary mirrors. Four different geometries were selected for the forward truss structure for gravity as well as wind loading. The four

trusses are shown in the Figure 3.1 are Modified Serrurier, Quad-Tripod, Double, and Octopod were analyzed for gravity and free vibration.

Free vibration analyses as well as static analyses were performed on all four structures and the modified Serrurier truss was chosen for best performance among the selected geometries. Listed in Table 3.2 are the natural frequencies and the maximum gravity deflections in both zenith and horizon cases. All four trusses approximately have the same mass. The Serrurier truss performed well in vibration and in the gravity field.

3.2 Trunnion Beam

Trunnion beam provides the link between primary mirror cell and the forward truss structure. It supports the elevation axis bearings. Also, it provides the adequate stiffness required to prevent vibration modes involving translation of the OSS along the elevation axis. The design goal for trunnion beam was to achieve the frequency of mode described above to a value greater than 12 Hz. The trunnion beam is a 15 inch \times 30 inch deep box fabricated with half inch plates. The corners were cut to provide clearance with the fork when the telescope is horizon pointing. The trunnion beam has interior stiffeners and load plates to create structural connections. Stiffeners were necessary at the elevation bearings, attachment points for the forward tube truss members, cell plate attachments, and side plate corners. The trunnion beam was analyzed along with the primary mirror cell and it is discussed in the next chapter.

3.3 Forward Truss Structure for the Four Meter Telescope

Serrurier truss was chosen for the forward truss structure. This structure provides support for the forty inch secondary mirror. The design criteria for this structure were as follows:

- 1) The nodding mode frequency of 12 Hz or more and
- 2) Deflections due to gravity within the range to be compensated by the secondary mirror.

Truss members were chosen to be standard tubular sections. These members connect the secondary mirror support structure to the trunnion beam.

The forward truss extends from the forward face of the trunnion beam to the secondary mirror support beams. It is composed of rectangular steel members on the top and the bottom planes of OSS. Secondary spider members are the part of secondary mirror support system. Individual spider members were designed to have frequencies higher than 40 Hz. The spider should be removable so as to allow installation and removal of the primary mirror. The forward truss structure without optimization was analyzed for free vibration modes. The modal frequencies and the shapes are described in Table 3.3. Optimization procedure described in chapter 6 was used to optimize the frequencies. Listed in Table 3.4 are the frequencies of the optimized structure after two iterations.

3.4 Summary

The results of the optimized trusses showed considerable improvement in all the cases considered for the study. This particular truss showed an increase of about 50% in the fundamental frequency. The gravity deflections were down by about 10%. The absolute deflection values of this forward truss alone do not describe the behavior of the OSS. Therefore the gravity deflections are reported for the assembled telescope only. The fore-aft or nodding frequency of the forward truss structure was 13.1 Hz after optimization which is above the 12 Hz minimum.

TABLE 3.1 PRIMARY AND SECONDARY MIRROR SPECIFICATIONS

PARAMETER	Primary Mirror	Secondary Mirror
Weight	8060 lbs	282 lbs
Outer Diameter	160 inches	40 inches
Inner Diameter	30 inches	No Hole

TABLE 3.2 FREQUENCIES AND DEFLECTIONS OF DIFFERENT TELESCOPE TRUSSES

Mode #	Modified Serrurier	Quad-Tripod	Double	Octopod
1	641	493	499	557
2	828	587	601	754
3	1074	978	989	1021
4	1393	1117	1065	1336
5	1722	1385	1424	1689
Maximum Deflection (Zenith)	4.37×10^{-6}	10.95×10^{-6}	10.48×10^{-6}	6.89×10^{-6}
Maximum Deflection (Horizon)	1.49×10^{-5}	2.91×10^{-5}	2.80×10^{-5}	1.93×10^{-5}

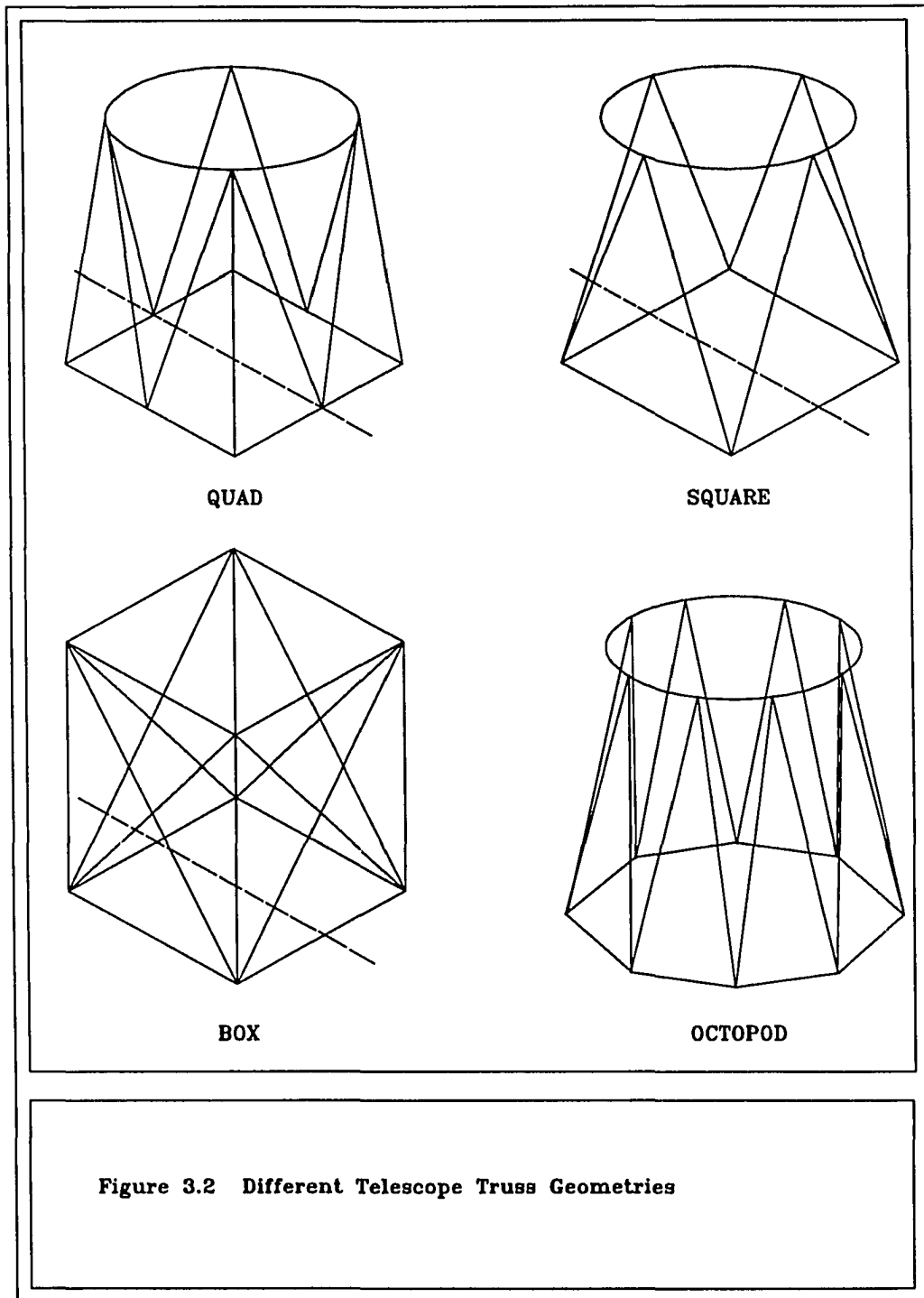
Note: All the frequencies are in Hertz and the deflections are in inches.

TABLE 3.3 Mode Shapes of the Original Structure

Mode	Frequency (Hz)	Mode Shape
1	8.5	Fore-Aft Translation
2	8.7	Lateral Translation
3	10.8	Rotation about Altitude Axis
4	12.7	Altitude Disks Out of Plane Bending
5	12.7	Orthogonal to Mode 4

TABLE 3.4 Mode Shapes of the Optimized Structure

Mode	Frequency (Hz)	Mode Shape
1	13.1	Fore-Aft translation
2	13.5	Lateral translation
3	14.0	Rotation about azimuth axis
4	16.1	Rotation about altitude axis
5	18.7	Out of plane bending



CHAPTER 4

DESIGN OF THE PRIMARY MIRROR CELL, FORK, AND SECONDARY MIRROR

4.1 Background

Design of the primary mirror cell, fork, and analysis of a support system of secondary mirror are described in this chapter. The primary mirror cell houses the primary mirror, instruments, counter weights, bellofram supports, and elevation drive. Therefore, the mirror cell should be stiff enough to withstand the gravity load and the wind load. Also, the mirror cell design depends on the axial and radial support systems of the primary mirror. The four meter telescope design consists of an alt-azimuth fork mount. This fork serves as the support structure for the OSS. The OSS transfers the load to the fork through the altitude bearings. The rolling element bearings define the altitude axis and azimuth axis. The fork assembly consists of azimuth drive disk, fork weldments, pillow blocks, altitude axles, and azimuthal bearings. Shown in Figure 4.3 is an alt-azimuth fork mount.

4.2 Design of the Primary Cell

The mirror cell mainly consists of cell bottom and cell wall. The cell bottom holds bellofram supports for the passive control system as described in Chapter 2, supports the hard points (mirror defining points), and counterweights. The cell wall connects the cell bottom and the trunnion beam. If the primary mirror is

supported by the outer edge and inner edge support system, the wall provides hard radial support to the mirror. The cell bottom consists of radial and circumferential web plates, covered by a top plate. The top plate was a curved plate with the curvature same as that of the primary mirror. This top plate supports belloframs. The mirror cell has Cassegrain hole in the center. The choice of the material depends on the primary mirror material, because well matched coefficients of thermal expansion yields better results from the thermal point of view. Steel was chosen here. The mirror weight is distributed according to the bellofram support locations. Shown in Figure 4.2 are the dimensions of the primary mirror cell. Static and free vibration analyses were performed.

For the design and analysis of the cell structure it has been assumed that the primary mirror, a thin meniscus mirror supported axially and radially by 66 point forces, which are arranged in 4 rings. The total load on the cell for this configuration was about 14000 lbs. The main cell structure consists of 6 radial ribs, which were connected by four rings. The central hole of the cell has a diameter of 32 inches and may house a Cassegrain adapter and instruments.

The finite element model of the cell which has been prepared for the static and dynamic analyses is shown in Figure 4.2.

When the telescope is in operation, the primary mirror cell and consequently the mirror suffer from the vibrations which are induced by the drives and the wind forces. Free vibration analysis was done to study the natural vibration modes and the eigen-frequencies related to them to make sure that no resonances occur. Listed in Table 4.1 are the eigen-frequencies and the mode shapes.

4.3 Design of the Fork

The fork structural design was intended to maximize stiffness and reduce weight to achieve relatively high modal performance, so that the hydrostatic bearings were not necessary.

Low weight and stiff structure yields smaller gravity deflections and higher structural resonant frequencies. Low weight also improves the thermal performance to the ambient temperature changes. Stiff structure guarantees a proper tracking stability under all loading conditions. The design of the fork structure was optimized using the stress optimization program which was described in Chapter 6, in order to transfer the load of the tube from the altitude to the azimuthal bearings in the most efficient way. The fork basically consists of two pedestals and a base. Main functions of the pedestals are to provide the bending and torsional stiffness. The distance between the altitude and the plane of azimuth pads has been minimized to obtain the best vibrational performance. Listed in Table 4.2 is the distribution of weight which comes on to the elevation axis. Listed in Table 4.3 are the mass moments of inertia. Finite element analyses of the fork for vibrational performance were made and the mode shapes described in Table 4.4 belong to the optimized structure. The finite element model is shown in the Figure 4.4. The first three frequencies were low because of the lack of stiffness of the azimuthal bearings. The fourth mode was the bending mode at 14.2 Hz.

4.4 Analysis of Support System of a Secondary Mirror

A forty inch honeycomb mirror was selected for the secondary mirror. The geometry is shown in the Figure 4.5. Finite element model of the honeycomb mirror is shown in Figure 4.6. Only half model was created to save CPU time. A simplified

equation was presented by Barnes (1972) for computing the equivalent thickness of the hexagonal honeycomb structure was used to compute equivalent thickness of the mirror. The equation for computing equivalent plate thickness (t_b) was given by:

$$t_b^3 = (2t_f + h_c)^3 - (1 - \frac{\eta}{2}) h_c^3$$

where,

t_b = Equivalent plate thickness

t_f = Flange thickness

h_c = Thickness of the core

$\eta = \left(\frac{2b + t_w}{b + t_w} \right) t_w$

b = Length of the hexagonal side

t_w = Web thickness

The values for these parameters are given in Table 4.5. Material properties are listed in Table 4.6.

The equivalent thickness (t_b) was computed to be 4.59 inches. The finite element model shown in Figure 4.6 (B) represents the model with equivalent thickness. Both the mirrors were supported at three points at a radius of 14 inches. Both the mirrors were analyzed under gravity loading for structural deformations and program FRINGE was used to compute the values of rms deflections and spot diagram radius. The deflections and spot diagram radius from the analysis of the meniscus mirror compare very well with that of the honeycomb mirror analysis. Listed in Table 4.7 are the rms and spot diagram size for both the mirrors and for both the orientations. A total number of 388 nodes and 650 elements were created for the half honeycomb mirror. For the meniscus mirror with the equivalent thickness, a total number of 157 nodes and 252 elements were created for the full model.

The rms values exceeded the error budget with a three point support. A six point support system was introduced and analysed for the ZENITH and HORIZON cases. Shown in Table 4.8 are the results from this analysis. The results were within the allowable error budget.

4.5 Summary

The fundamental frequency of 14.2 Hz for the primary mirror cell has been achieved. The bending mode criterion with a frequency of 14.2 Hz has been achieved for the fork. The optimization procedure using mode shapes as described in chapter 6 was useful. Only modes 4 through 6 were used to optimize the fork. A six point support system was necessary to achieve the rms error under 0.1 waves for the secondary mirror. Gravity deflections for the complete assembly are presented in Chapter 5.

TABLE 4.1 Mode Shapes of the Optimized Cell Structure

Mode	Frequency (Hz)	Mode Shape
1	14.2	Rotation about the optical axis
2	15.9	Lateral cell movement
3	18.3	Bending about altitude axis
4	20.1	Piston action

TABLE 4.2 TOTAL WEIGHT ON THE ELEVATION AXIS

DESCRIPTION	WEIGHT (lbs)
Primary Mirror	8060
Axial and Radial Support System	4752
Secondary Mirror	282
Secondary Mirror Cell	400
Instruments	1600
Counter Weight	1500
OSS Assembly	21904
Total Weight	38498

TABLE 4.3 MASS MOMENTS OF INERTIA ON THE ELEVATION AXIS

AXIS	MASS MOMENT OF INERTIA (lbs-in ²)
I_{xx} (Altitude)	2.96×10^8
I_{yy} (Perpendicular)	2.73×10^8
I_{zz} (Optical)	2.56×10^8

TABLE 4.4 Mode Shapes of the Optimized Fork

Mode	Frequency (Hz)	Mode Shape
1	6.1	Rotation about optical axis
2	9.2	Rocking motion in x direction
3	11.6	Rocking motion in y direction
4	14.2	In plane bending of the arms
5	16.7	Out of plane bending

TABLE 4.5 HONEYCOMB MIRROR SPECIFICATIONS

PARAMETER	VALUE (INCHES)
t_f	0.500
h_c	5.000
b	2.500
t_w	0.125
η	0.909

TABLE 4.6 MATERIAL PROPERTIES OF THE SECONDARY MIRROR

MATERIAL PROPERTY	VALUE
Mass density (ρ)	0.08058 lb/in^3
Young's Modulus (E)	8.9487 lb/in^2
Poisson's Ratio (ν)	0.20

TABLE 4.7 (A) GRAVITY DEFLECTIONS OF THE SECONDARY MIRROR (ZENITH)
with a Three Point Support System

MIRROR	MAXIMUM DEFLECTION (inches)	rms (waves)	pv (waves)	SPOT DIAGRAM RADIUS (arc secs)
Honeycomb Mirror	-1.97×10^{-5}	0.36	1.59	0.9189
Meniscus Mirror	-2.02×10^{-5}	0.41	1.62	0.9021

TABLE 4.7 (B) GRAVITY DEFLECTIONS OF THE SECONDARY MIRROR (HORIZON)
with a Three Point Support System

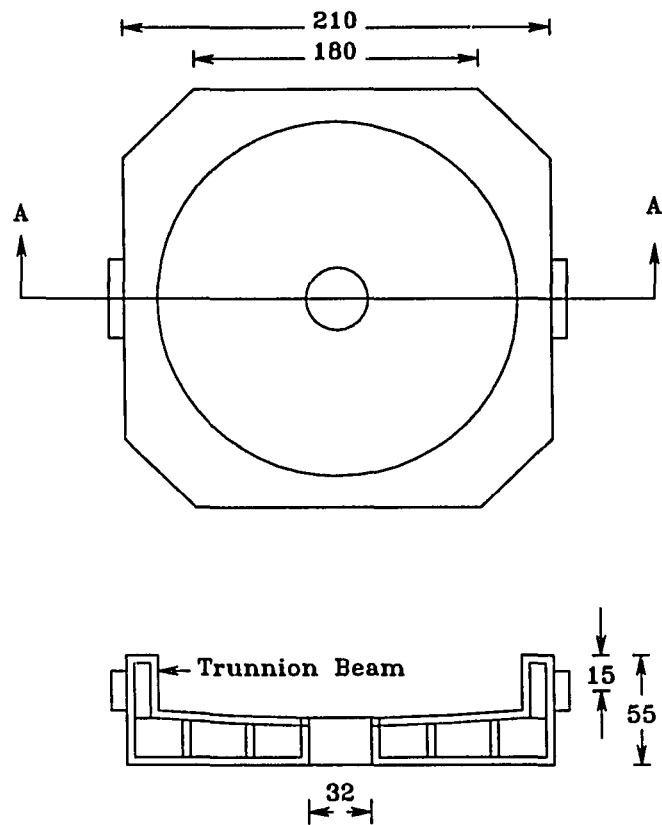
MIRROR	MAXIMUM DEFLECTION (inches)	rms (waves)	pv (waves)	SPOT DIAGRAM RADIUS (arc secs)
Honeycomb Mirror	-2.33×10^{-6}	0.08	0.377	0.2652
Meniscus Mirror	-2.48×10^{-6}	0.09	0.395	0.2701

TABLE 4.8 (A) GRAVITY DEFLECTIONS OF THE SECONDARY MIRROR (ZENITH)
with a Six Point Support System

MIRROR	MAXIMUM DEFLECTION (inches)	rms (waves)	pv (waves)	SPOT DIAGRAM RADIUS (arc secs)
Honeycomb Mirror	-3.12×10^{-6}	0.060	0.30	0.1021
Meniscus Mirror	-3.26×10^{-6}	0.071	0.31	0.0989

TABLE 4.8 (B) GRAVITY DEFLECTIONS OF SECONDARY MIRROR (HORIZON)
with a Six Point Support System

MIRROR	MAXIMUM DEFLECTION (inches)	rms (waves)	pv (waves)	SPOT DIAGRAM RADIUS (arc secs)
Honeycomb Mirror	-0.40×10^{-6}	0.021	0.061	0.0451
Meniscus Mirror	-0.42×10^{-6}	0.026	0.065	0.0432



Section A-A

Units : Inches

Plot not to scale

Figure 4.1 Primary Mirror Cell and Trunnion Beam

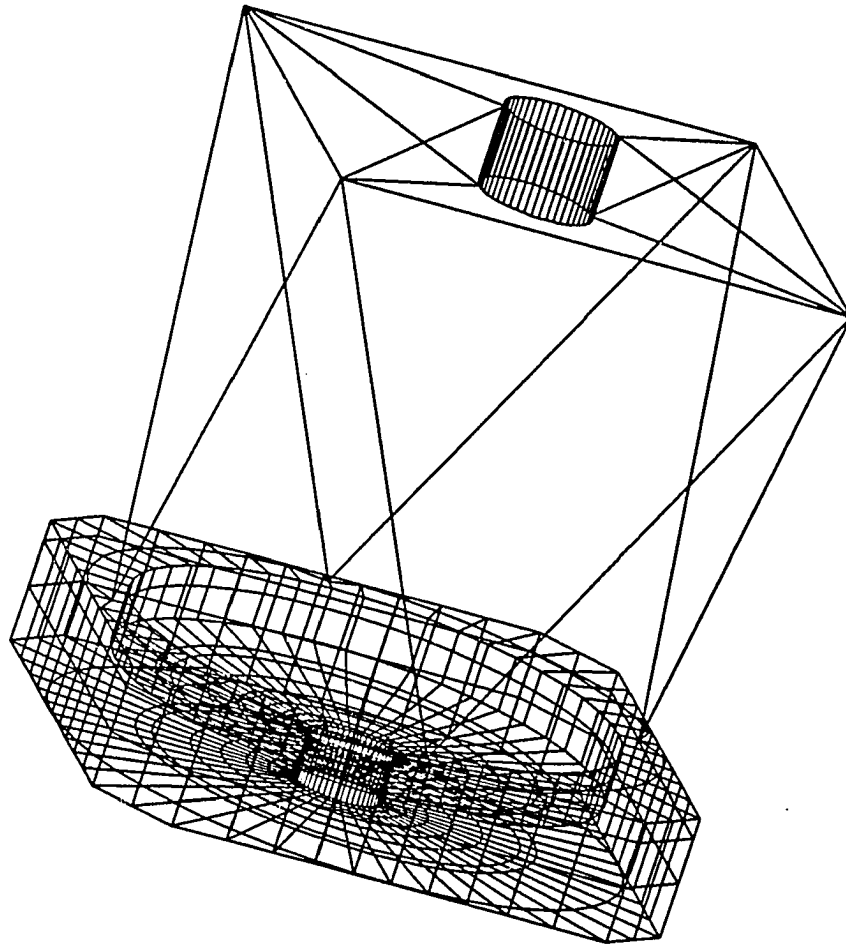


Figure 4.2 Finite Element Model of the Cell and OSS

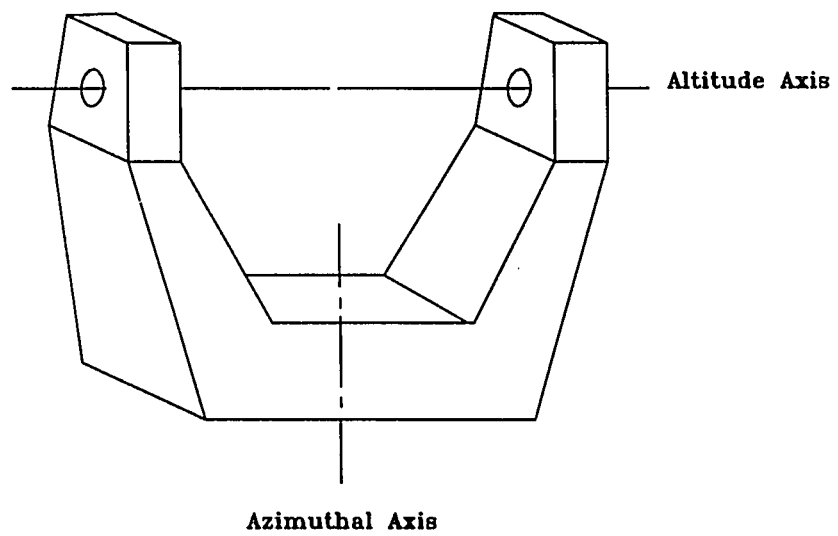


Figure 5.1 Altazimuth Fork

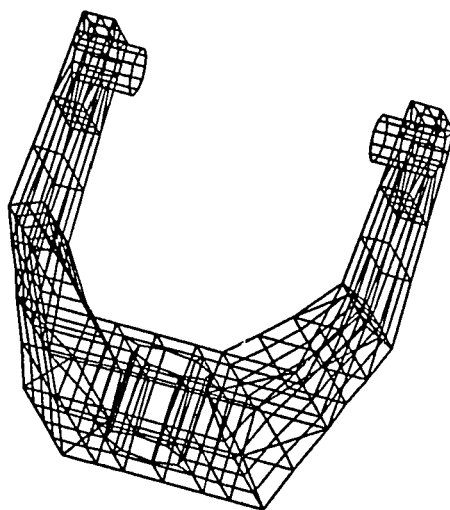
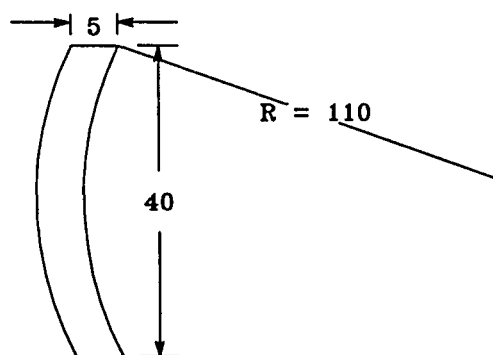


Figure 4.4 Finite Element Model of the Fork

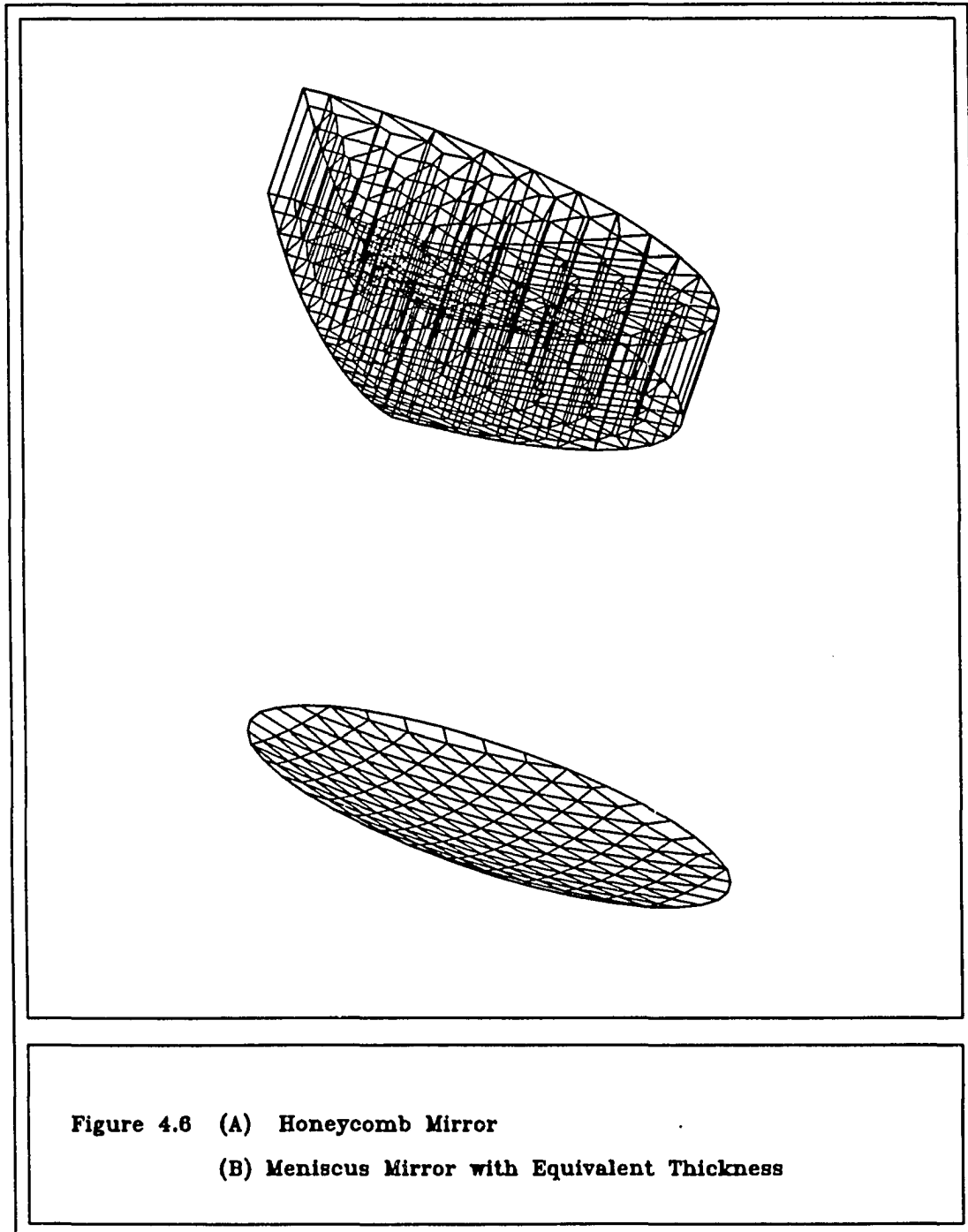


Honeycomb Secondary Mirror

Units : Inches

Plot not to Scale

Figure 4.5 Secondary Mirror for the Four Meter Telescope



CHAPTER 5

ANALYSIS OF THE TELESCOPE ASSEMBLY

The telescope assembly is analyzed for the gravity deflections as well as the resonant frequencies to study the overall performance. The finite element model shown in the Figure 5.1 represents the complete model without the azimuthal bearings. Listed in Table 5.1 are the resonant frequencies of the telescope. The translational modes are reliant on stiffness of the fork structure than on support stiffness. The locked rotor azimuth mode is much more reliant on drive stiffness than it is on the stiffness of the fork structure. The finite element model was created to determine optical misalignments due to rotating through the gravity field. This was done by applying zenith and horizon gravity loads separately and combining their effects. Listed in Table 5.2 are the gravity deflections of the center nodes of primary and secondary mirrors, when the telescope is rotated from zenith to horizon. The telescope structure has to keep the mirrors in place with tolerances as allowable static deflections which are set at 0.02 inches for the maximum translation and 0.04 degrees for the maximum rotation. The deflections values listed in Table 5.2 show that they are within these limits.

TABLE 5.1 Mode Shapes of the Optimized Telescope

Mode	Frequency (Hz)	Mode Shape
1	12.1	Nodding about elevation axis
2	13.2	Lateral translation
3	16.1	Axial movement secondary mirror support spider
4	18.2	Fork rotation about azimuthal axis
5	22.1	Rotation about altitude axis
6	24.2	Flexure of tube truss members

TABLE 5.2 GRAVITY DEFLECTIONS (HORIZON-ZENITH)

Mirror	Translations			Rotations		
	TX	TY	TZ	RX	RY	RZ
Primary	4.89×10^{-4}	1.42×10^{-2}	1.62×10^{-2}	1.41×10^{-2}	-0.77×10^{-5}	1.61×10^{-4}
Secondary	0.72×10^{-4}	1.82×10^{-2}	1.89×10^{-2}	2.01×10^{-2}	3.10×10^{-6}	-2.92×10^{-6}

Units: Displacements – Inches

Rotations – Degrees

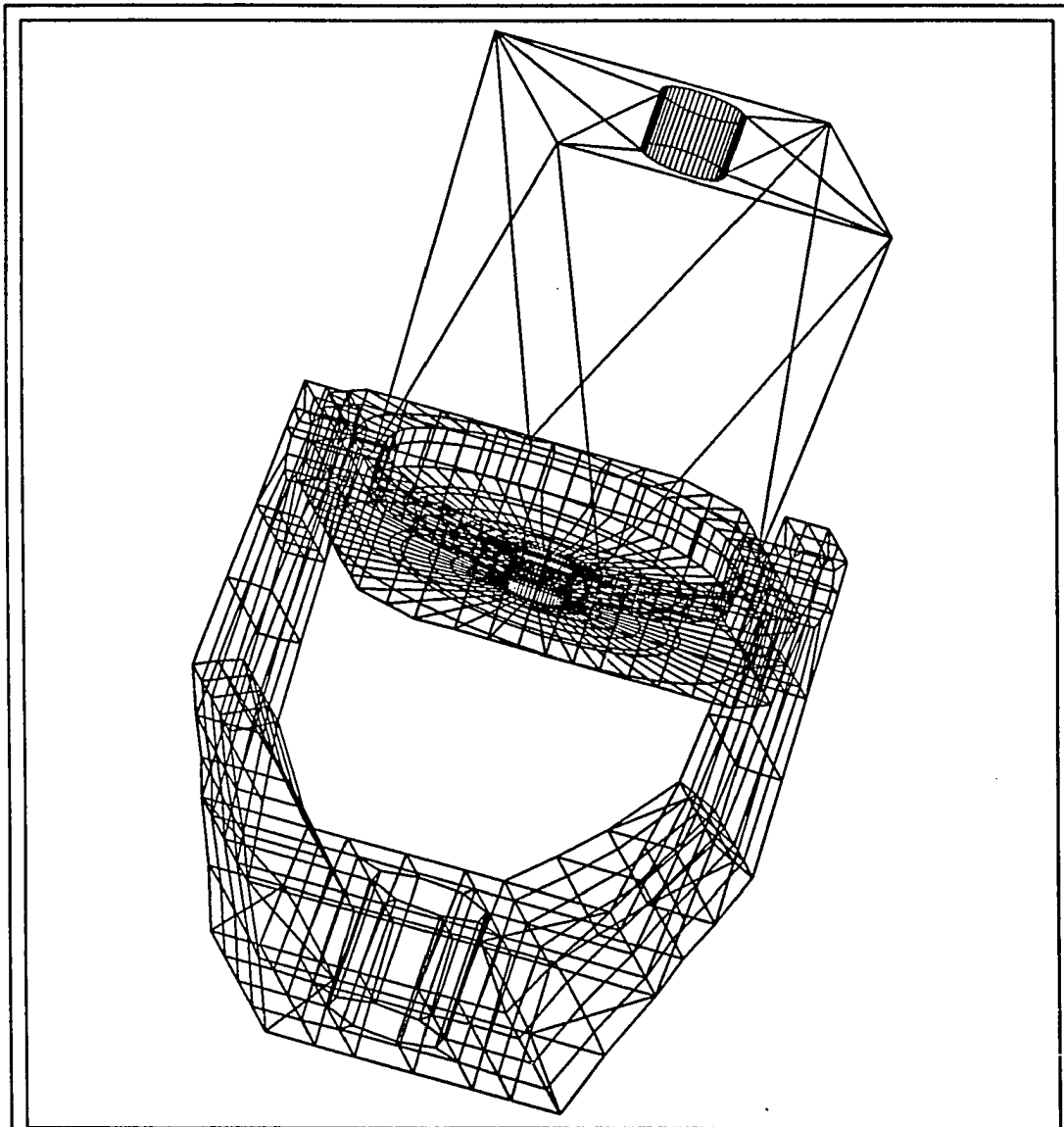


Figure 5.1 Finite Element Model of the Telescope Assembly

CHAPTER 6

OPTIMIZATION PROCEDURES

6.1 Background

The objective in structural optimization is generally to minimize the weight of the structure and satisfy all the imposed constraints. The loads applied to the structure and the geometry are specified, and the unknowns are the individual sizes of the members. The constraints imposed on the structure may include maximum allowable stress, displacement limits at the nodal points, frequency constraints, etc. The main purpose of many optimal design research projects is to find the most effective optimization technique. In the design of optimal structures it is customary to have a wide choice of design variables whose variations may influence the magnitude of the quality criterion. For example, a reduction in the weight in structure may be accomplished by altering the distribution of the thickness of the members, controlling anisotropy, reinforcing, prestressing, etc. From engineering point of view the constraints of structural optimization may be classified in two groups: behavioral constraints and technological constraints. Behavioral constraints refer, for example, to strength, stiffness, stability, vibration of structures under given system of loading. Manufacturing reasons may require that the cross-section of individual members are the same: such a requirement is a technological constraint. It is important to discover which specific

methodology of optimization or which combination of techniques results in the largest gain for a given functional.

Classical single purpose problems of structural optimization are characterized by the assumption that the loads, the manner of support, and various demands concerning the stressed - deformed state are stated in definite unique fashion, and that the purpose of the structure is also unique. Therefore, the design process may be accomplished within the framework of a single computational scheme. For example, in beam designs only the bending loads as external forces may be considered, and in the design of columns, only the buckling loads. A simple and efficient method known as the "Fully Stressed Design (F.S.D)" concept is the most popular resizing algorithm. This intuitive approach filled the need for automated sizing for strength requirements and no such method is available for automating the strength as well as stiffness requirements.

Finite element techniques enable the structural engineer to analyze the extremely complex structural systems. The trend is now towards automated design methods. During recent years, a number of advances have been made in the automated design of structures. Such advances generally fall into one of the following three categories:

- 1) Application of mathematical programming methods to relatively small components of structures. Tocher and Karnes (1971) described these methods.
- 2) Application of the above mentioned "optimality criteria" methods to large structural assemblies: for example, the well known "Fully Stressed Design (F.S.D)" to design for strength. This procedure is described by Giles (1971).
- 3) Application of weight-strength analysis to determine efficient structural properties, a method proposed by Shanley (1972).

As discussed earlier, there can be several optimization schemes available for a given problem. It is important to study the effectiveness and the validity of the method.

6.2 Optimization Procedures

The minimization of weight is the most typical objective in many structural optimization problems. In the design of telescope structures, it is important to note that, stiffness is as important as the strength of the structure. When structure design criteria are first considered the subject turns to the eigen-frequency as a measure of performance. The reason this is used is that for any telescope the fundamental eigen-frequency is proportional to the square root of the deflections under gravity, and thus it is a measure of telescope sag and it is the most important mechanical input into the servo analysis. It determines how well the optics have positioned and how well the telescope tracks. The reason that eigen-frequencies are important to servos is that they cause a phase shift. This means that well below the eigen-frequency, when a servo position is low, one pushes it higher to get it to the desired position. But above the eigen-frequency, if it is low, and one pushes it higher, by the time the servo activates (phase lag) the error has moved higher and makes it worse. The structural eigen-frequencies should be as high as possible in order to have good dynamic performance of the telescope in order to maximize the frequency response of the telescope drives. The performance requirements for telescope structures have been increasing nearly as fast as the aperture requirements. The more sophisticated tools that are available to current designer have predicated the very efficient design in use today.

Engineering tools such as truss design, the finite element method and optimization are necessary to make an efficient design. Basic assumptions and initial constraints are probably more important in determining the telescope performance. Design and optimization just determine how close to that performance one can get. Several types of optimum design procedures for structures are of interest from practical engineering stand points of view. In this study, a method of optimum structural design is proposed and the validity and effectiveness of the methods are revealed by two numerical examples. The procedure is summarized in Table 6.1. This method uses the stresses obtained from free vibration analyses and gravity loading analyses. The stresses obtained from the free vibrational analyses are not actual stresses, because of the fact that they are obtained for a normalized eigen-vector. The following three methods are studied to evaluate the effectiveness:

- A) Optimization without weighting the frequencies.
- B) Optimization with weighting by the frequencies linearly.
- C) Optimization with weighting by the square of the frequencies.

From hereon, these methods are referred to methods A, B, and C. These optimization procedures are applied to the design of the optical support structure, mirror cell, and the fork and evaluated for the effectiveness. The procedure is described in this section. Beams and framed structures are taken as simple structures in the following numerical examples. These structures are idealized as connected systems of n uniform finite elements by the finite element method. The free vibrational and gravity analyses were done using finite element method. The length, density, and Young's modulus were the same for all elements. However, the cross sectional area and the moments of inertia were modified to achieve the

optimum frequency. A simple truss , a cantilever beam, and a simply supported beam were optimized using the methods A, B, and C to demonstrate the effectiveness of these procedures which were implemented by a FORTRAN program. The NASTRAN output was the input to this program for optimization. The steps involved in the procedure are as follows:

- 1) Run the free vibration analysis with the option to normalize the eigen vector to unit value of the largest displacement component in the analysis set

- 2) Obtain the stresses for the first six mode shapes. The number of mode shapes necessary to optimize the stiffness of the structure was determined after analysing several structures. Initially, only the first mode shape was considered. But, the manipulation of stiffnesses of the structural members during optimization using mode 1 only affected the higher modes. When optimization using mode 1 only, the fundamental frequency decreased for some telescope structures. When the difference in the first few eigen-frequencies is very small, the above phenomena were observed. After analysing several different structures, it was concluded that at least six modes are necessary for this optimization procedure.

- 3) Run the gravity loading analyses for the zenith and horizon cases

- 4) Obtain the stresses under these gravity loadings

- 5) Input these stress data to the FORTRAN program. This program evaluates the participation of each member of the structure in terms of stress, in first six mode shapes under free vibration, and both the gravity (Zenith and Horizon) cases

- 6) The optimization FORTRAN program rates the active members and inactive members in a scale of 1 to 10 for methods A, B, and C. The stresses (axial, bending, effective, maximum, etc.) are sorted out for the complete

structure and divided into ten groups. Then each member of the structure is rated depending on the value of stresses. Most active member is given a value of 1 and a value of 10 is given to the least active member.

- 7) Stiffnesses of the members are then changed accordingly
- 8) Then the model is run for the free vibration and for the gravity loading
- 9) The gravity stresses are then compared with the stress limits.

The results for the simple truss shown in Figure 6.1 show an increase of about 15 % in the fundamental frequency and a decrease of about 15 % in the gravity deflections. The total mass was kept approximately the same in this analysis. Listed in Table 6.2 are the modal frequencies for this optimized model and the original model. A cantilever beam was analysed under free vibration and the eigen-frequencies are listed in the Table 6.3, and the optimization process described previously was applied to this model. This model has 10 beam elements and 11 nodes. The fundamental frequency increased from 1107 Hz to 1544 Hz. Total mass of the original model and that of the optimized model was kept the same in order to make a comparison. Shown in Figure 6.2 are the original and optimized cantilever beams. Listed in Table 6.3 are the first six frequencies of the original and optimized cantilever model. Also, a simply supported beam was analysed under free vibration and the eigen-frequencies are listed in the Table 6.4. Then, the optimization process described previously has been applied to this model. This model also has 10 beam elements and 11 nodes. The fundamental frequency increased from 3022 Hz to 3259 Hz. Total mass of the original model and that of the optimized model was kept the same to make a comparison. Shown in Figure 6.3 are the original and optimized simply supported beams. Listed in Table 6.4 are the first six frequencies of the original and optimized model.

6.3 Optimization of Mirror Support System Using Modal Frequencies

As described in Chapter 2, the primary mirror support design is the critical part of a telescope design. Optimization of the support system using the procedure described in Figure 2.14 is a lengthy process. From the analysis procedure describes in Chapter 2, an estimate of the time required by the lengthy procedure to optimize the support system for a mirror can be made. The procedure of preparation of the data for the finite element program, FRINGE command file generation, extraction of the structural deformations from the NASTRAN output, using that data in the program FRINGE, and extracting the optical parameters from the FRINGE is very cumbersome. Since the modal frequencies are directly proportional to the stiffness of the structure, and the stiffness is proportional to the deflections of the structure under gravity loading, a simplified procedure is presented using modal frequencies to reduce the time involved in this initial iterative process. Instead of computing the rms deflections, 80 % encircled energy diameter, etc., computation of the modal frequencies could yield the same optimized support system. A four meter mirror with the support locations shown in Figure 6.4 with fewer nodes was used to demonstrate this procedure. A six point support system was used and the support radius for each of the four models is listed in Table 6.5. This model with four different support topologies demonstrates the effectiveness of the above procedure. Spot diagram radius and rms deflections were calculated for these four support conditions. A detailed study was performed to understand which mode shapes or modal frequencies directly predict the behavior of the support structure and the deflections of the mirror in terms of optical aberrations. It was concluded that the fundamental frequency or piston frequency is directly proportional to the rms deflections and

the radius of the spot diagram. Listed in Table 6.5 are the fundamental frequencies and the piston frequencies along with the rms and spot diagram values. The higher fundamental or piston frequency means a better support system for the mirror. The regular procedure described in the previous sections and the procedure described in this section yield the same results. Therefore, this simplified procedure should be used, as it reduces significantly the amount of time involved in the above described iterative process.

6.4 Summary

The procedures to optimize structural eigen-frequencies and deflections were proven effective for all the structures considered. Method A was used to analyze an eight meter telescope. This procedure improved the fundamental frequency from 8.1 Hz to 11.7 Hz. Similar improvements were observed for a 1.8 meter Vatican telescope and a 6.5 meter Multiple Mirror Telescope. Method A is more effective in increasing the values of higher frequencies as it weighs all the modes equally. Methods B and C weigh the modes according to the corresponding eigen-frequency as described above. Thus, the fundamental frequency is represented with the highest ratio. The higher eigen-frequencies for structures analyzed decreased in value, during optimization when methods B and C were used. Method A was found to be effective for beams as well as truss structures. The modal frequencies procedure to optimize the mirror support structure was very useful in the design process.

TABLE 6.1 OPTIMALITY CRITERIA

Model	Description
Analyses	Free Vibration and Gravity Analyses (Zenith and Horizon)
Design Variable	Element Mass (m_i)
Constraints	$\sum_{i=1}^N m_i = \text{Constant}$
Objective	Increase the Fundamental Frequency

TABLE 6.2 STRUCTURAL OPTIMIZATION OF A TRUSS
USING MODAL ANALYSIS

Mode #	Original Frequency	Method A	Method B	Method C
1	505	633	682	697
2	505	633	682	697
3	624	735	689	641
4	1183	1262	1101	1082
5	1340	1531	1287	1243

TABLE 6.3 STRUCTURAL OPTIMIZATION OF A CANTILEVER BEAM
USING MODAL ANALYSIS

Mode #	Original Frequency	Method A	Method B	Method C
1	1107	1544	1689	1701
2	1107	1544	1689	1701
3	4964	5835	5362	5287
4	6862	7424	6782	6663
5	6862	7424	6782	6663
6	14771	15013	13042	12872

TABLE 6.4 STRUCTURAL OPTIMIZATION OF A SIMPLY SUPPORTED BEAM
USING MODAL ANALYSIS

Mode #	Original Frequency	Method A	Method B	Method C
1	3022	3259	3490	3511
2	3022	3259	3490	3511
3	8898	9032	8642	8317
4	12488	13047	11488	11112
5	12488	13047	13047	11112
6	19552	20064	18154	17689

TABLE 6.5 OPTIMIZATION USING MODAL FREQUENCIES

r/R	RMS (WAVES)	SPOT DIAGRAM RADIUS (ARC SECS)	PISTON MODE FREQUENCY (HERTZ)	FUNDAMENTAL FREQUENCY (HERTZ)
0.33	183.96	10916	48.90	34.50
0.50	88.61	9333	65.36	53.51
0.70	49.10	5155	81.03	58.79
1.00	161.74	14754	46.14	46.14

R = Outer Radius

r = Support Radius

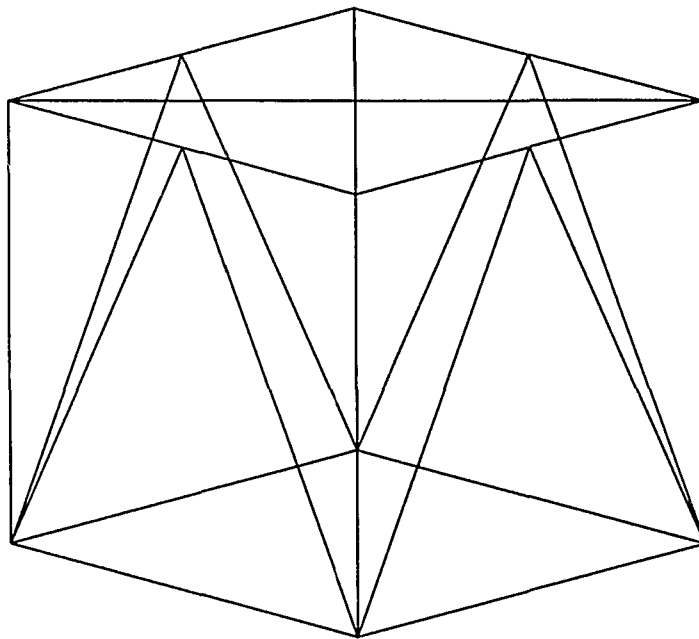
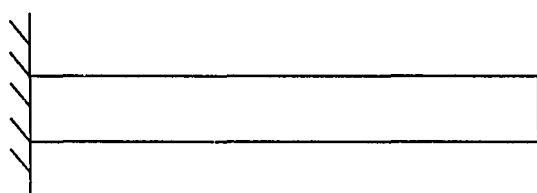
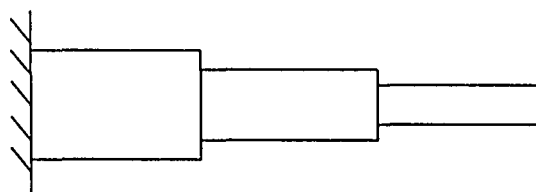


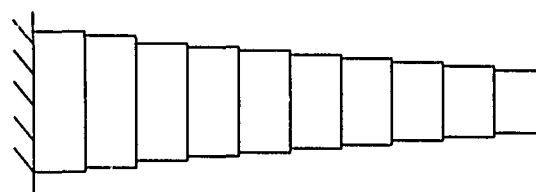
Figure 6.1 Simple Truss for Optimization Procedure



Original Model (Uniform Cross Section)

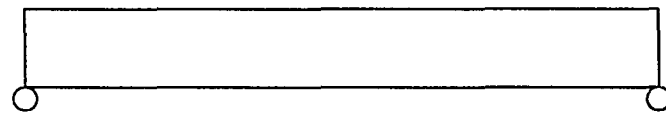


Optimized Model (without weighting frequencies)



Optimized Model (weighting frequencies linearly)

Figure 6.2 Optimization of a Cantilever Beam



Original Model (Uniform Cross Section)



Optimized Model (without weighting frequencies)



Optimized Model (weighting frequencies linearly)

Figure 6.3 Optimization of a Simply Supported Beam

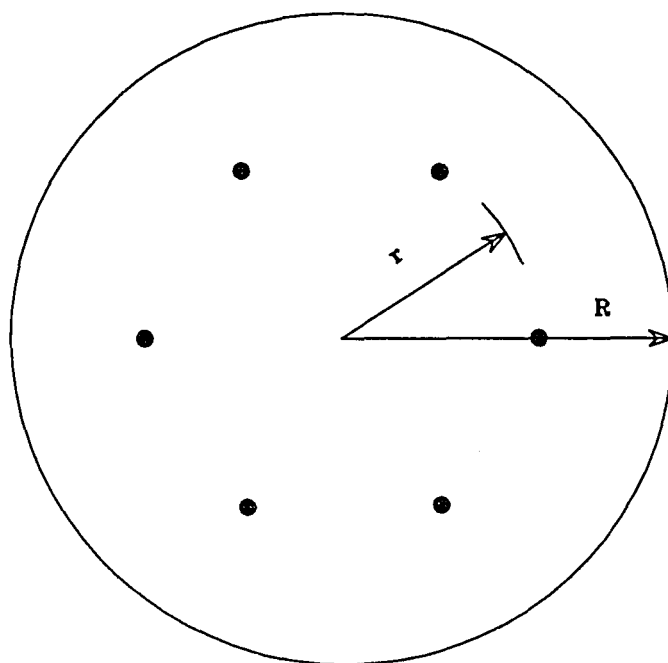


Figure 6.4 Model used for the modal frequencies procedure

CHAPTER 7

CONCLUSIONS

In this dissertation, a support topology for axial and radial support systems for a four meter meniscus mirror for an optimum optical performance is presented. A procedure is developed using modal frequencies to minimize the steps to obtain the optimum support locations for a four meter meniscus mirror. The optical performance evaluation for a forty inch honeycomb as well as the equivalent meniscus mirror is performed. The support conditions were designed to limit the optical aberrations within a selected error budget.

A handling stress analysis was done for the four meter meniscus mirror for various conditions with stress limited to 500 psi. Effects of finite element grid pattern such as quadrilateral and triangular mesh on the optical parameters such as spot diagram radius and rms are studied. Quadrilateral mesh yielded aberrations of about 7% more than that of triangular mesh. An analysis to determine the minimum number of nodes in the finite element model without losing the accuracy in the FRINGE analysis is presented. A free vibration analysis is performed to study the vibration modes of the primary mirror.

The structural performance is evaluated for the other telescope components, i.e. the fork, optical support structure, and mirror cell. A procedure to optimize the stiffness as well as the strength is proposed and applied to the analysis of fork, optical support structure, and cell. Results showed an increase of about 15% in the fundamental frequency and similar improvements are observed in the

higher frequencies and the gravity deflections. The telescope assembly is analyzed for the gravity deflections as well as the resonant frequencies to study the overall performance. The four meter telescope presented here performs well under gravity deflections as well as under vibration.

GLOSSARY

ABERRATION:

The degree an image passed through a lens differs from first order equation predictions of where it should be and what it should it look like.

ASPECT RATIO:

The ratio of the diameter of a lens or mirror to its thickness, e.g., 10:1 - mirror diameter is 10 times its thickness.

ASTIGMATISM:

An aberration that occurs when the tangential and radial images do not coincide. The image of a point source is not a point but takes the form of two lines.

CELL:

A housing surrounding a lens element.

COMA:

The variation of magnification with aperture. Rays passing through the edge portions of lens are focussed at a different height on the focal plane from those passing through the centre. The image resembles a comet or flare, rather than a point.

FOCAL LENGTH:

The distance from the principal surface of an element or system to the point where parallel rays of light impinging on it are focussed.

f/NUMBER:

The ratio of the focal length of a lens to its clear aperture.

SAG:

This term is used two ways:

- 1)The distance a curved optical surface deviates from flat surface over its aperture or diameter (also called "sagitta")
- 2)The amount an optical element droops under gravity loading.

WAVEFRONT:

The optical distortion observed or photographed after reflection from or transmission through a tested optical component.

WAVEFRONT DISTORTION:

The departure of a wavefront from a plane or spherical wave as it passes through an optical element (or reflected from it).

WAVELENGTH:

The wavelength of the electromagnetic radiation for a helium neon laser (red) is 0.633×10^{-6} metres.

REFERENCES

- Anderson, D., 1982, *Fringe Manual*, Version 3 , Optical Sciences Center, University of Arizona, Tucson, AZ.
- Anderson, D. and R. E. Parks, 1982, *SPIE - The International Society for Optical Engineering*, Vol. 332, " Gravity Deflections of Light Weight Mirrors. "
- Balick, B. and Ed Mannery, 1983, *SPIE Advanced Technology Optical Telescopes II*, Vol. 444, pp. 12-18 : " Concept Design of a Precision, Versatile, Inexpensive 3- to 4-Meter Class Telescope. "
- Ballio, G., R. Contro, C. Poggi, and O. Citterio, 1984, *IAU Colloquium : Very Large Telescopes, Their Instrumentation and Programs*, N. 79, pp. 75-94 : " A Finite Element Approach to the Design of the Support System for the ESO 1 m Active Optics Experiment."
- Barnes, W. P., Jr., 1969, *Applied Optics*, Vol. 8, No. 6, pp. 1191-1196 : " Optimal Design of Cored Mirror Structures. "
- Baustian, W. W., 1966, *A Symposium on Support and Testing of Large Astronomical Mirrors*, pp. 150-154 : " Mirror Cell Design. "
- Bella, D. F., 1988, *Optical Engineering*, Vol. 27, No. 2, pp. 111-114 : " Combining Optical Fringe Analysis and the Finite Element Method. "
- Blanco, D. R., C. Corbally, R. H. Nagel, and N. J. Woolf, 1990, *SPIE Advanced Technology Optical Telescopes IV*, Vol. 1236, pp. 905-911 : "Advanced Technology in the VATT. "
- Bliss, R., 1966, *A Symposium on Support and Testing of Large Astronomical Mirrors*, pp. 234-243 : " Axial Support Systems Utilizing Pneumatic or Hydraulic Cylinders, Servo controlled by Measurement of Defining Pad Load. ", Kitt Peak National Observatory and University of Arizona, Tucson, Arizona.
- Chi, C., Aaron Ostroff and Praveen Mehta, 1980, " Vibrational Modes Of The Primary Mirror Structure In The Large Space Telescope System", The Perkin-Elmer Corporation, Wilton, Connecticut.
- Cho, M. K. and R.M. Richard, 1989, *PCFRINGE*, " An Optical Performance Program Using Structural Deflections", University of Arizona, Tucson, AZ.
- Cho, M. K., 1989, *PhD Dissertation*, " Structural Deflections and Optical Performances of Light Weight Mirrors", University of Arizona, Tucson, AZ.

- Couder, A., 1931, *Bulletin Astronomique*, Vol. 7, "Research on the Deformations of Large Mirrors Used for Astronomical Observations."
- Crawford, D. L., A. B. Meinel, and M. W. Stockton, 1968, *Symposium Proceedings*, "Support and Testing of Large Astronomical Mirrors," Tucson, Arizona.
- Davison, W. B., *Columbus Project*, Technical Report No. 1, pp. 1-7 : "A Big Binocular Telescope Mount Concept."
- Davison, W. B., 1987, *SPIE Structural Mechanics of Optical Systems II*, Vol. 748, pp. 31-38 : "Structural Innovations in the Columbus Project: An 11.3 Meter Optical Telescope."
- Davison, W. B., Rambabu Bavirisetty, Roger Angel, 1987, *Columbus Project*, Technical Memo UA-87-16, pp. 1-4 : "Comparison of Finite Element Models of Telescopes A and B."
- Davison, W. B., 1990, *SPIE Advanced Technology Optical Telescopes IV*, Vol. 1236, pp. 878-883 : "Design Strategies for Very Large Telescopes."
- Dwyer, W. M., Emerton, R. K., and Ojalvo, I. J., 1971, *AFDL-TR-70-118*, "An Automated Procedure for the Optimization of Practical Aerospace Structures."
- European Southern Observatory, 1987, *VLT Report No. 57*, "16-Meter Very Large Telescope."
- Farrell, J., 1966, *A Symposium on Support and Testing of Large Astronomical Mirrors*, pp. 131-137 : "Tension and Compression Radial Support System for the Primary Mirror.", Kitt Peak National Observatory and University of Arizona, Tucson, Arizona.
- Fehrenbach, C., 1966, *A Symposium on Support and Testing of Large Astronomical Mirrors*, pp. 66-68 : "Summary of Axial Supports.", Kitt Peak National Observatory and University of Arizona, Tucson, Arizona.
- Giles, G. L., 1971, *Journal of Structural Division, ASCE*, Vol. 97, No. ST1, "Procedure for Automating Aircraft Wing Structural Design."
- Gillett, P. E., 1983, *The NNTT Technology Development Program Report No. 5*, "Gravity Deflection Analysis of a Structured Mirror."
- Grundmann, W. A., 1983, *SPIE Advanced Technology Optical Telescopes II*, Vol. 444, pp. 218-225 : "Passive Support Systems for Thin Mirrors."
- Gunnels, S. M., 1990, *SPIE Advanced Technology Optical Telescopes IV*, Vol. 1236, pp. 854-865 : "Detail Design Problems and their Solutions: Apache Point Observatory 3.5 Meter Telescope."
- Hatheway, A. E., 1987, *SPIE Structural Mechanics of Optical Systems II*, Vol. 748, pp. 96-104 : "Optomechanical Analysis Strategies."

- Hill, J. M., 1990, *Columbus Project Technical Memo*, " Mirror Support System for Large Honeycomb Mirrors. "
- Iraninejad, B., Jacob Lubliner, Terry Mast, and Jerry Nelson, 1987, *SPIE Structural Mechanics of Optical Systems II*, Vol. 748, pp. 206-214 : " Mirror Deformations Due to Thermal Expansion of Inserts Bonded to Glass. "
- Isobe, S., Shiro Nishimura, and Minoru Shimizu, 1983, *SPIE Advanced Technology Optical Telescopes II*, Vol. 444, pp. 19-22 : " Proposed 3-Meter Alt-Az Telescope as the Japanese Next Large Telescope. "
- Itoh, N., 1987, *Workshop on Japanese National Large Telescope*, pp. 212-215 : " Mirror Support System. "
- Itoh, N., I. Mikami, T. Noguchi, Y. Shimizu, Y. Yamashita, J. Sovka, R. A. McLaren, and A. Erasmus, 1990, *SPIE Advanced Technology Optical Telescopes IV*, Vol. 1236, pp. 866-877 : " Mechanical Structure of JNLT : Analysis of Mirror Deflection due to Wind Loading. "
- Iye, M., T. Noguchi, Y. Torii, Y. Mikami, Y. Yamashita, W. Tanaka, M. Tabata, and N. Itoh, 1990, *SPIE Advanced Technology Optical Telescopes IV*, Vol. 1236, pp. 929-939: "Active Optics Experiments with a 62-cm Thin Mirror."
- Johns, M. W. and C. Pilachowski, 1990, *SPIE Advanced Technology Optical Telescopes IV*, Vol. 1236, pp. 2-12 : " WIN 3.5 Meter Telescope Project. "
- Jones, C. W., 1966, *A Symposium on Support and Testing of Large Astronomical Mirrors*, pp. 113-123 : " Mirror Axial Support Hardware. ", Kitt Peak National Observatory and University of Arizona, Tucson, Arizona.
- Knohl, E. D., 1983, *SPIE Cryogenic Optical Systems and Instruments III*, Vol. 973, pp. 201-208 : " Supporting and Figuring of SOFIA F/1.0 Thin ZERODUR Meniscus. "
- Kodaira, K., 1990, *SPIE Advanced Technology Optical Telescopes IV*, Vol. 1236, pp. 56-62 : " Present Status of the JNLT project. "
- Kowalskie, B.J., 1978, *A User's Guide to Designing and Mounting Lenses and Mirrors*, UCRL-52411, Lawrence Livermore Laboratory, University of California, Livermore, CA.
- L & F Industries, 1990, *Engineering Report - Preliminary Design Study of Wisconsin - Indiana - Yale - NOAO (WIYN) 3.5 Meter Telescope*, Huntington Park, CA.
- Lubliner, J., 1982, *UC TMT Technical note*, No. 25, " Deflections of a Circular Plate on a Ring of Point Supports", University Of California, Berkely, CA.

- Malvick, A. J., 1972, *Applied Optics*, Vol. 11, No. 3, pp. 575–584 : “ Theoretical Elastic Deformations of the Steward Observatory 230-cm and the Optical Sciences Center 154-cm Mirrors. ”
- Mehta, P., 1983, *SPIE - The International Society for Optical Engineering*, Vol. 450, “ Flat Circular Optical Elements on a 9 Point Hindle Mount in a 1-g Force Field. ”
- Mehta, P., 1987, *SPIE Structural Mechanics of Optical Systems II*, Vol. 748, pp. 158–171 : “ Flexural Rigidity Characteristics of Leight Weighted Mirrors. ”
- Meier, H. J., 1988, *Carl Zeiss, West Germany*, “ Support of Thin Meniscus Primary for SOFIA . ”
- Meinel, A. B. and Meinel, M. P., 1986, *SPIE Advanced Technology Telescopes III*, Vol. 628, pp. 403–411: “Wind Deflection Compensated, Zero-Coma Telescope Truss Geometries.”
- Meinel, A. B. and Meinel, M. P., 1987, *SPIE Structural Mechanics of Optical Systems II*, Vol. 748, pp. 2–5 : “ Telescope Structures: An Evolutionary Overview.”
- Melugin, R. K., L. S. Chang, J. A. Mansfield, and S. D. Howard, 1983, *SPIE Cryogenic Optical Systems and Instruments III*, Vol. 973, pp. 184–200 : “ Primary Mirror and Mount Technology for a Stratospheric Observatory for Infrared Astronomy (SOFIA) Telescope. ”
- Mohn, W. R. and Daniel Vukabratovich, 1988, *Optical Engineering*, Vol. 27, No. 2, pp. 90–98 : “ Recent Applications of Metal Matrix Composites in Precision Instruments and Optical Systems. ”
- MSC/NASTRAN, *User's Manual*, MacNeil Schwendler Corporation, Los Angeles, CA.
- MSC/NASTRAN, *Application Manual*, MacNeil Schwendler Corporation, Los Angeles, CA.
- Nelson, J. E., Jacob Lubliner, and Terry S. Mast., 1982, *UC TMT Report*, Report No. 74, “ Telescope Mirror Supports: Plate Deflections on Point Supports. ”, University of California, Berkely, California.
- Nelson, J. E., 1983, *UC TMT Technical note*, No. 69, “ Deflections of a Circular Plate on 3 and 6 Points”, University Of California, Berkely, CA.
- Niedenfuhr, A. W. Leissa, and M. J. Gaitens, “ A Method of Analysis for Shallow Shells of Revolution Supported Elastically on Concentric Rings.”

- Odgers, G. J., 1966, *A Symposium on Support and Testing of Large Astronomical Mirrors*, pp. 174-179 : " Canadian 150-Inch Telescope. ", Kitt Peak National Observatory and University of Arizona, Tucson, Arizona.
- Pearson, E. T., 1966, *A Symposium on Support and Testing of Large Astronomical Mirrors*, pp. 77-83 : " Effects of Cassegrain Hole On Axial Ring Supports. "
- Pearson, E. and I. Stepp, 1987, *SPIE Structural Mechanics of Optical Systems II*, Vol. 748, pp. 215-228 : " Response of large Optical Mirrors to Thermal Distributions. " Kitt Peak National Observatory and University of Arizona, Tucson, Arizona.
- Pearson, E., 1980, *Kitt Peak National Observatory Conference*, " Optical and Infrared Telescopes for the 1990s. " Kitt Peak National Observatory and University of Arizona, Tucson, Arizona.
- Pepi, J. W., 1987, *SPIE - The International Society for Optical Engineering*, Vol. 748, " Analytical prediction for light weight optics in a gravitational and thermal environment. "
- Pope, J. D., 1983, *SPIE Advanced Technology Optical Telescopes II*, Vol. 444, pp. 8-11 : " The UK 4.2 meter Optical Telescope. "
- Prevensic, T. V., 1968, *Applied Optics*, Vol. 7, No. 10, " The deflection of circular mirrors of linearly varying thickness supported along a central hole and free along the outer edge. "
- Ray, F. B. and Anthony Perroni, 1982, *SPIE Advanced Technology Optical Telescopes*, Vol. 332, pp. 206-211 : " Structural Analysis of the Mirror of the University of Texas 7.6 m Telescope. "
- Ray, F. B., Y. T. Chung, and B. S. Mani, 1983, *SPIE Advanced Technology Optical Telescopes II*, Vol. 444, pp. 228-240 : " Surface Error Analysis for the University of Texas 7.6m Telescope Primary Mirror. "
- Ray, F. B. and J.H. Chang, 1986, *SPIE Advanced Technology Telescopes III*, Vol. 628, pp. 526-528 : " Nastran Analysis for a Sequence of Cellular Primary Mirrors of the 8 Meter Class. "
- Richard, R. M. and George C. Williams, 1985, *A Design Report Prepared for NOAO*, " Optical Performance Analysis of 4-Meter Altazimuth Mounted Primary Telescope Mirrors. "
- Roark, R. J., 1975, *Formulas for Stress and Strain*, 5th Edition, McGraw Hill, New York, 1975.
- Robertson, H. J., 1966, *A Symposium on Support and Testing of Large Astronomical Mirrors*, pp. 244-249 : " Active Optics for Large Orbiting Astronomical

- Telescopes. ", Kitt Peak National Observatory and University of Arizona, Tucson, Arizona.
- Rule, B., 1966, *A Symposium on Support and Testing of Large Astronomical Mirrors*, pp. 143–149 : " Defining of Large Mirror Support Systems. ", Kitt Peak National Observatory and University of Arizona, Tucson, Arizona.
- Rule, B., 1966, *A Symposium on Support and Testing of Large Astronomical Mirrors*, pp. 84–104 : " Lever Support Systems. ", Kitt Peak National Observatory and University of Arizona, Tucson, Arizona.
- Schaeffer, H., 1984, *MSC/NASTRAN Primer*, "Static and Normal Modes Analysis."
- Schneermann, M., X. Cui, D. Enard, L. Noethe, and H. Postema, 1990, *SPIE Advanced Technology Optical Telescopes IV*, Vol. 1236, pp. 920–928 : " ESO VLT: III. The Support System of the Primary Mirrors. "
- Schwesinger, G., 1954, *Journal of the Optical Society of America*, Vol. 44, No. 5, pp. 417–424 : " Optical Effect of Flexure in Vertically Mounted Precision Mirrors."
- Schwesinger, G., 1966, *A Symposium on Support and Testing of Large Astronomical Mirrors*, pp. 11–23 : " Theoretical Aspects of Mirror Support. ", Kitt Peak National Observatory and University of Arizona, Tucson, Arizona.
- Seigmund, W. A., Edward J. Mannery, James Radochia, and Paul E. Gillett, 1986, *SPIE Advanced Technology Telescopes III*, Vol. 628, pp. 377–389 : " Design of the Apache Point Observatory 3.5 m Telescope : Deformation Analysis of the Primary Mirror. "
- Selke, L. A., 1970, *Applied Optics*, Vol. 9, No. 1, " Theoretical Elastic Deflections of a Thick Horizontal Circular Mirror on a Ring Support."
- Selke, L. A., 1971, *Applied Optics*, Vol. 10, No. 4, " Theoretical Elastic Deformations of Solid and Cored Horizontal Circular Mirrors having a Central Hole on a Ring Support."
- Sheng, S. C. F., 1988, *Applied Optics*, Vol. 27, No. 2, pp. 354–359 : " Lightweight mirror structures best core shapes: a reversal of historical belief. "
- Simpson Gumpertz & Heger Inc. 1990, *Final Conceptual Design – Conversion of MMT to 6.5 Meter Telescope*, Consulting Engineers, Arlington, MA.
- Smith, F. D., 1966, *A Symposium on Support and Testing of Large Astronomical Mirrors*, pp. 213–224 : " Interferometric Testing of Precision Optics. ", Kitt Peak National Observatory and University of Arizona, Tucson, Arizona.
- Stepp, L. M., 1990, *SPIE Advanced Technology Optical Telescopes IV*, Vol. 1236, pp. 615–627 : " 3.5 Meter Project at NOAO. "

- Timoshenko, S. , 1959, *Theory of Plates and Shells*, McGraw-Hill, New York.
- Tocher, J. L., and Karnes, R. N., 1971, *AIAA/ASME 12th Structures, Structural Dynamics, and Materials Conference*, AIAA Paper 71-361, " The Impact of Automated Structural Optimization on Actual Design. "
- Tokyo Astronomical Observatory, 1986, *Feasibility Study Interim Report on Japanese National Large Telescope*.
- Tokyo Astronomical Observatory, 1987, *Workshop On Japanese National Large Telescope*.
- Vukobratovich, D., Iraninejad, B., Richard, R. M., Hansen, Q. M., and Melugin, R., 1982, *Proceedings of SPIE*, Vol. 332, No. 54, " Optimum Shapes for Light Weight Mirrors. "
- Vukobratovich, D., 1988, *Optical Sciences Center, University of Arizona, Tucson, Arizona*, " Advanced Topics in Opto-Mechanics. "
- Wand, D. S., J. R. P. Angel, and Robert E. Parks, 1989, *Applied Optics*, Vol. 28, No. 2, " Mirror Deflection on Multiple Axial Supports. "
- Williams R. and H. F. Brinson, 1974, *Journal of Franklin Institute*, No. 6, " Circular Plate on Multipoint Supports. "
- Wilson, R. N., F. Franza, and L. Noethe, 1984, *IAU Colloquium : Very Large Telescopes, Their Instrumentation and Programs*, No. 79, pp. 23-40 : " From Passive Support Systems to the NTT Active Support. "
- Wizinowich, P. L. and Angel, J. R. P., 1987, " A demonstration of aspheric polishing with a full size stressed lap " , Steward Observatory, Tucson, AZ.
- Yoder, P. R. Jr., 1986, *Optomechanical System Design*, Marcel Dekker Inc., New York.
- Zavarise, G., C. Majorana, and B. Schrefler, 1987, *Columbus Project*, " Static and Dynamic Analyses of The Elevation Structure of a 2 × 8 Meter Optical Telescope. "